

CHAPTER 7

Lower Stratospheric Processes

Lead Authors:

A.R. Ravishankara

T.G. Shepherd

Coauthors:

M.P. Chipperfield

P.H. Haynes

S.R. Kawa

T. Peter

R.A. Plumb

R.W. Portmann

W.J. Randel

D.W. Waugh

D.R. Worsnop

Contributors:

S. Borrmann

B.A. Boville

K.S. Carslaw

R.L. Jones

M. Mozurkewich

R. Müller

D. O'Sullivan

G. Poulet

M. Rossi

S.P. Sander

CHAPTER 7

LOWER STRATOSPHERIC PROCESSES

Contents

SCIENTIFIC SUMMARY	7.1
7.1 INTRODUCTION	7.5
7.2 CHEMICAL AND MICROPHYSICAL PROCESSES	7.6
7.2.1 Gas Phase Processes	7.6
7.2.2 Microphysics	7.9
7.2.3 Reactions on Condensed Matter	7.12
7.3 RADIATIVE-DYNAMICAL AND TRANSPORT PROCESSES	7.16
7.3.1 Large-Scale Temperature and Wind Distribution	7.16
7.3.2 Global View of Transport and Mixing	7.19
7.3.3 Quantification of Transport and Mixing	7.21
7.3.3.1 Transport Time Scales	7.22
7.3.3.2 Exchange Time Scales	7.23
7.3.3.3 Mixing Time Scales	7.26
7.3.4 Stratosphere-Troposphere Transport and Exchange	7.27
7.3.4.1 Lowermost Stratosphere	7.28
7.3.4.2 Water Vapor and the Tropical Tropopause	7.29
7.4 COUPLED PROCESSES	7.30
7.4.1 Mesoscale Structure and Its Impact	7.30
7.4.1.1 Temperature Fluctuations	7.31
7.4.1.2 Filamentary Structure	7.32
7.4.2 Seasonal Evolution of Inorganic Chlorine	7.33
7.4.3 Lessons from Mt. Pinatubo	7.35
7.5 QUANTIFICATION AND PREDICTION OF OZONE CHANGES	7.36
7.5.1 Local Chemical Ozone Loss	7.37
7.5.2 2-D Models	7.40
7.5.3 General Circulation Models	7.42
7.5.4 3-D Chemical Models	7.43
7.6 CURRENT UNDERSTANDING OF OZONE DEPLETION IN THE LOWER STRATOSPHERE	7.47
7.6.1 Polar Seasonal Depletion	7.47
7.6.2 Midlatitude Trends	7.53
7.7 SYNTHESIS	7.57
REFERENCES	7.59

SCIENTIFIC SUMMARY

Chemical, microphysical, radiative-dynamical, and transport processes all play important roles in determining ozone abundance in the lower stratosphere. Since the last Assessment (WMO, 1995), there have been significant advances in our understanding of these processes and of the way in which they couple together to produce the observed distribution of ozone, and changes in this distribution.

Current understanding of lower stratospheric ozone depletion

- The large ozone losses during spring over Antarctica continue unabated, with approximately the same magnitude and areal extent as in the early 1990s. The near-constant extent of seasonal column ozone losses from year to year reflects the near-complete destruction of ozone within the Antarctic lower stratosphere during spring-time, and is consistent with our understanding of polar processes.
- Low abundances of late-winter/spring column ozone have been recorded both inside and outside the Arctic vortex in six of the last nine years. Observations show those years to be characterized by specific meteorological conditions: lower-than-normal late-winter/spring Arctic temperatures, which lead to enhanced activated chlorine; and a more isolated vortex and weaker planetary-wave driving, which lead to less transport of ozone-rich air into the Arctic. Under these meteorological conditions, both chemistry and dynamics act to reduce the seasonal levels of column ozone.
- During these years of low late-winter/spring column ozone, high abundances of active chlorine have been observed inside the Arctic vortex, and chemical ozone losses inside the vortex have been unambiguously identified. These chemical losses are associated with activated chlorine augmented by bromine. The total seasonal chemical ozone losses within the vortex have been estimated to be approximately 100 milli-atm cm (Dobson units), although this magnitude is subject to considerable uncertainty.
- Low polar temperatures, an isolated vortex, and reduced wave driving are coupled processes that occur in concert in the stratosphere; but their intensity and duration are highly variable. With the present high chlorine loading and winter/spring temperatures close to the threshold for significant chlorine activation, late-winter/spring Arctic chemical ozone loss is particularly sensitive to meteorological conditions (temperature and vortex isolation). Thus, it is not possible to predict the year-to-year variations.
- The decadal trend in springtime Arctic depletion during the 1990s is reminiscent of the early years of the Antarctic ozone hole. However, while the decadal trend in the Antarctic during the late 1970s and 1980s was driven by the trend in chlorine loading, the decadal trend in the Arctic during the 1990s has been driven by a decadal change in late-winter/spring meteorological conditions in the presence of already high chlorine loading. Thus, a reduced chemical ozone loss in the coming years would not necessarily indicate chemical recovery. The Arctic will remain vulnerable to extreme seasonal loss as long as chlorine loading remains high.
- The major contribution to the midlatitude column ozone decline during the last two decades has come from decreases in the lower stratosphere. This region is influenced by local chemical ozone loss, enhanced by volcanic aerosol, and by transport from other regions. The vertical, latitudinal, and seasonal characteristics of the decadal depletion of midlatitude ozone are broadly consistent with the understanding that halogens are the primary cause. The expected low ozone amounts in the midlatitude lower stratosphere following the Mt. Pinatubo eruption, and the progressively smaller decreases in the following years as the volcanic aerosol loading decreased, further strengthened the connection between ozone destruction and anthropogenic chlorine. (In the absence of chlorine, an increase in sulfate loading is expected to increase ozone abundance.)

LOWER STRATOSPHERIC PROCESSES

- The apparent leveling-off in midlatitude column ozone losses since the last Assessment is consistent with recovery from the large losses following the Mt. Pinatubo eruption as the volcanic aerosol loading slowly declined. Recent modeling studies have shown that it takes several years for the chemical effects of a volcanic eruption to disappear. Indeed, the trend in midlatitude ozone depletion during the 1980s (prior to Mt. Pinatubo) is now understood to have been exacerbated by volcanic influences during that decade.

Processes

- Chlorine activation in or on liquid particles in the lower stratosphere (both stratospheric sulfate aerosol (SSA) and supercooled ternary solutions (STS)) increases strongly with decreases in temperature. The rate coefficients are at least as large as those on solid polar stratospheric clouds (PSCs) close to nitric acid trihydrate (NAT) equilibrium temperatures. Thus, chlorine activation is to a first approximation controlled by temperature and water vapor pressure, and only secondarily by the phase of the condensed matter.
- Rapid polar ozone loss requires elevated chlorine monoxide (ClO) in the presence of sunlight. Maintenance of elevated ClO in late-winter/spring was previously thought to require denitrification. Since the last Assessment, new understanding has shown that cold liquid aerosol and/or repeated heterogeneous processing can also maintain elevated ClO in non-denitrified air.
- Some rate coefficients and photochemical parameters have been revised since the last Assessment. Although the impact of these findings has not yet been fully evaluated, our understanding of the lower stratosphere is not expected to change significantly. The lower measured rate coefficients for the reactions of iodine monoxide (IO) radicals mean that iodine may not contribute very significantly to the observed ozone depletion in the lower stratosphere.
- One of the most important new heterogeneous reactions identified since the last Assessment is the hydrolysis of bromine nitrate (BrONO_2), which serves to enhance odd hydrogen radicals (HO_x) and suppress nitrogen oxides (NO_x) and thereby plays a significant role in the midlatitude ozone chemistry.
- An individual stratospheric air parcel is made up of molecules that have spent differing amounts of time in the stratosphere. To calculate the composition of a given air parcel, one therefore needs to know the distribution of such times. The distribution varies as a function of height and latitude of the parcel. Different two-dimensional (2-D) and three-dimensional (3-D) model calculations of the distributions vary greatly and are generally inconsistent with measurements.
- The balance between radiation and dynamics controls upwelling and temperature in the tropics, and hence the amount of water vapor entering the stratosphere. This represents a potentially important mechanism by which stratospheric ozone depletion could be altered by changes in climate. The nature of this radiative-dynamical control is better understood since the last Assessment, although some important details remain unresolved.
- Constituent measurements show that the tropics are relatively isolated from midlatitudes, in some ways analogous to the wintertime polar vortex. The extent of isolation affects the budgets (and lifetimes) of chemical species. Simplified models that represent this dynamical feature (e.g., a leaky tropical pipe model) have been used to provide rough estimates of mixing time scales.
- Small-scale chemical tracer structure in the lower stratosphere, manifested as filaments or laminae, can arise from stirring by the large-scale flow. The importance of this process has been demonstrated since the last Assessment through transport calculations supported by in situ measurements. There have been significant advances in our understanding and quantification of this process, which affects mixing time scales in the lower stratosphere.

- Observations together with process-based modeling suggest that mesoscale PSC formation can activate chlorine in lee wave clouds. It is estimated that ozone can be destroyed downstream of such clouds for many days. Mesoscale chemical structure due to filamentation may also systematically impact rates of reactions (e.g., chlorine deactivation or ozone loss) on a larger spatial scale. However, the contribution of these two phenomena to midlatitude or polar ozone changes is yet to be quantified.

Quantification and prediction of ozone changes

- Field measurements of the abundances of free radical catalysts involved in lower stratospheric ozone loss are consistent with model calculations and have enabled calculation of ozone loss rates in certain parts of the lower stratosphere. For example, it is now known that HO_x is the dominant catalytic ozone destroyer in the midlatitude stratosphere below ~ 20 km. However, observations in the lowest part of the extratropical stratosphere within a few km above the tropopause remain very limited.
- Two-dimensional models, despite their shortcomings, are useful for characterizing radiative/chemical effects in the present climate system. They are able to calculate variations in total ozone amounts that are broadly consistent with the observed midlatitude column ozone trend. In particular, the models reproduce the lower ozone amounts observed immediately following Mt. Pinatubo and the subsequent increases as the aerosol disappeared.
- The major hindrance for future prognosis of ozone levels in the Arctic is the limited ability of models to predict the dynamics (hence temperatures and transport), due to the inherent chaotic variability of the atmospheric circulation on interannual and decadal time scales.
- Dynamical forcing of the stratosphere by gravity-wave drag is now believed to be a more important effect than was previously realized. Most gravity-wave drag parameterizations remain crude. This represents a significant obstacle for general circulation modeling and prediction of stratospheric climate change.

7.1 INTRODUCTION

When the possibility of stratospheric ozone depletion was first predicted in the 1970s, it was not expected to occur in the lower stratosphere. Now we know that it does (see Chapter 4). We also now know this region to be the major contributor to the observed column ozone changes. This is true both in midlatitudes and in polar regions, where the springtime ozone holes are confined to altitudes below 30 km. However, the extent of the observed depletion and the confidence with which it can be quantified vary significantly with location and season. In polar regions, ozone depletion is seasonal and well outside the natural variability. It is always associated with cold temperatures, a lack of local ozone production, and a rapid loss of ozone following exposure of polar air parcels to sunlight. Natural variability is however manifested in a year-to-year variability in late-winter/spring ozone depletion, especially in the Arctic. In contrast, ozone depletion in midlatitudes can only be identified as a statistical trend after removing the seasonal cycle. In this region one needs to understand the natural variability before quantifying the depletion and, especially, attributing the depletion to known (or unknown) forcings.

The lower stratosphere has a number of unique features that are relevant to its ozone abundance. (1) It is far removed from the major ozone production region, the more so the closer one gets to the poles. (2) It is somewhat removed from the regions where chlorine and nitrogen oxides are released from their precursor gases. Thus, transport plays a major role in bringing catalysts, as well as ozone itself, to the lower stratosphere. (3) It is the region that contains most of the sulfate aerosol and is vulnerable to enhanced sulfate loading following volcanic eruptions. (4) It contains the coldest parts of the stratosphere, to the extent that the sulfate aerosol can become highly reactive. Thus, heterogeneous reactions (those taking place on a solid substrate) and multiphase reactions (those taking place in a liquid droplet) play a major role in the chemistry of this region. The high degree of nonlinearity in the rates of these reactions with temperature also makes temperature, and temperature fluctuations, very important. (5) In the extrapolar upper stratosphere, outside the polar night, a balance between chemical production and destruction of ozone is established much faster than air can be transported from one region to another. However, in the lower midlatitude stratosphere, there is no clear separation of the time scales

for chemistry and transport. (6) In the polar regions, radiative cooling together with the dynamics of air motions sets up a vortex during winter and early spring. This polar vortex and its immediate outer surroundings provide very cold temperatures to produce condensed matter (solid and liquid polar stratospheric clouds (PSCs)) that is generally not possible in other parts of the stratosphere. At the same time – and for related reasons – the vortex also inhibits the transport of air from the inside to the outside of the vortex, and vice versa. Thus, the coldest parts of the stratosphere can sustain large concentrations of active species. The contents of the vortex are episodically leaked out to, and mixed into, the midlatitude lower stratosphere during winter and spring.

The stratosphere cannot be considered in isolation from the troposphere, because the processes that determine the structure and composition of the stratosphere are not local to the stratosphere. For example, increases in tropospheric carbon dioxide (CO₂) are predicted to lead to reduced temperatures in the lower stratosphere because there will be less upward penetration of upwelling longwave radiation. The Rossby and gravity waves that play an important role in forcing dynamical heating are primarily forced in the troposphere, and future changes in tropospheric climate may therefore lead to changes in dynamical heating in the stratosphere. Changes in the chemical composition of the troposphere, e.g., increases in methane (CH₄), will lead to changes in the stratosphere. The chemical composition of the lower extratropical stratosphere is affected by exchange with the troposphere. Finally, the water vapor content of the stratosphere is determined to a great extent by the temperature of the tropical tropopause, which is affected by the radiative-convective dynamics of the troposphere.

In order to understand ozone changes, it is necessary to first understand the natural (background) ozone distribution and its time evolution, on both seasonal and interannual time scales. The seasonal cycle of column ozone is well documented from ground-based and satellite data (e.g., Bowman and Kruger, 1985; London, 1985). There is relatively weak seasonality in the tropics ($\pm 4\%$ variations about a mean of ~ 260 Dobson units (DU)) but much larger seasonal changes in high latitudes ($\pm 20\%$ or so, depending on location). Most of the seasonality and latitudinal structure in column ozone occurs in the lower stratosphere between about 10–20 km. Because the ozone photochemical lifetime is

LOWER STRATOSPHERIC PROCESSES

relatively long in this region, seasonal variations are largely attributable to transport. The seasonal maximum occurs in both hemispheres during late winter and spring; in the Northern Hemisphere (NH) the maximum (~440 DU) occurs in polar regions, whereas in the Southern Hemisphere (SH) the maximum (~360 DU) occurs near 40-60°S, with a relative minimum over the pole. There is a similar amount of ozone in high latitudes of both hemispheres in late summer (~300 DU). The springtime high-latitude maximum in both hemispheres is a result of poleward and downward transport of ozone from the tropics (the photochemical source region) throughout winter and spring (i.e., the Brewer-Dobson circulation); the higher values of ozone in the NH result from stronger transport, associated with larger planetary wave activity during NH winter (e.g., Holton *et al.*, 1995). In the NH, this transport reaches all the way to the pole, and the climatological ozone maximum therefore extends to the pole. In the SH, in contrast, the ozone maximum occurs over 40-60°S because the strongest diabatic descent in this region of the lower stratosphere occurs near the edge of the polar vortex (Manney *et al.*, 1995a), and the Antarctic vortex is well isolated. Thus the relative minimum in ozone over the SH pole is a climatological feature related to transport (see Bojkov and Fioletov (1995), their Figure 15).

Interannual variability in column ozone is also well documented from observations (e.g., Randel and Cobb, 1994), although quantification of the long-term variations (such as the solar cycle) is limited by the shortness of the record. In the tropics the interannual variability ($\pm 4\%$) is comparable in magnitude to the seasonal cycle and is dominated by the quasi-biennial oscillation (QBO), with no apparent trend. In midlatitudes the interannual variability is substantially smaller than the seasonal cycle. After removal of the seasonal cycle, there is a significant (seasonally dependent) decadal-scale negative trend (see Chapter 4), episodic decreases following volcanic eruptions (especially in 1992-1993 following the Mt. Pinatubo eruption in mid-1991, when decreases reached ~5-10%), a small signal ($\pm 1\%$) associated with the 11-year solar cycle, and additional dynamical effects due to the QBO ($\pm 2-4\%$, and out of phase with the tropical QBO), the El Niño-Southern Oscillation (episodic $\pm 1\%$ variations in zonal means, with larger longitudinally localized values), and year-to-year meteorological variations (~1-2%). The seasonal and interannual variations in midlatitude ozone are due to a combination of transport and chemistry. Accurate knowledge of the

processes controlling the seasonal and interannual dynamical variability is thus central to understanding trend-related issues.

As noted above, the lower stratosphere is a region where chemical, microphysical, radiative-dynamical, and transport processes all play an important role in the determination of ozone abundance. It follows that our accounting of the past and prediction of the future trends in the lower stratospheric ozone depend on our understanding of these various component processes and of the way in which they couple together. This chapter attempts to build such an integrated understanding from a process-based perspective, in terms of quantifiable fundamentals. In the first part of the chapter, our current understanding of the fundamentals, individually and together, is assessed. Then, based on the assessed information, our current best understanding for the cause of the observed ozone changes is presented. Each subsection begins with a summary (in italics) that highlights the state of our present understanding and the principal new findings since the last Assessment (WMO, 1995). These summaries are supported by the more technical descriptions in the individual subsections. Thus, the summaries serve as a bridge between the scientific summary of the chapter and the text; an overall view of the chapter can be obtained by reading only the summaries. A synthesis (not a summary) of our overall understanding of lower stratospheric ozone depletion is provided in Section 7.7.

7.2 CHEMICAL AND MICROPHYSICAL PROCESSES

7.2.1 Gas Phase Processes

There have been no major changes in the values of the rate coefficients and photochemical parameters since the most recent evaluations. The findings during the past two years, though they are not necessarily already incorporated in current models and thus are not yet fully evaluated, are not expected to significantly affect our understanding of lower stratospheric ozone depletion. Such findings include the finite (~5%) hydrogen chloride (HCl) production in the reaction of hydroxyl radicals (OH) with chlorine monoxide (ClO); rate coefficients for reactions of many brominated species; and the finite quantum yields for the production of excited-state oxygen atoms ($O(^1D)$) in the photolysis of ozone beyond ~320 nm. The measured abundance

and diurnal variations of odd nitrogen (NO_y) and inorganic chlorine (Cl_y) species are generally in agreement with calculations based on laboratory data.

Table 7-1 lists some of the changes in gas phase reaction rate coefficients that have been reported since the 1994 Assessment (WMO, 1995). The small HCl production in the $\text{OH} + \text{ClO}$ reaction, in the absence of rapid heterogeneous conversion of HCl to atomic chlorine (Cl), will significantly shift the balance between the active and inactive forms of chlorine, possibly affect the rate of chlorine recovery in the Arctic spring, and make chlorine less effective. The impact of this finding is discussed further in Chapter 6. The better definition of the rate coefficient for the reaction of ClO with itself improves the polar ozone depletion calculation. The current assumption of Cl atom production in the photolysis of the ClO dimer (Cl_2O_2) appears to be valid. However, the photolysis rate of Cl_2O_2 is still somewhat uncertain.

In the winter/spring polar lower stratosphere, higher chlorine and, possibly, bromine oxides and oxyacids may be formed and, thus, sequester a fraction of the inorganic halogen as temporary reservoirs (Sander *et al.*, 1989). Studies of Burkholder *et al.* (1993) imply that Cl_2O_3 , the prime candidate that could lead to higher oxides of chlorine, is too short-lived under polar conditions to result in significant higher chlorine oxide formation. Electronic structure calculations suggest otherwise (Clark and Francisco, 1997; Flesch *et al.*, 1994). The role of higher oxides of halogens is still somewhat uncertain but not expected to be a major factor.

The loss processes for the source gases for bromine are discussed in Chapter 2. The updates on the stratospheric reactions involving the brominated species are given in Table 7-1. The partitioning of bromine species between active and inactive forms in the stratosphere is discussed in Chapter 2 and Section 7.5.1. None of these changes alter the conclusions of the previous Assessment that on a per-atom basis, bromine is approximately 50 times more efficient than chlorine in destroying stratospheric ozone.

Nickolaisen *et al.* (1996) reported the quantum yields of ClO and nitrate radical (NO_3) formation in chlorine nitrate (ClONO_2) photolysis to vary with pressure when photolyzed above 300 nm and attributed the less-than-unity quantum yield to the quenching of a metastable state formed subsequent to light absorption. Recent studies suggest that the photolysis rate of ClONO_2 is not pressure dependent below 350 nm. If the ClONO_2

photodissociation quantum yield is pressure dependent at long wavelengths, the photodissociation rates (J-values) will be ~50% lower at high solar zenith angles; at lower solar zenith angles, the reduction in J-values will be much less. A smaller J-value would reduce the ClO/ Cl_y ratio in the lower stratosphere. The partitioning amongst ClO, nitrogen dioxide (NO_2), and ClONO_2 calculated by assuming a unit quantum yield agree, within their measurement uncertainties, with data from the Upper Atmosphere Research Satellite (UARS) (Dessler *et al.*, 1996), the National Aeronautics and Space Administration (NASA) ER-2 high-altitude aircraft (Stimpfle *et al.*, 1994), and the Atmospheric Trace Molecule Spectroscopy (ATMOS) instrument (Chang *et al.*, 1996); these studies suggest that the photolysis rate of ClONO_2 is not much smaller than that calculated using unit photodissociation quantum yield. The most recent information on bromine nitrate (BrONO_2) photolysis is listed in Table 7-1. It appears that the partitioning of ClO/ Cl_y and BrO/ Br_y (bromine monoxide/inorganic bromine), and the ozone depletion efficiencies, which are affected by photolysis rates of ClONO_2 and BrONO_2 , are reasonably well quantified.

The rate coefficient for the reactions of ClO with iodine monoxide (IO) is measured to be a factor of 5 smaller (Turnipseed *et al.*, 1997) than that assumed by Solomon *et al.* (1994). As discussed in Section 7.6.2, this finding greatly reduces the calculated influence of iodine compounds on stratospheric ozone.

In the lower stratosphere, odd-hydrogen radicals (HO_x) are produced mostly via the reaction of $\text{O}(^1\text{D})$ atoms, formed by the photodissociation of ozone (O_3), with water and methane. An assessment of the impact of a higher OH production rate based on the new determinations of the $\text{O}(^1\text{D})$ quantum yields (Table 7-1) on the stratosphere awaits further studies.

No major revisions to the rate parameters that determine the abundance and partitioning of nitrogen oxide species have been made since the last Assessment. However, available field observations indicate that processes controlling NO_y partitioning in the lower stratosphere are reasonably well characterized for spring and winter. Nitric oxide (NO) and NO_2 measured over a wide range of latitudes (Gao *et al.*, 1997) yield NO/ NO_2 ratios (uncertainty ± 20 -30%) within 8% of the steady-state relationship and imply that the NO_2 photolysis rate and reaction rate coefficients controlling this ratio in spring and winter are accurate, in spite of some earlier contradictions (Jaeglé *et al.*, 1994; Sen *et al.*, 1998).

Table 7-1. Changes in the data on gas phase reactions that affect stratospheric ozone chemistry. Minor changes in some of the other reactions are not listed. In most cases, the data obtained after the 1994 Assessment are listed in DeMore *et al.* (1997).

Reaction	Information for 1994 Assessment (WMO, 1995)	Update	Impact	Reference
OH + ClO →HO ₂ + Cl or →HCl + O ₂	HCl yield = 0.	~5% HCl yield.	Reduces the impact of chlorine.	Lipson <i>et al.</i> (1997).
ClO + ClO + M → Cl ₂ O ₂ + M	10 to 60% uncertainty in rate constant.	No new data. Reanalysis reduced uncertainty to <30%.	Better definition of ozone loss rates.	Nickolaisen <i>et al.</i> (1994).
ClO + BrO → products	Uncertain to ~30%.	No change.	Contribution of this reaction still uncertain.	DeMore <i>et al.</i> (1997).
ClOOCl + hv → products	Limited information on products. Cross sections uncertain.	Quantum yields measured at 248 & 308 nm.	Assumption of Cl atom production OK. Photolysis rate still uncertain.	DeMore <i>et al.</i> (1997).
HO ₂ + BrO → products	Not well defined.	Many studies. Defined to better than 50%.	Role of bromine-catalyzed ozone loss in midlatitudes better defined.	Cronkhite <i>et al.</i> (1998), Elrod <i>et al.</i> (1996), Larichev <i>et al.</i> (1995), and Li <i>et al.</i> (1997).
HOBr + hv → products	Inconsistent data on cross sections.	New band of HOBr discovered. Cross sections a little better defined.	HOBr photolysis rate will not determine the rate of O ₃ loss. Helps explain the early morning OH.	DeMore <i>et al.</i> (1997), Ingham <i>et al.</i> (1998), and Deters <i>et al.</i> (1996).
OH + BrO → products	No information.	Fast reaction. Products unknown.	Small yield of HBr will help explain observations.	DeMore <i>et al.</i> (1997).
BrO + O → products		Better defined.	Little impact.	DeMore <i>et al.</i> (1997).
BrO + O ₃ → products		Lower upper limit.	Makes this reaction unimportant.	Rowley <i>et al.</i> (1996).
ClONO ₂ + hv → products	Possibility of pressure dependence in photolysis.	Pressure dependence of photolysis rate, if it exists, is small. Products are Cl and NO ₃ .	The pressure dependence of photolysis rate is not responsible for measured ClONO ₂ to HCl ratio.	Moore <i>et al.</i> (1995), Tyndall <i>et al.</i> (1997), Yokelson <i>et al.</i> (1997), and Nickolaisen <i>et al.</i> (1996).
BrONO ₂ + hv → products	Cross section measured by only one group at 298 K only.	Cross sections known as function of temperature. Quantum yields measured. Photolysis rate not pressure dependent.	Role of bromine better defined.	Harwood <i>et al.</i> (1998), Burkholder <i>et al.</i> (1995), and Deters <i>et al.</i> (1998).
IO + ClO → products IO + BrO → products	Rate coefficients unknown.	Rate coefficients defined and some information on product yields available.	The role of iodine is better quantified.	DeMore <i>et al.</i> (1997).
O ₃ + hv → O(¹ D)+O ₂		Production of O(¹ D) at long wavelengths and lower T.	HO _x production rate is enhanced. Full impact not yet assessed.	Ball <i>et al.</i> (1997), Silvente <i>et al.</i> (1997), Takahashi <i>et al.</i> (1996), and Talukdar <i>et al.</i> (1998).

7.2.2 Microphysics

Nitric acid-containing PSCs can exist 2-6 K above the frost point. The surface area of PSCs critically depends on their type. Particles of different composition and phase can coexist, but may not necessarily be in thermodynamic equilibrium with each other or with the gas phase. In particular there is evidence that solid PSCs, e.g., nitric acid trihydrate (NAT) clouds, often do not grow to their equilibrium sizes (Type-1a). In the absence of solid PSCs, gaseous nitric acid is taken up by solution droplets when temperatures fall to within 2-3 K of the frost point. The resulting ternary solution droplets form liquid PSCs (Type-1b) with a surface area typically 10-fold higher than background aerosols. While the thermodynamics and non-reactive kinetics of liquid PSCs are understood, the conditions that lead to the formation of solid PSCs are still highly uncertain. The role of solid particles in ozone depletion through sedimentary redistribution of NO_y and water (H_2O) and through direct chemical processing of halogen species cannot yet be quantified.

The size, phase, growth, and evaporation of stratospheric aerosol are fully governed by the highly temperature-dependent partitioning of nitric acid (HNO_3), sulfuric acid (H_2SO_4), and H_2O and not by other species, such as those involved in chemical processing or nucleation (e.g., freezing). Despite the expected simplicity of such a ternary system, the composition and the phase of wintertime stratospheric particles are unclear.

The strong supercooling of supercooled ternary solutions (STS) leads to overall rates of chemical processing that vary continuously in going from sulfuric acid aerosols to PSCs (see Section 7.2.3). Due to increasing solubilities of reactants, the chemical processing increases very rapidly with decreasing temperature. Activation of chlorine occurs in a day or so around the NAT equilibrium temperature. This continuous but rapid activation was confused previously with a threshold process.

Currently, it is uncertain when gas-to-solid, liquid-to-solid, and solid-to-solid phase transitions (deposition-nucleation, freezing, and incongruent melting, respectively) occur. As long as these processes are poorly understood, the relevance of solid PSCs in chemical processing and sedimentary redistribution of HNO_3 and H_2O remains unclear. This impedes a proper analysis of current ozone loss and prohibits accurate prognosis of future ozone levels.

THERMODYNAMICS OF SOLID AND LIQUID STRATOSPHERIC PARTICLES

As noted in Chapter 3, under typical Arctic conditions, quasi-binary $\text{H}_2\text{SO}_4/\text{H}_2\text{O}$ solution droplets turn into quasi-binary $\text{HNO}_3/\text{H}_2\text{O}$ droplets upon cooling from 193 to 190 K. Under these conditions, species such as hydrogen chloride (HCl), hypochlorous acid (HOCl), and hydrogen bromide (HBr) can also take part in multiphase reactions in/on the liquid particles because of their increased solubility at low temperatures (see Figure 3-1 and Section 7.2.3). Other temperature-dependent contributions, such as liquid phase diffusion coefficients, second-order reaction rate coefficients, or the increase in surface area due to $\text{HNO}_3/\text{H}_2\text{O}$ uptake, are of relatively minor importance (Peter, 1997; Ravishankara and Hanson, 1996). Solubilities at very low temperatures have been mostly derived from thermodynamic models rather than direct experimental vapor pressure data but are believed to be robust (Carslaw *et al.*, 1997).

The thermodynamic stability of hydrates of nitric and sulfuric acid and their complex interactions are summarized in Figure 7-1. Under typical stratospheric conditions, nitric acid hydrates (NAX = NAT, nitric acid dihydrate (NAD), or nitric acid pentahydrate (NAP)) may coexist either with a liquid or with hydrates containing the H_2SO_4 of the background aerosol droplet. On the other hand, sulfuric acid hydrates (SAX = sulfuric acid tetrahydrate (SAT) or sulfuric acid hemihexahydrate (SAH)) or the mixed hydrate (MIX) in general cannot coexist with HNO_3 -containing liquids, because they deliquesce below a certain temperature (e.g., at 191 K for SAT in Figure 7-1). As Koop and Carslaw (1996) noted, deliquescence leads to a "reset mechanism" of frozen H_2SO_4 aerosols back to the liquid state, provided NAT does not nucleate on these particles before the deliquescence temperature is reached.

ARE PSCs SOLIDS, LIQUIDS, OR BOTH?

The only solid unambiguously known to be formed under stratospheric conditions is ice, which nucleates a few degrees below the frost point (see, for example, Carslaw *et al.*, 1997). Originally, PSCs were suggested to form upon freezing of the sulfate aerosols and condensation of HNO_3 and H_2O onto it (Poole and McCormick, 1988), as indicated by the SAT-NAX-ice path in Figure 7-1. However, laboratory studies indicate

LOWER STRATOSPHERIC PROCESSES

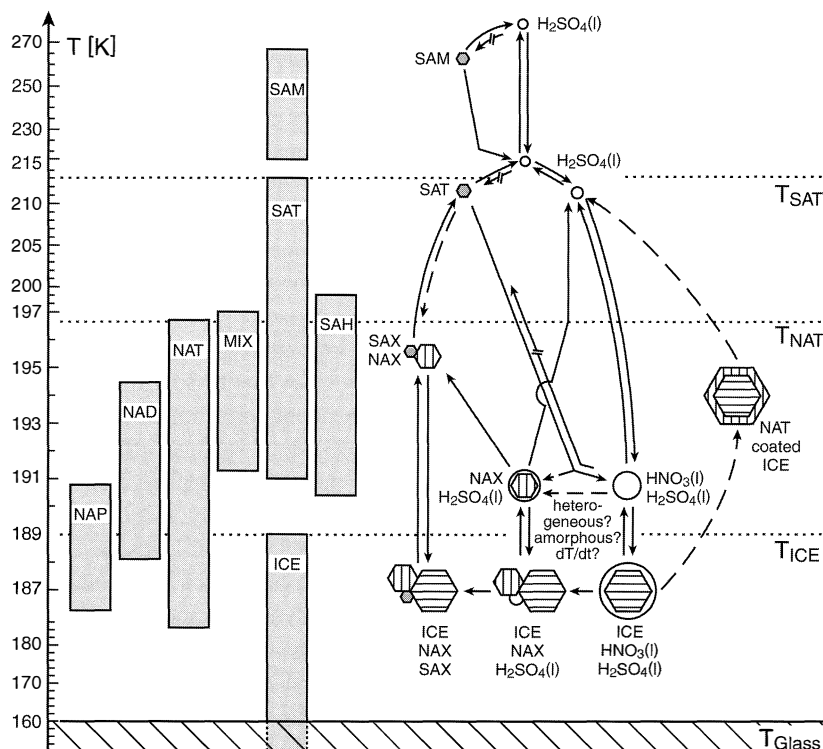


Figure 7-1. Stability regions of HNO_3 and H_2SO_4 hydrates and water ice (left) and phase transitions among these solids and with ternary solutions (right) for the following conditions: 50 hPa, 5 ppmv H_2O , and 10 ppbv HNO_3 . Horizontal lines mark equilibrium temperatures for SAT, NAT, and ice. Solid arrows: kinetically allowed transitions. Crossed arrows: kinetically hindered. Particles in thermodynamic equilibrium are connected by solid arrows, in nonequilibrium by dashed arrows. Abbreviations for crystalline phases: NAX is generic name for nitric acid hydrates, NAT = $\text{HNO}_3 \cdot 3\text{H}_2\text{O}$, NAD = $\text{HNO}_3 \cdot 2\text{H}_2\text{O}$, NAP = $\text{HNO}_3 \cdot 5\text{H}_2\text{O}$; SAX is generic name for sulfuric acid hydrates, SAT = $\text{H}_2\text{SO}_4 \cdot 4\text{H}_2\text{O}$, SAH = $\text{H}_2\text{SO}_4 \cdot 6.5\text{H}_2\text{O}$, SAM = $\text{H}_2\text{SO}_4 \cdot \text{H}_2\text{O}$; MIX = $\text{H}_2\text{SO}_4 \cdot \text{HNO}_3 \cdot 5\text{H}_2\text{O}$, ICE = water ice. (l) marks aqueous liquids. Adapted from Peter (1997) after Koop *et al.* (1997b).

that precipitation of SAT from binary or ternary solutions ($\text{H}_2\text{SO}_4(l) \rightarrow \text{SAT}$) is kinetically unfavorable down to temperatures below the frost point (Carslaw *et al.*, 1997; Martin *et al.*, 1998), and that even ice crystals in STS are probably not suited for heterogeneous nucleation of acidic hydrates (Koop *et al.*, 1995; Koop *et al.*, 1997a). On the other hand, deposition nucleation (gas-to-solid) on ice without liquid intermediates sets in at moderate supersaturations (Hanson, 1992) and was suggested as a mechanism for NAT formation (Carslaw *et al.*, 1997).

Temperatures do not often drop below the frost point in the Arctic (at least on large scales). The need for such low temperatures could be circumvented if HNO_3 hydrates nucleated on H_2SO_4 hydrates, thereby avoiding their deliquescence. There are conflicting data

on whether NAT can nucleate on SAT (dashed line from SAT to NAX in Figure 7-1) due to a pre-conditioning of the SAT (Iraci *et al.*, 1998; Zhang *et al.*, 1996). A differentiation between deliquescence or pre-activation, which is difficult to obtain from presently available observations (Larsen *et al.*, 1997) or laboratory investigations (Iraci *et al.*, 1998), is necessary to determine the evolution of the physical state of PSC particles. It has been suggested that solids could form above the frost point via crystallization of amorphous solids upon warming (Tabazadeh and Toon, 1996) or the freezing of highly nonequilibrium liquid states (Tsiaras *et al.*, 1997) (see dashed horizontal arrow in Figure 7-1).

It was thought that solid particles (ice, NAT, and other hydrates of HNO_3 and H_2SO_4) would nucleate close

to the NAT equilibrium temperature, leading to abrupt changes in surface area and chemical processing rates (WMO, 1995). Modeling and laboratory work have since revealed that PSCs could consist of supercooled ternary (liquid) solution (STS) droplets (Carslaw *et al.*, 1994; Tabazadeh *et al.*, 1994) and have led to the identification of Type-1b PSCs as liquid aerosol. Thus, PSCs can be solids or liquids. However, the circumstances that lead to solid PSCs remain unclear.

NON-REACTIVE UPTAKE KINETICS

Particles and the gas phase can be out of equilibrium due to gas diffusion and partial pressure limitations. Growth/evaporation times depend on particle size and the saturation ratio (i.e., the difference between the vapor pressure and partial pressure of the condensing species). Therefore, the growth/evaporation of HNO₃-containing particles, such as NAT and STS particles, are much slower than that of ice particles. For 1- μ m particles, typical growth times (or lifetimes) vary from less than one minute for ice (Toon *et al.*, 1989b) to more than one day for NAT (Peter *et al.*, 1994). Diffusion resistances may also lead to highly nonequilibrium compositions in growing/evaporating STS clouds, with small droplets acquiring HNO₃ concentrations well above the maximum equilibrium value (Meilinger *et al.*, 1995). The extent of deviation from equilibrium depends on the time rate of temperature change. Cooling/heating rates of 100 K/h, for example in mountain-induced gravity waves (lee waves; see Section 7.4.1.1) can lead to droplets with negligible H₂SO₄ concentrations and about 60 wt% HNO₃ (Tsias *et al.*, 1997). It is likely that NAD nucleates (Disselkamp *et al.*, 1996) in these wave-induced highly nonequilibrium solution droplets, which may subsequently convert into NAT.

Solid particles, which are few in number but can grow to large sizes, often take long times to grow. For example, from lidar measurements, Toon *et al.* (1990) concluded that Type-1a particles have radii on the order of 1 μ m or larger, but that possibly only a part of the available HNO₃ condensed. This might be due to long growth/evaporation times, which are supported by balloon and aircraft-borne in situ observations that have frequently found nonequilibrium conditions. In Chapter 3 of this Assessment, Figure 3-12 shows particle counter measurements made on board the ER-2 in the Arctic. Each point in that figure corresponds to a size-resolved measurement. Particles in panel 1 (bottom left panel

corresponding to the encircled 1 in the main panel) show a log-normal distribution shifted with respect to the background, most likely indicating STS droplets. In contrast, panel 2 shows a large particle mode with small number density but radii of about 1 μ m immersed in a small particle mode representative of a background distribution. Most likely, the large mode consists of an HNO₃ hydrate and the small mode of liquid H₂SO₄/H₂O droplets (with very small amounts of dissolved HNO₃). If the hydrate was NAT and had grown to its full equilibrium size, point (2) in the main panel of Figure 3-12 would lie on the NAT curve (dotted). At their small number density, however, it would take roughly a day for these particles to deplete the gas phase. Because air parcels in the Arctic rarely remain cold for such long periods, clouds with fully condensed large solid particles are rarely observed there.

Tabazadeh *et al.* (1995) and Tabazadeh and Toon (1996) have interpreted the flight observations in Figure 3-12 as the manifestation of a new thermodynamic phase rather than an indication of nonequilibrium particle distributions. By eliminating particles with radii larger than 2 μ m from the particle counter measurements and constraining the evaluation to a certain time window, they obtained the more compact volume-temperature relationship shown in the insert in Figure 3-12. They argued that this relationship could represent a glass-like amorphous phase, as trajectory analyses indicate crystallization of the particles upon warming. However, the only laboratory investigation bearing directly on this issue suggests that crystal embryos in binary or ternary solutions show no growth impedance at stratospheric temperatures (Koop *et al.*, 1997a), thereby not supporting an amorphous high-viscosity state.

MICROPHYSICAL ASPECTS OF SEDIMENTARY REDISTRIBUTION

Sedimentary redistribution of HNO₃ (also called denitrification and re-nitrification) and H₂O (dehydration and rehydration) has been observed in the Antarctic (WMO, 1995) and, to a lesser extent, in the Arctic (Arnold *et al.*, 1998; Fahey *et al.*, 1990; Hübner *et al.*, 1990). Sedimentation rates depend critically on particle size. To sediment down by 5 km, representative of the observed redistributions, it takes 7 months to a week for 1 to 5 μ m particles, respectively (Müller and Peter, 1992). For a particle number density of 10 cm⁻³, NAT particles would reach radii of about 0.3 μ m and ice particles of

LOWER STRATOSPHERIC PROCESSES

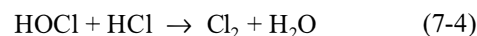
about 1.6 μm , if all the HNO_3 and H_2O , respectively, in a lower stratospheric air parcel condensed. Such small particles obviously do not allow for significant sedimentary redistribution and a very small number of particles must grow to large sizes via some highly selective nucleation mechanism.

In the Arctic, matters are complicated because planetary waves make the air parcels go through temperature oscillations with a period of about 5 days and 15-30 K peak-to-peak amplitude. This warms the air well above the NAT evaporation temperature. Therefore, sedimentary redistribution could occur in many successive steps, possibly enhanced by mesoscale temperature fluctuations in mountain waves (Section 7.4.1.1). Another possibility is that HNO_3 coats an ice particle (Wofsy *et al.*, 1990; Peter *et al.*, 1994); see rightmost path in Figure 7-1. If particles grow to radii above 10 μm , sedimentation could proceed in a single step, which is unlikely for NAT. Goodman *et al.* (1997) found ice particles containing small amounts of HNO_3 with radii between 6 and 8 μm in the Antarctic stratosphere at temperatures 2-4 K above the frost point. They observed increases in the HNO_3 fraction with decreasing particle size and concluded that the ice might be protected by a NAT coating. In conclusion, redistribution of HNO_3 requires a selective nucleation mechanism whose nature is still uncertain and does not necessarily require significant dehydration.

7.2.3 Reactions on Condensed Matter

The rates of the major stratospheric multiphase reactions in liquid aerosol are known to about a factor of 2. The rates of reactions on solids are very uncertain; inclusion of more detailed kinetic formulations in models requires improved laboratory data and analysis. Cl_y activation rates vary with various stratospheric parameters as follows: a factor of 2 in heterogeneous processing rate corresponds to a factor of 2 in aerosol surface area; a change in T of 2-4 K; a factor of 2 to 4 change in HCl vapor pressure; or a 20% change in water vapor pressure (the latter corresponding to about 2 km in altitude). Within that uncertainty, the role of liquid aerosol from measurements of the partitioning of reactive families (NO_x and Cl_y) is reasonably well understood at mid and high latitudes, particularly at low aerosol loading. Uncertainties remain at high aerosol loading and for coldest conditions (where solid particles may be important).

Five reactions that take place in liquid droplets as well as on solid surfaces are routinely included in stratospheric models:



In addition, the reaction of hypobromous acid (HOBr) with HCl is included in a few models:



Reaction (7-1) on sulfate aerosol controls the relative weighting of NO_x (where $\text{NO}_x \equiv \text{NO} + \text{NO}_2$) and HO_x ozone loss cycles by converting NO_x to HNO_3 . At colder temperatures ($T < 200\text{K}$), reactions (7-2 to 7-4) shift Cl_y speciation toward ClO_x and NO_x to HNO_3 , enhancing Cl-induced ozone loss. The activation of Cl_y via reactions (7-2 to 7-4) increases strongly with decrease in temperature. Br_y reactions (7-5 and 7-6) are now believed to impact ClO_x and HO_x levels. Other reactions between species of different radical families ($\text{N}_2\text{O}_5 + \text{HCl}$ and $\text{BrONO}_2 + \text{HCl}$, for example) are not currently included routinely in models.

Laboratory measurements of reactive uptake coefficients and physico-chemical parameters involved in these coefficients on many solids and liquids have been evaluated (Atkinson *et al.*, 1997; DeMore *et al.*, 1997). Overall, there is good agreement for reactions with condensed H_2O (7-1, 7-2, and 7-5), especially on liquids. However, laboratory results for reactions of two gas phase species on or in condensed matter, e.g., reactions (7-3), (7-4), and (7-6), are still uncertain, especially on solid surfaces. Understanding of chemical mechanisms in terms of fundamental physico-chemical parameters is required to reduce uncertainties and apply kinetic formulations to all stratospheric conditions (see for example, Kolb *et al.*, 1995).

There has been much progress in understanding the mechanism of liquid phase reactivity, exemplified by the formulations of reactions (7-2) and (7-3) by Hanson *et al.* (1994). Figure 7-2 shows ClONO_2

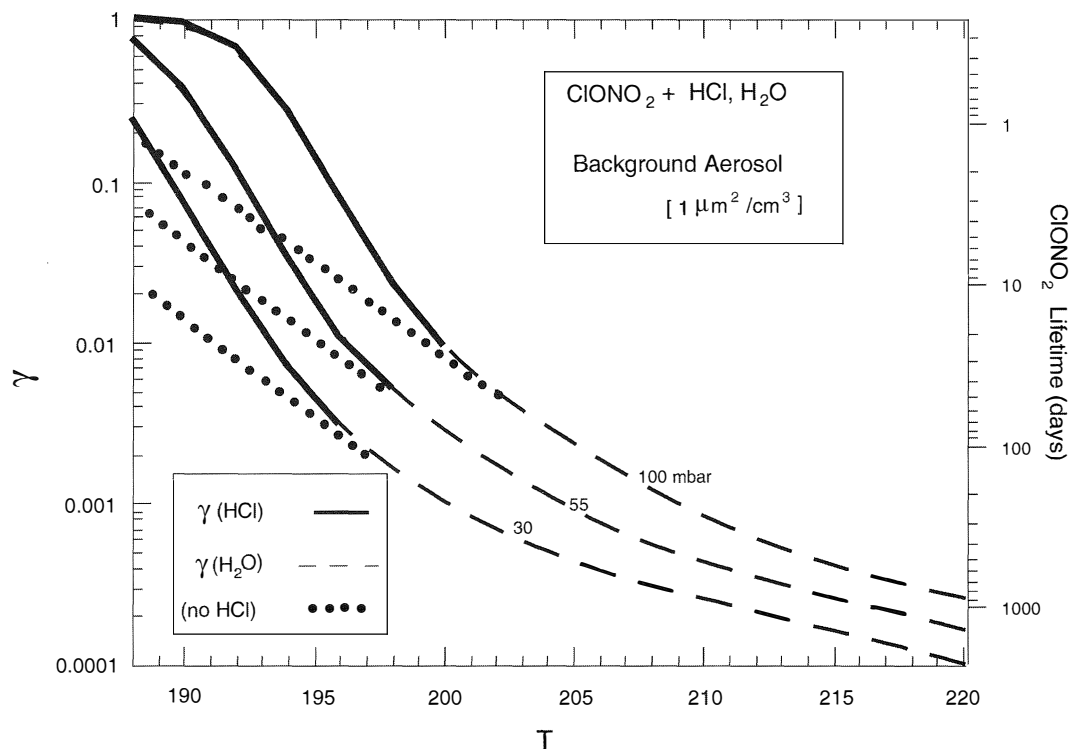


Figure 7-2. Reactivity of ClONO_2 with H_2O and HCl (reactions (7-2) and (7-3)) as a function of stratospheric temperature (T). ClONO_2 processing lifetime on right axis is derived from reactive uptake coefficient (γ) on left axis, assuming background aerosol (ignoring PSC condensation below 195 K). Stratospheric pressures of 30, 55, and 100 mbar correspond roughly to 24, 20, and 16 km altitude, respectively. The steep rise in γ below 195-200 K reflects increasing H_2O and HCl condensation into the sulfuric acid solution. The corresponding shift from reaction with H_2O (dashed line) to faster reaction with HCl (solid line) defines cold (polar) Cl_y processing. The dotted line shows H_2O reaction in absence of HCl . Curves come from updated formulation of the Henry's law solubility (H) and the rate coefficient (k) for reaction (7-2), derived from analysis of all experimental results (Robinson *et al.*, 1997). For reaction (7-3), H for HCl was taken from Carslaw *et al.* (1995) and k was derived from Hanson and Ravishankara (1994). Also included is a detailed formulation of the liquid phase diffusion coefficient (D_l) in $\text{H}_2\text{SO}_4/\text{H}_2\text{O}$ solution (Hanson and Ravishankara, 1993; Klassen *et al.*, 1998; Williams and Long, 1995). Adapted from Ravishankara and Hanson (1996) and Robinson *et al.* (1997).

reactivity on sulfuric acid/water mixtures under lower stratospheric conditions. The rate of Cl_y processing shows a steep temperature dependence, largely due to condensation or dissolution of reactants (H_2O and HCl) at cold temperatures (see Chapter 3). Rates of multiphase processing depend on Henry's law solubility (H), liquid phase diffusion coefficient (D_l), and rate coefficients (k) for the reaction in the liquid. Figure 7-2 uses an updated kinetic formulation (Robinson *et al.*, 1997) that refines previous work (Hanson *et al.*, 1994) by more comprehensively treating H , D_l , and k in variable aerosol

acid composition. This is particularly important for predicting variability with altitude, because the relationship between acid composition and stratospheric temperature (T) depends on absolute water vapor density, and because D_l and k determine how processing rates vary with the size of the particle.

The sharp increase in the ClONO_2 processing rate as T gets close to 200 K is largely from reaction (7-3) in liquid aerosols. Reaction (7-2) is now identified to be acid-catalyzed (Robinson *et al.*, 1997) and is consistent with recent observation of protonated HOCl at high acid

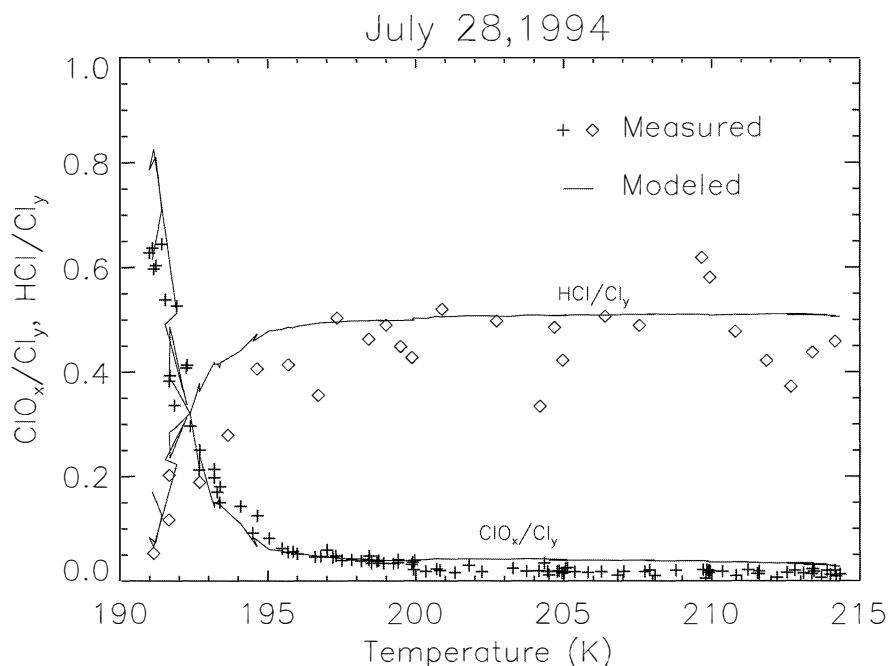


Figure 7-3. Measurements of ClO_x/Cl_y and HCl/Cl_y from the flight of 28 July 1994 near the southern vortex plotted versus temperature. On this day the measured temperature was the minimum of the previous 10 days for all trajectories originating south of 57°S . (Adapted from Kawa *et al.*, 1997.)

concentration (Hanson and Lovejoy, 1996; Donaldson *et al.*, 1997). Although reaction (7-3) dominates the Cl activation process, these faster rates for reactions (7-2) and (7-4) for $T < 200\text{K}$ alter the $\text{HCl}/\text{ClONO}_2$ partitioning, particularly at low HCl levels (Carslaw and Peter, 1997). Reaction (7-6) is also potentially important (Abbatt, 1994). Reaction (7-5) remains fast even at lower H_2O concentrations and, hence, at higher wt% (i.e., temperatures well above 200 K in the stratosphere) (Hanson *et al.*, 1996). Therefore, it is important in the lower stratosphere during all seasons and over a wide range of altitudes.

In contrast to reaction (7-2), the rate of N_2O_5 hydrolysis (reaction 7-1) is virtually independent of water activity. While a constant value of 0.1 for the reactive uptake coefficient (γ) represents results for background stratospheric aerosol conditions, the detailed mechanism is likely more complex (Robinson *et al.*, 1997). There are uncertainties in the rate of reaction (7-1) in STS (Hanson, 1997a; Zhang *et al.*, 1995). Reaction (7-1) is reported to be slower in warmer aerosols (Hu and Abbatt, 1997).

Parameterizations of chemical mechanisms in liquids, including estimation of surface reactivity

(Hanson, 1997b) and the reacto-diffusive length for aerosol-size-dependent processing (Hanson and Lovejoy, 1995; Lovejoy and Hanson, 1995), are known well enough to quantify the rates of reactions (7-1)-(7-6) within a factor of 2 under various stratospheric conditions. The calculated processing rates are consistent with many field observations of HNO_3 and chlorine species, including Arctic ER-2 (Webster *et al.*, 1994) and balloon measurements (Oelhaf *et al.*, 1994; von Clarmann *et al.*, 1997) and global satellite measurements (Müller *et al.*, 1996; Roche *et al.*, 1994; Santee *et al.*, 1995). A recent example is plotted in Figure 7-3, showing sharp temperature-dependent shifts in Cl_y partitioning measured from the ER-2 in the Southern Hemisphere (Kawa *et al.*, 1997) that match the predicted rates for reactions (7-2)-(7-4) on liquid aerosols (see Figure 7-2). Likewise, analyses of field observations of midlatitude NO_x/NO_y ratios confirm the importance of N_2O_5 hydrolysis (reaction 7-1) on liquid sulfate aerosol in the lower stratosphere. This includes ER-2 (Gao *et al.*, 1997), balloon (Kondo *et al.*, 1997; Sen *et al.*, 1998), and UARS satellite (Morris *et al.*, 1997) observations. There are examples of models underpredicting NO_x levels, such as sunrise measurements at high southern

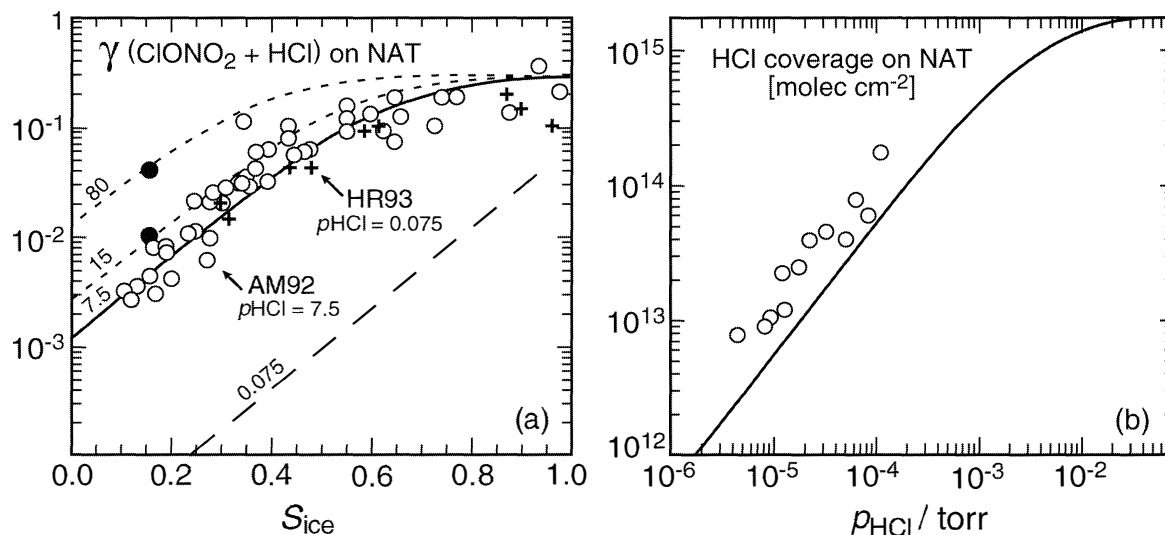


Figure 7-4. Left panel: Measured (from the data of Abbatt and Molina (1992) and from Hanson and Ravishankara (1993); see Carslaw and Peter (1997) for details) and calculated (by Carslaw and Peter) reactive uptake coefficients (γ) on NAT. Depending on the assumed surface coverage of HCl on NAT (S_{ice}), the calculated reactive uptake coefficients can be different by factors of 50 to 100 (see text). Right panel: Surface coverage of HCl on NAT as a function of the partial pressure of HCl measured by various investigators (see Carslaw and Peter (1997) for details). Adapted from Figure 2 of Carslaw and Peter (1997).

latitudes from ATMOS (Newchurch *et al.*, 1996; Rinsland *et al.*, 1996a), perhaps indicative of incomplete heterogeneous or gas phase chemistry.

On solid particles, characteristic of some PSCs or cirrus clouds in the lower stratosphere, uncertainties in reaction mechanisms are greater. Cl_y activation rates on solids are similar to those in liquids; in fact, when solid formation thresholds are included, temperature-dependent reactivity on solids is virtually indistinguishable from that on liquids shown in Figure 7-2 (Ravishankara and Hanson, 1996). Rate measurements on a variety of surfaces (NAT, NAD, SAT, ice) indicate Cl_y reactivity is somewhat slower than on liquids, with dependencies on relative humidity giving effective negative temperature dependencies (Ravishankara and Hanson, 1996).

Much of the uncertainty in reactivity on solids is associated with lack of knowledge of surface densities of reactants (Carslaw and Peter, 1997; Henson *et al.*, 1996), for which there are no good thermodynamic models, in contrast to gas condensation in liquids (see Section 7.2.2 and Figure 3-1). Uncertainties in fundamental quantities, such as surface area of solids prepared in the laboratory (e.g., see discussion of ice

structure in Kolb *et al.*, 1995), lead to contradictory data and interpretation concerning surface coverage of HCl and other gases (Chu *et al.*, 1993; Hanson and Ravishankara, 1992; Oppliger *et al.*, 1997). For example, a reinterpretation of reaction (7-3) on NAT surfaces (Carslaw *et al.*, 1997) is shown in Figure 7-4. Extrapolation of data obtained at higher HCl concentration by assuming a linear variation in surface coverage with HCl partial pressure and a rate of reaction that is proportional to HCl surface coverage gives an effective rate of reaction (7-3) that is 100 times slower than that measured at lower concentrations. However, it is not known if the surface coverage increases linearly with HCl partial pressure and if the rate of reaction of ClONO_2 on the surface increases linearly with HCl surface coverage. Some experiments clearly show that the rate of reaction (7-3) is nearly independent of HCl partial pressure (Hanson and Ravishankara, 1992). If reaction (7-3) on NAT were as slow as that shown in Figure 7-4, and if a significant fraction of the surface area is due to NAT, solid PSC formation would slow Cl_y activation (Carslaw and Peter, 1997).

Kinetic formulations on solid phases still require coupled models of chemical mechanisms and surface

LOWER STRATOSPHERIC PROCESSES

morphology. For example, though protonation of HOCl adsorbed in ice matrices has been observed (see, e.g., Banham *et al.*, 1995), such behavior is not quantified as with Henry's law solubility for liquids. Despite much discussion, there is little quantitative knowledge on the existence and role of quasi-liquid like layers (see Ravishankara (1997) and references therein), for example on ice in the presence of condensable vapors such as HCl and HNO₃. A recent example involves laboratory results indicating that at stratospheric concentrations of a few parts per billion by volume (ppbv), HNO₃ will completely coat ice (Abbatt, 1997; Zondlo *et al.*, 1997). Formulation of generalized mechanisms of surface coverage and reactivity that might include such HNO₃ surface coverage requires more information before quantitative application to stratospheric models will be feasible (Carslaw and Peter, 1997).

Other heterogeneous reaction pathways have been discussed in the literature. These include solubility and reactivity of formaldehyde (CH₂O) in acid solution (Iraci and Tolbert (1997) and references therein), solubility and reactivity of nitrous acid (HONO) in sulfuric acid (DeMore *et al.*, 1997; Seisel and Rossi, 1997; Longfellow *et al.*, 1998; and references therein), and formation of peroxy nitric acid (Zhang *et al.*, 1997). Recent studies have also reported fast rates for HOBr, BrONO₂, and HCl reacting on ice (Allanic *et al.*, 1997), but they are unlikely to be very important in the stratosphere. However, none of these studies appears to indicate a significant perturbation of stratospheric photochemistry, though the mechanisms still need better characterization to quantify their relevance in the stratosphere. For example, despite much interest, a heterogeneous pathway for reduction of HNO₃ has not been demonstrated (Chatfield, 1994). Another example is the potential reactivity of carbonaceous soot particles (Rogaski *et al.*, 1997; Wyslouzil *et al.*, 1994). Modeling studies have suggested significant effects of reactions on carbonaceous aerosol (Bekki, 1997; Lary *et al.*, 1997). It seems very unlikely that a particle that is reactive enough to reduce an oxidized species such as HNO₃ will remain reactive in an oxidizing stratosphere. Further, it is unlikely that such a particle will not be covered with condensables such as sulfuric acid and water. If the soot particle is destroyed in the reaction, in view of the low stratospheric density of soot particles, it is unlikely that they will lead to significant non-local effects in the stratosphere.

7.3 RADIATIVE-DYNAMICAL AND TRANSPORT PROCESSES

7.3.1 Large-Scale Temperature and Wind Distribution

The dynamical and radiative processes controlling the structure of the temperature and wind distribution in the lower stratosphere and its seasonal evolution are, broadly speaking, well understood. There remain some uncertainties over what balance of processes determines tropical temperature distributions and, by implication, tropical upwelling. The current troposphere-stratosphere general circulation models quantitatively differ from observations because there is still an insufficient understanding of how all these processes interact to determine the stratospheric climate (see Section 7.5.3). Small changes, or small uncertainties, in temperatures in the high latitudes and tropics will imply large changes, or large uncertainties, in chemical distributions.

Significant coupling exists between radiation, dynamics, and ozone abundance in the lower stratosphere. Temperatures affect photochemistry and the distribution of condensed matter. Ozone in turn affects temperatures through both longwave and shortwave radiative processes. Because of the Earth's rotation there is a strong constraint between temperatures and winds, particularly in the extratropics, which has direct implications for transport.

The lower boundary of the stratosphere, the tropopause, is generally characterized by a change in static stability, from relatively high values in the stratosphere to relatively low values in the troposphere. This definition has limitations, as discussed by Holton *et al.* (1995) for example, but is a useful starting point. The height of the tropopause varies from about 15 km in the tropics to about 7 km at high latitudes. The tropical tropopause, which corresponds roughly to an isentropic surface, appears to be consistent with formation by radiative-convective adjustment, with the height of the tropopause set by the top of the region of moist convection. The extratropical tropopause, on the other hand, slopes across a number of isentropic surfaces and is more plausibly formed through the action of baroclinic eddies (Holton *et al.* (1995) and references therein). These different formation mechanisms, and the strong latitudinal variation of the height of the tropopause, have implications for chemistry and transport in the lowest part of the stratosphere (see Section 7.3.4.1).

The temperature field in the stratosphere arises from a balance between radiative and dynamical heating (or cooling). Dynamical heating is caused by vertical (adiabatic) motion, which occurs partly in response to the annually varying distribution of solar radiation. However, a substantial part of the vertical motion occurs in response to forces arising from the breaking and dissipation of Rossby waves and gravity waves (e.g., Andrews *et al.*, 1987). In the extratropical stratosphere, the wave-induced forces are almost exclusively westward and act to drive air poleward, thus producing a meridional Brewer-Dobson circulation that is generally rising at low latitudes and sinking at high latitudes. The Brewer-Dobson circulation transports ozone poleward and downward from its photochemical production region into the extratropical lower stratosphere. It follows that variations in ozone transport are likely to be associated with variations in dynamical heating, with less transport corresponding to colder temperatures. This correlation is indeed seen in observations (e.g., Randel and Cobb, 1994).

The mechanism by which the meridional circulation is driven by breaking waves was termed the “extratropical pump” by Holton *et al.* (1995). However, extratropical wave driving cannot adequately explain the location of the tropical upwelling, which occurs throughout the year and maximizes on the summer side of the equator. This cannot be accomplished by “pumping” from the winter hemisphere alone, which would require air to cross angular momentum surfaces within the tropics. Plumb and Eluszkiewicz (1998) have suggested that forces within the tropics may be needed.

The extratropical lower stratosphere exhibits a strong seasonal cycle in temperatures, with coldest temperatures in winter. Although this is what one would expect from radiative considerations, the role of wave-driven vertical motion in modifying the temperature field is apparent from differences in the seasonal cycle between the hemispheres. The greater longitudinal asymmetry in surface conditions of the Northern Hemisphere, which is communicated up into the stratosphere by wave propagation, means that wave driving is stronger there. Since wave driving acts to increase temperatures in the extratropical lower stratosphere, the NH winter polar vortex is warmer (and hence also weaker) than the SH vortex. Indeed the NH vortex is often highly disturbed by strong dynamical events, called sudden warmings. These events tend to break up the vortex by early spring. In the SH, in contrast, the lower stratospheric vortex usually persists as a

coherent dynamical entity, with correspondingly cold temperatures, at least until mid to late spring. The stronger dynamical activity in the NH extratropical stratosphere leads to greater interannual variability of temperatures and circulation. This inherently limits predictability and attribution of ozone depletion (see Section 7.6.1).

The contrast between the NH and SH winter vortices illustrates the particularly strong effect of dynamical forcing on wintertime polar temperatures and vortex stability. Because polar ozone chemistry exhibits strong sensitivity to these meteorological conditions (see Section 7.6.1), this points to a mechanism by which long-term changes in dynamical forcing, associated with climate change, could affect stratospheric ozone — quite apart from changes in ozone transport that would also result from a change in dynamical forcing. That such a mechanism is potentially significant is illustrated by the climate simulation results of Shindell *et al.* (1998b), who find an altered dynamical forcing resulting from greenhouse-gas-induced climate change, which leads to a colder, more isolated Arctic vortex and hence a delayed ozone recovery (see Chapter 12).

The effects of dynamical forcing on stratospheric temperatures tend to cancel out in the global mean at any given altitude. This is because downwelling (and dynamical heating) in the extratropics must, by mass conservation, be compensated by upwelling (and dynamical cooling) in the tropics. It follows that global-mean temperatures are largely insensitive to dynamical variability compared to mean temperatures defined over the tropics or extratropics alone (Figure 7-5). Long-term changes in global-mean stratospheric temperatures, such as those in Figure 7-5, must therefore be associated with changes in radiative forcing; conversely, long-term changes in dynamical forcing should be manifested as compensating changes, of opposite sign, in tropical and extratropical temperatures.

The tropical lower stratosphere represents a local temperature minimum, a combined effect of deep tropical tropospheric convection and dynamical cooling associated with stratospheric upwelling (the ascending branch of the Brewer-Dobson circulation). Upwelling rates within the tropics have been estimated from diabatic circulation calculations based on satellite measurements (e.g., Rosenlof, 1995; Eluszkiewicz *et al.*, 1996) and indicate a large seasonal variation with the value during NH winter ($0.4 \times 10^{-3} \text{ m s}^{-1}$) being around 2 to 3 times that in NH summer ($0.15 - 0.2 \times 10^{-3} \text{ m s}^{-1}$). There are

LOWER STRATOSPHERIC PROCESSES

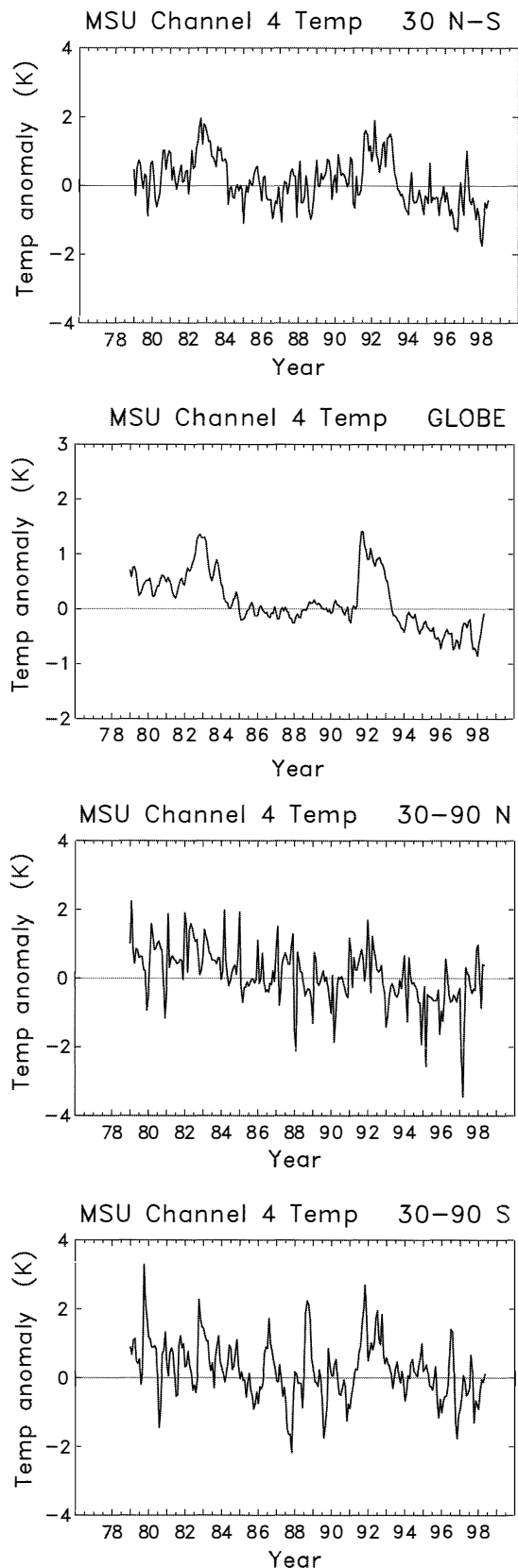


Figure 7-5. Time series of lower stratospheric temperatures measured by Microwave Sounding Unit (MSU) Channel 4, from which the annual cycle has been removed. Panel 1: tropical lower stratosphere. Panel 2: the same, but for globally averaged temperatures. The smaller variation in panel 2 shows the strong compensation between temperature variations in the tropics and extratropics, which variations are therefore presumably associated with the diabatic circulation (i.e., with dynamics). Exceptions are the strong signals from 1982 to 1984 and from 1991 to 1994, which are plausibly driven by heating effects associated with El Chichón and Mt. Pinatubo aerosol, and the long-term cooling, which has been attributed to decadal ozone depletion (see Chapter 5). Panels 3 and 4 are the lower stratospheric temperatures for northern and southern extratropics.

large uncertainties in the derived values, particularly near the tropical tropopause, although independent tracer observations (see Section 7.3.3.1) imply an upwelling rate in this region that is generally consistent with these values. The strength and seasonal cycle of this upwelling have important implications for understanding stratospheric water vapor (see Section 7.3.4.2).

Consistent with this seasonal cycle in tropical upwelling, tropical temperatures exhibit a weak but nonetheless clearly identifiable seasonal cycle, with coldest temperatures during NH winter. Early explanations for this cycle appealed to the seasonal cycle in tropospheric convection. It has recently been suggested by Yulaeva *et al.* (1994) that the seasonal cycle may be due instead to the seasonal cycle in extratropical wave driving, which is larger in the NH winter than in the SH winter for reasons stated earlier. Part of the evidence used by Yulaeva *et al.* (1994) is the observed compensation between tropical and extratropical temperatures. Recent studies (Holton *et al.*, 1995; Plumb and Eluszkiewicz, 1998) suggest that wave driving at subtropical or lower latitudes, perhaps together with the annual cycle of thermal forcing, is needed to account for the observed annual cycle in tropical temperatures.

The dominant component of interannual variability in tropical lower stratospheric temperatures is the quasi-biennial oscillation (QBO). It has long been recognized that the QBO is driven by wave momentum transport, but it remains unclear exactly which waves are involved

(see, e.g., Dunkerton, 1997). The role of Rossby waves has been particularly uncertain, though recent direct wind (Ortland, 1997) and constituent observations (O'Sullivan and Chen, 1996) have shown clear evidence of stratospheric Rossby waves radiating into the tropics when the QBO phase is westerly. In addition to the QBO, the observed interannual variability in extratropical wave driving might also, on the basis of the arguments of Yulaeva *et al.* (1994), be expected to affect interannual variability of tropical lower stratospheric temperatures. Certainly the extratropical compensation observed in the seasonal cycle is also seen in the interannual variation, suggesting that dynamical mechanisms account for much of this variation (Figure 7-5).

The influence of the QBO extends globally, particularly into the winter hemisphere. In general, the winter polar vortex is observed to be stronger and temperatures colder, with fewer sudden warmings in the NH, when the phase of the QBO in the lower stratosphere is westerly (Holton and Tan, 1980). As noted by Holton and Tan, this is plausibly due to the effect of tropical winds on the location of extratropical Rossby wave driving; when the tropical winds are westerly the wave driving occurs closer to the equator, and reduces descent (and therefore dynamical heating) over the pole. A recent study with the Geophysical Fluid Dynamics Laboratory (GFDL) "SKYHI" general circulation model, using an imposed forcing to create a QBO, reproduced this tropical-extratropical coupling and produced an extratropical QBO in NH winter in good agreement with observations (Hamilton, 1998).

The QBO is clearly evident in column ozone data, both in the tropics and extratropics (Bowman, 1989). The vertical structure in the tropics shows two cells, with a change of sign near 28 km altitude (Hasebe, 1994; Randel and Wu, 1996). Below 28 km, it appears that ozone is behaving as a tracer, so the QBO signal is a direct response to the QBO in tropical circulation; above 28 km, model studies indicate the link to be chemical, ozone at these altitudes responding to QBO transport of reactive nitrogen (Chipperfield *et al.*, 1994b). The extratropical QBO signal in (column) ozone is oppositely phased to the tropical signal, indicating that it is not caused by transport of the tropical ozone anomaly. Also, the midlatitude ozone QBO is seasonally synchronized (maximum in winter). The QBO effect on the location of extratropical wave driving mentioned above suggests the possibility of increased ozone transport by the Brewer-Dobson circulation during easterly QBO winters

(e.g., Tung and Yang, 1994; Hess and O'Sullivan, 1995). However, a recent study by Jones *et al.* (1998) suggests that wave-drag feedbacks are not needed, since the solstitial QBO-driven circulation is equatorially asymmetric (extending into the winter hemisphere).

An important new development in the quantitative study of stratospheric transport has been the use of data assimilation techniques to produce comprehensive global datasets of stratospheric temperatures and winds (Swinbank and O'Neill, 1994; Gelman *et al.*, 1994). These datasets have been the basis for a large number of papers on chemical transport over the last five years or so, including simulations of polar seasonal ozone depletion (see Sections 7.5.4 and 7.6.1). Manney *et al.* (1996) and Coy and Swinbank (1997) compare such datasets and note differences between them, as well as differences with radiosonde observations. Agreement is generally good, with the largest numerical disagreements tending to occur at the most dynamically active times, e.g., during sudden warmings. The global datasets tend to weaken vertical temperature gradients compared with individual high-resolution satellite instruments. There are also systematic differences in some cases between the global datasets and radiosonde ascents, especially over Antarctica (Manney *et al.*, 1996).

7.3.2 Global View of Transport and Mixing

Long-lived tracers are observed to have similar global distributions, whose morphology is controlled by the competing effects of diabatic advection and isentropic mixing. Many tracers exhibit compact relationships in the lower stratosphere, where their lifetimes are long. These relationships are understood theoretically in terms of stratospheric mixing and may differ between tropics and extratropics, and between the wintertime polar vortex and midlatitudes. Isentropic mixing is most intense within the midlatitude "surfzone" and weakest at its edges. Below about 16 km altitude, the vortex edge barrier disappears, and mixing reaches high latitudes. In this region, known as the "lowermost stratosphere," isentropic surfaces are no longer confined to the stratosphere but intersect the midlatitude tropopause, and rapid isentropic mixing with the troposphere is possible.

Since Jones and Pyle (1984) noted the similar meridional distributions of N₂O and CH₄ in Limb Infrared Monitor of the Stratosphere (LIMS) observations of the

LOWER STRATOSPHERIC PROCESSES

stratosphere, it has been recognized that long-lived stratospheric constituent mixing ratios display similar structures. The characteristic observed structure is illustrated in Figure 6-3 of Chapter 6 of this Assessment. For a tracer of tropospheric origin, high concentrations are found in the tropics, corresponding to “young” air (see Section 7.3.3.1 for a discussion of “age”); there are regions of strong gradients in the subtropics, weak gradients in midlatitudes and, in winter, strong gradients at the edge of the polar vortex, within which the oldest air, low in tropospheric source gases, is found.

Holton (1986) and Mahlman *et al.* (1986) explained the slopes of zonal-mean tracer contours as a balance between the slope-steepening effects of the diabatic circulation and the slope-flattening effects of mixing, resulting in a characteristic poleward-downward slope of such contours that is determined by transport alone, and so is the same for all sufficiently long-lived species. Plumb and Ko (1992) showed that these same arguments explained the observations of compact relationships between different long-lived species (e.g., Fahey *et al.*, 1990; Murphy *et al.*, 1993), provided mixing is sufficiently fast. (True compactness can be achieved only when mixing is infinitely fast, and so is never

achieved in reality.) The characteristics of the tracer-tracer relationships have been used to determine net global fluxes (Murphy and Fahey, 1994), lifetimes (Volk *et al.*, 1997; see Section 7.3.3.1), and mixing rates (see Section 7.3.3.3).

The classical picture of the Brewer-Dobson circulation has been significantly refined in recent years. The phenomenology of stratospheric transport and mixing reveals a number of distinct regions, depicted in Figure 7-6. Evolution of wintertime stratospheric potential vorticity (PV) maps indicates a contrast between the “surf zone” of midlatitudes, stirred by breaking of the dominant quasi-stationary Rossby waves, and the relatively undisturbed polar vortex (McIntyre and Palmer, 1983). High-resolution modeling results show that the wave-breaking process is associated with erosion of the vortex through detrainment of air from the vortex edge, thus sharpening the edge (Jukes and McIntyre, 1987). This air is typically stretched out into filaments, as seen clearly in high-resolution transport calculations and inferred from aircraft observations (e.g., Waugh *et al.*, 1994; Newman *et al.*, 1996). Although there are occasional events in which small amounts of midlatitude air are injected into the vortex (Plumb *et al.*, 1994),

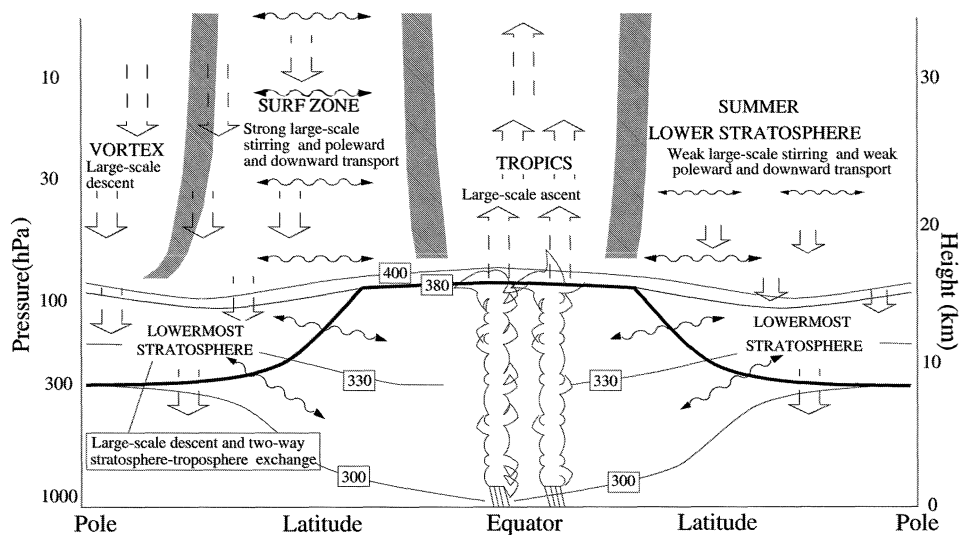


Figure 7-6. Schematic of the principal regions of the lower stratosphere with distinct transport characteristics. Broad arrows denote the diabatic circulation, wavy arrows denote stirring along isentropic surfaces. The thick solid line starting at about 7 km at the pole and ending at about 15 km at the equator is the tropopause, i.e., the notional boundary between troposphere below and stratosphere above. Isentropic surfaces (300K, 330K, 380K, and 400K) are drawn as thin solid lines in the troposphere and lower stratosphere. Isentropic surfaces in the remainder of the stratosphere may be assumed to be roughly horizontal. See text for further discussion.

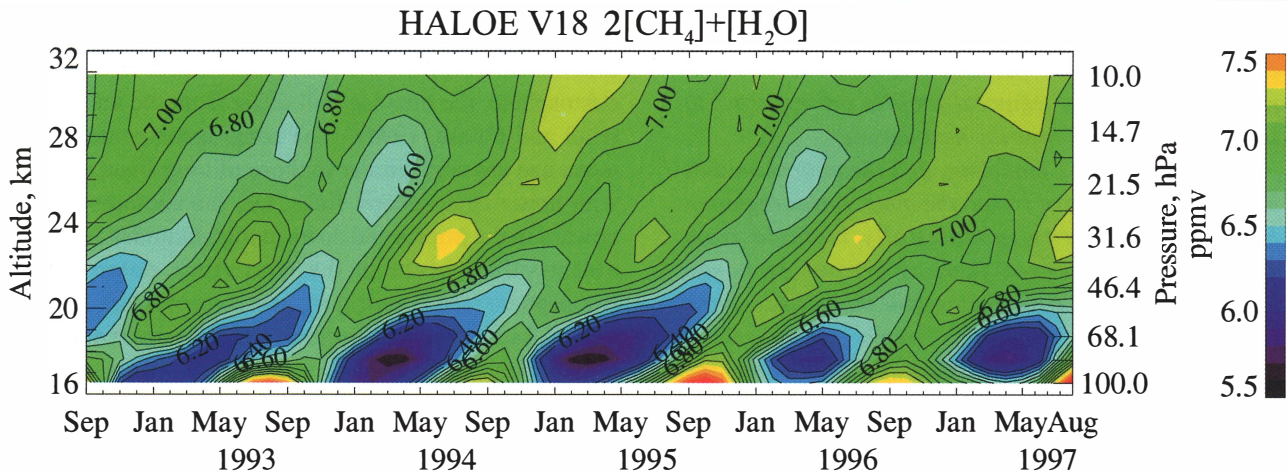


Figure 7-7. Height-time section of the quantity $2\text{CH}_4 + \text{H}_2\text{O}$ (the variable part of total hydrogen) between 12°S and 12°N , derived from HALOE data from Mote *et al.* (1998).

particularly in the NH, the vortex itself is less disturbed than the “surf zone,” and the inner regions of the vortex are substantially isolated from midlatitudes (see Section 7.3.3.2). In situ data from ER-2 transects often show extremely sharp gradients of tracers close to the vortex edge (e.g., Schoeberl *et al.*, 1992).

McIntyre (1990) suggested on dynamical grounds that the surf zone also possesses a subtropical edge, isolating the tropics from surf zone stirring. Such a supposition is supported by observations of a “tropical stratospheric reservoir” of aerosols from tropical volcanic eruptions (Dyer and Hicks, 1968; Grant *et al.*, 1996) and of material from nuclear bomb tests (Feely and Spar, 1960); of strong subtropical tracer gradients (Randel *et al.*, 1993; Tuck *et al.*, 1997); of different tracer relationships between tropical and midlatitude air (Murphy *et al.*, 1993; Plumb, 1996; Volk *et al.*, 1996); and of the relatively undiluted ascent within the tropics of the “tape recorder” signal of the annual cycle of water vapor (Mote *et al.*, 1996) (see Figure 7-7). Erosion processes, similar to those seen at the vortex edge, are evident in high resolution transport calculations based on observed winds (Chen *et al.*, 1994; Waugh, 1996) and in dynamical models (Norton, 1994; Polvani *et al.*, 1995; O’Sullivan, 1997).

The location of the tropical reservoir and the gradients at its edge exhibit a seasonal variation, with the center in the summer hemisphere and steeper gradients during winter (Randel *et al.*, 1993; Grant *et al.*, 1996). This variation is consistent with the seasonal variation in upwelling discussed earlier, together with

the seasonal variation in Rossby wave breaking: there is stronger wave breaking during winter and this produces a wider surf zone and increased transport away from the tropical edge, producing steeper gradients (Waugh, 1996). The seasonal variation in location of the tropical reservoir increases with altitude, and there is also a significant influence from the QBO (Randel *et al.*, 1998).

Because diabatic transport is so slow in the stratosphere, there is an important dynamical distinction between isentropic surfaces that lie entirely within the stratosphere, and those that intersect the midlatitude tropopause. Holton *et al.* (1995) refer to the region containing the latter, where there may be rapid isentropic exchange with the troposphere, as the “lowermost stratosphere” (see Section 7.3.4.1). Thus, in contrast to the region above, the lowermost stratosphere is bounded on its equatorward side by the tropopause, rather than by the tropical stratosphere. It seems that the distinct vortex/surf zone separation does not exist within the lowermost stratosphere (see Section 7.3.3.2), although why this should be the case is not well understood.

7.3.3 Quantification of Transport and Mixing

The time lag between tropospheric and stratospheric concentrations of time-varying species is a probability distribution of transit times. The time lag of a conserved tracer with linear trend is equal to the mean of this probability distribution (the so-called “mean age”), but the time lag for tracers with nonlinear time dependence or loss processes differs from the mean age.

LOWER STRATOSPHERIC PROCESSES

Mean age may not be appropriate for dealing with chlorofluorocarbons (CFCs) and short-lived CFC replacements whose temporal profiles are expected to be highly nonlinear over the next decade.

Observational, modeling, and theoretical studies all indicate that above 16 km, the inner vortex region in both hemispheres is substantially isolated from midlatitudes. However, there is greater exchange between the vortex edge region and midlatitudes, and below 16 km (the “sub-vortex” region). Analysis of tracer observations shows that the time scale for entrainment into the tropics is around 15 months in the lowest few kilometers of the stratosphere. This entrainment rate is much weaker than both the detrainment rate from the tropics and the mixing rates within the surf zone.

In the surfzone, air drawn out of the polar vortex or the tropics is stirred by the large-scale flow, leading to the formation of filaments and laminae in chemical tracer fields. Analysis of high-resolution aircraft tracer data suggests that, in some average sense, air is well mixed on vertical scales of about 50 m and horizontal scales of about 10 km. It follows that for typical surf-zone stretching rates, filaments of polar or tropical air will survive for about 20-25 days before they become mixed with their surroundings.

7.3.3.1 TRANSPORT TIME SCALES

Tropospheric concentrations of many long-lived trace gases vary with time, and there is a time lag between these concentrations and those in the stratosphere. Determining these time lags is crucial for calculating the concentrations of many species, and especially the available inorganic chlorine and hence the potentially active chlorine.

If the diabatic circulation alone was responsible for transport, then there would be a single pathway and “transit” time for transport from the tropopause to a given location in the stratosphere, and the time lag in concentration would be the same for all species. However, because of mixing within the stratosphere, air parcels comprise many components with different transport histories and there is not a single transit time; rather, there is a probability distribution of transit times, known as the “age spectrum” (Kida, 1983).

The mean of the probability distribution is the “mean age” (Hall and Plumb, 1994). The mean age is equivalent to the time lag in concentration only for a

conserved tracer with linear trend; if the time dependence is nonlinear or if there are chemical loss processes in the stratosphere, the time lag will differ from the mean age (Hall and Plumb, 1994). The zonal-mean contours of mean age are very similar to those of long-lived tracers with upper stratospheric sinks, i.e., the contours bulge upward in the tropics and down at high latitudes, and the oldest values occur in the wintertime polar upper stratosphere (see Figure 7-8a, and compare with Figure 6-3 of Chapter 6 of this Assessment). Note that the spatial distribution of mean age is very different from what it would be if air were transported only by the diabatic circulation; in the latter case, the oldest air would be found in the polar lower stratosphere (Rosenlof, 1995).

The mean age has been estimated from measurements of several different tracers with approximately linear trends, e.g., sulfur hexafluoride (SF_6) (Harnisch *et al.*, 1996; Waugh *et al.*, 1997b; Volk *et al.*, 1997), CO_2 (Bischof *et al.*, 1985; Schmidt and Khedim, 1991; Boering *et al.*, 1996), CFC-115 (CClF_2CF_3) (Pollock *et al.*, 1992; Daniel *et al.*, 1996), and hydrogen fluoride (HF) (Russell *et al.*, 1996). Note that although CO_2 has an approximately linear trend, it also has a strong seasonal variation, which complicates calculations of the mean age (Hall and Prather, 1995). Also chemical loss processes in the upper stratosphere affect estimates of mean age from CFC-115. Results from the above studies show that the mean age (relative to the tropical tropopause) at 20 km varies from around 1 year in the tropics to 4 to 6 years at high latitudes (see examples given in Figure 7-8b), and at 30 km it varies from 4 to 5 years in the subtropics to 7 to 9 years at high latitudes. In general, both 2-D and 3-D model results vary widely and have difficulty reproducing these numbers.

The time scale for vertical propagation within the tropical stratosphere has been derived from measurements of both H_2O (Hintsa *et al.*, 1994; Mote *et al.*, 1996; Weinstock *et al.*, 1995) and CO_2 (Boering *et al.*, 1996). These calculations yield similar time scales, which are broadly consistent with ascent rates derived from diabatic circulation calculations based on satellite measurements, with more rapid ascent during northern winter than northern summer (see Section 7.3.1). Note that although model calculations suggest that the rate of propagation of the annual signal will be close to the diabatic vertical velocity, it is not clear that there should be exact agreement (Waugh *et al.*, 1997b).

Modeling studies indicate that the age spectrum is generally broad and asymmetric (Kida, 1983; Hall and

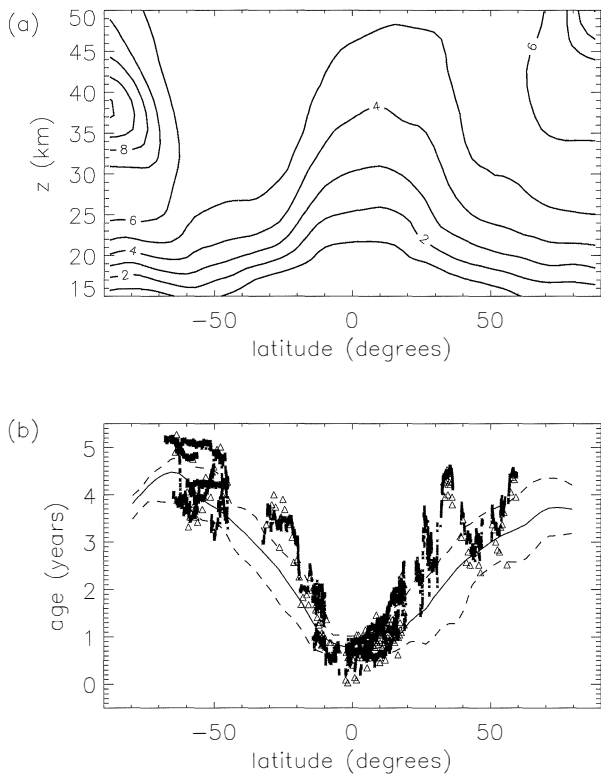


Figure 7-8. Mean age relative to the tropical tropopause as determined from a 3-D chemical transport model and from measurements. (a) Altitude-latitude contour plot of mean age for the zonal mean in October, as determined from a model calculation of a linearly increasing conserved tracer. Contours are for 1.0, 2.0, ..., 10.0 years. (b) Latitudinal variation of mean age at 20 km in October. The solid curve is the zonal-mean model value, while dashed curves are the minimum and maximum values around a latitude circle at this altitude. The symbols are mean age derived from aircraft measurements of SF₆ (triangles) and CO₂ (solid squares) from October and November 1994 (Boering *et al.*, 1996; Volk *et al.*, 1997). Note that the good agreement between the above model and data is not generally true; the modeled mean ages are younger than observed for most other models. Adapted from Waugh *et al.* (1997b).

Plumb, 1994; Hall and Waugh, 1997a) (see Figure 7-9) with the mean age much older than both the most likely transit time and the propagation time of an annually repeating tracer. It is only within the lower tropical stratosphere, where the age spectra are strongly peaked, that these various times are approximately equal.

The mean age has been used to account for the temporal variation in tropospheric concentrations when determining stratospheric halogen budgets from source gas measurements (see Section 7.5.1) and when using these tracers in tracer-tracer correlation studies (e.g., Vohralik *et al.*, 1998; Volk *et al.*, 1997). However the nonlinear growth and chemical losses of these species may affect these calculations. This effect may be significant over the next decade when the time trends in CFCs and short-lived CFC replacements are expected to be highly nonlinear (see Chapter 1).

A different class of transport time scale to the above is the time for transport out of the stratosphere from a given location. These time scales are important for understanding, for example, the impact of aircraft emissions and volcanic aerosols on stratospheric ozone. Several 2-D and 3-D modeling studies have calculated the mean lifetime (residence time) of aircraft emissions

(e.g., Weaver *et al.*, 1996; Schoeberl *et al.*, 1998). The calculated lifetimes vary from one to three years, with 3-D models generally yielding shorter lifetimes than 2-D models. As with transport into the stratosphere, there will be a probability distribution of (residence) times for transport out of the stratosphere, but the characteristics of this probability distribution have not been examined.

7.3.3.2 EXCHANGE TIME SCALES

As discussed in Section 7.3.2, there exist polar and tropical “reservoirs” in the lower and middle stratosphere, with weak exchange between these reservoirs and the midlatitude surf zone. Rates of exchange across the edges of these reservoirs play an important role in determining the global distribution of ozone and ozone-related species. This has long been recognized for the winter polar vortices. In the tropics, the impact is primarily on troposphere-stratosphere time lags and stratospheric residence times.

There is an extensive body of research into the rate of transport into and out of the polar vortices. A difficulty when comparing these studies is the different definitions of vortex edge that have been used (such as the wind

LOWER STRATOSPHERIC PROCESSES

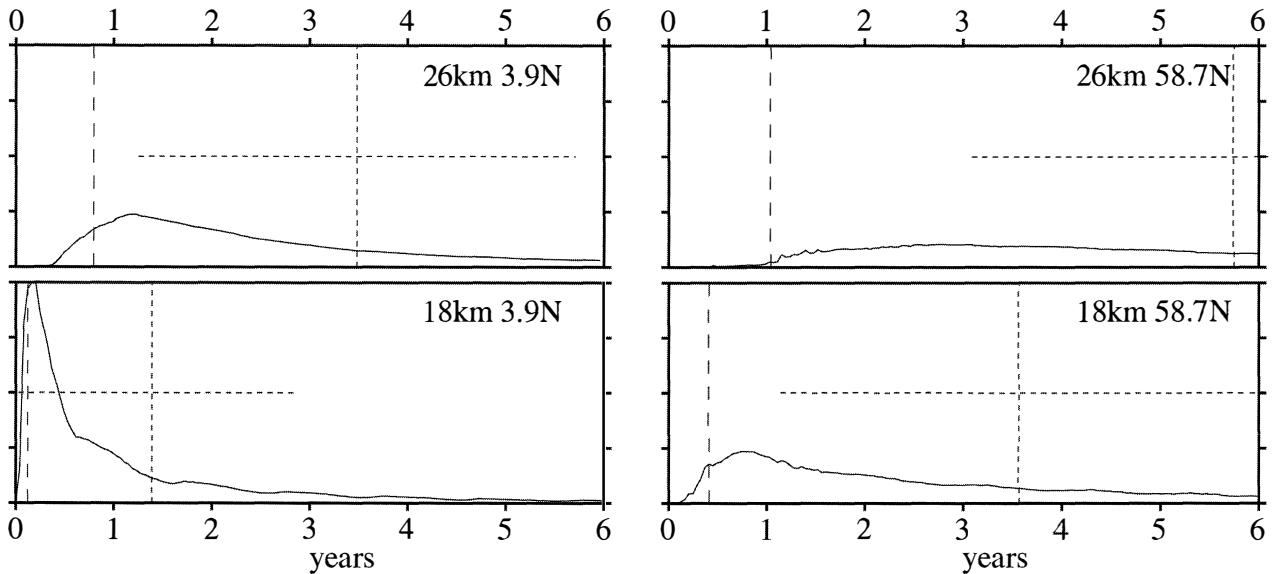


Figure 7-9. Modeled zonal-mean age spectra at latitudes 3.9°N and 58.7°N and altitudes 18 km and 26 km. The dotted vertical line is the mean age, the dotted horizontal line represents the width of the spectrum, and the dashed vertical line is the phase propagation time of an annual cycle. The mean age values differ from Figure 7-8 because the age spectra shown are relative to a surface point (resulting, for this model, in an offset of about 1 year) and represent annually averaged values. From Hall and Waugh (1997a).

maxima, maximum gradients in PV or tracers, or minima in stretching rates), as well as different techniques used to quantify the irreversible transport (e.g., Sobel *et al.*, 1997). High-resolution trace constituent observations and numerical simulations frequently show multiple fine-scale (filamentary) structures near the polar jet (e.g., Tuck *et al.*, 1992; Waugh *et al.*, 1994), indicating that it is more appropriate to consider a finite-width “vortex edge region” than a single, sharp vortex edge. This vortex edge region encloses the above definitions of the vortex edge and surrounds the so-called “inner vortex.”

Recent observational, modeling, and theoretical studies (e.g., Dahlberg and Bowman, 1995; Wauben *et al.*, 1997; Rosenlof *et al.*, 1997; Waugh *et al.*, 1997a) confirm the view of the previous Assessment (WMO, 1995) that during winter, the inner vortex region of both vortices is substantially isolated from midlatitudes above about 16 km (potential temperature 400 K). These studies also indicate that there is much greater exchange between the vortex edge region and the surroundings, and between polar regions and midlatitudes below 16 km. Exchange in either region may affect ozone loss through chemical processing. However, representing exchange in these regions by a single number is misleading, because calculations based on different choices of control surface

give substantially different rates of exchange.

From the point of view of understanding midlatitude ozone depletion, a more relevant quantity than total transport out of the edge region is the transport of “perturbed” air into midlatitudes. Such transport requires both cold vortex temperatures and a disturbed vortex; these two requirements are seldom met simultaneously, for reasons explained in Section 7.3.1, the exception being during strong anticyclonic blocking events. Transport of perturbed air has been quantified for three NH winters by Norton and Chipperfield (1995) using a high-resolution transport model driven by analyzed winds. Their calculations show large inter-annual and vertical variability, reflecting the inherent variability of the wave driving (Figure 7-10). Large transport of perturbed air into midlatitudes occurred in 1991/1992 during which there was a strong blocking anticyclone over Europe during mid to late January (e.g., Plumb *et al.*, 1994). Transport during the subsequent two winters was much smaller; in 1992/1993 there was a cold, undisturbed vortex with a large amount of processing but little transport into midlatitudes, while in 1993/1994 the vortex was warmer and more disturbed, with more transport but less processing.

A similar analysis of the transport of perturbed air

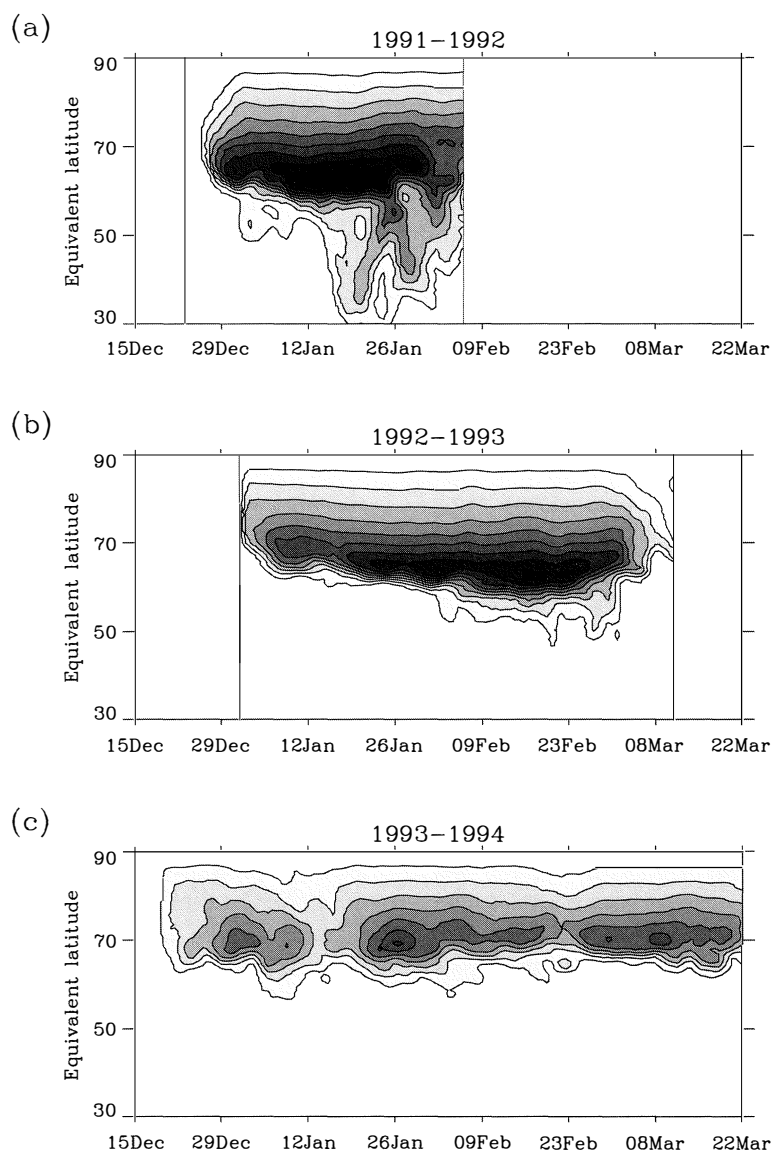


Figure 7-10. Temporal evolution of mass of perturbed air (kg) per unit equivalent latitude per unit potential temperature at 475 K as a function of time for (a) 1991-1992, (b) 1992-1993, and (c) 1993-1994 Northern Hemisphere winters. Contour interval is 4.9×10^{13} , with darker shading indicating greater amounts. From Norton and Chipperfield (1995).

into southern midlatitudes has not been performed. However the Antarctic vortex is always colder and less disturbed than the Arctic vortex. Of the three winters shown in Figure 7-10, the Arctic vortex during 1992/1993 is most like the Antarctic vortex, with large areas of processed air but little transport into midlatitudes.

Although there is strong evidence for larger meridional transport, in both hemispheres, between polar regions and midlatitudes below 16 km (e.g., Tuck, 1989;

Chen, 1994; McIntyre, 1995), the amount of transported air has not been fully quantified. Transport calculations for northern winter 1992/1993 indicate that the amount of perturbed air transported at 350 K was around 50% of the mass of midlatitudes (and around 5 times that at 475 K) (Norton and Chipperfield, 1995). However, similar calculations have not been performed for other northern winters or for the Southern Hemisphere. Until the transport of perturbed air in this region is better

LOWER STRATOSPHERIC PROCESSES

understood, it will be difficult to obtain a quantitative understanding of midlatitude ozone depletion (see Section 7.6.2).

Comparatively less is known about exchange rates across the edge of the tropical reservoir. However, recent trace gas measurements within the tropics have resulted in significant advances in our understanding of the transport within this region. Using ascent rates from radiative calculations together with a steady mass balance assumption, Volk *et al.* (1996) estimate a time scale of less than 6 months for detrainment from the tropics in the lower stratosphere. This detrainment time scale is broadly consistent with the rapid propagation of CO₂ and H₂O cycles into midlatitudes (Boering *et al.*, 1994) and with transport rates derived from calculations using analyzed winds (Chen *et al.*, 1994; Waugh, 1996). These latter studies indicate that there are large vertical and seasonal variations in transport, with enhanced transport near the tropopause and during winter months when westerlies exist in midlatitudes. These features are corroborated by measured aerosol distributions (Grant *et al.*, 1996).

Because of large uncertainties in analyzed tropical winds, it is not possible to examine reliably the transport into the tropics (and hence the isolation of the tropics) using transport calculations driven by these winds (Waugh, 1996). However, there have been several studies that have used (limited) measurements of trace constituents within the tropics to examine this isolation issue (e.g., Avallone and Prather, 1996; Minschwaner *et al.*, 1996; Volk *et al.*, 1996; Mote *et al.*, 1996; Schoeberl *et al.*, 1997; Hall and Waugh, 1997b; Tuck *et al.*, 1997). These studies indicate that the tropics are not totally isolated and that in the lower stratosphere, the time scale for mixing into the tropics is around 11 to 15 months (and around 30 to 60% of air at 20 km in the tropics is of midlatitude origin). Using high vertical resolution Halogen Occultation Experiment (HALOE) H₂O and CH₄ data, Mote *et al.* (1998) estimate the vertical profiles of the entrainment rate and find that the rate is much slower between 19 and 23 km (several years) than above or below (less than two years).

7.3.3.3 MIXING TIME SCALES

As noted in Section 7.3.2, intermittent erosion events transport air out of the tropics, or out of the vortex, into the surf zone, or vice versa. Such filaments ultimately mix with their surroundings, creating a

homogeneous air mass. Understanding how the mixing process occurs is important for quantitatively assessing the impact of perturbed air on ozone. Some chemical implications of mixing are discussed later in Section 7.4.1.2. Here we focus on the process of mixing itself.

Stretching is important as a route to genuine molecular mixing, by increasing spatial gradients and thereby reducing time scales for molecular diffusion. Estimates of stretching rates have been calculated from observed wind fields by various techniques (Pierrehumbert, 1991; Bowman, 1993; Chen, 1994; Waugh *et al.*, 1994) and confirm the midlatitude surf zones in both hemispheres as regions of large stretching rates, typically 0.1-0.2 day⁻¹. Haynes and Anglade (1997) showed that in simple stretching flows with vertical shear, horizontal and vertical tracer gradients tend to increase exponentially with time at the same rate. For the surf zone in the lower stratosphere, they estimated the aspect ratio of vertical to horizontal gradients to be about 250. The decreases in vertical scale are, therefore, potentially far more important for mixing than the decreases in horizontal scale (e.g., Jukes and McIntyre, 1987).

Features with small vertical scales are routinely observed in tracer profiles obtained from ozonesondes (Dobson, 1973; Reid and Vaughan, 1991), aircraft measurements (Murphy *et al.*, 1989), and lidar (Reid *et al.*, 1993; Orsolini *et al.*, 1997). Although some of these features may be associated with inertia-gravity waves (e.g., Teitelbaum *et al.*, 1996), recent high-resolution transport calculations have shown that quasi-horizontal advection alone, as described above, can lead to tracer features with vertical structures that are in qualitative and in some cases quantitative agreement with those observed (Newman *et al.*, 1996; Orsolini *et al.*, 1997). Appenzeller and Holton (1997) noted that formation of tracer laminae depends not only on vertical shear, but also on pre-existing horizontal tracer gradients on which quasi-horizontal advection can act. They estimated climatological tracer lamination rates using large-scale tracer observations and found large values associated with the vortex edge, in the lowermost stratosphere, and in the subtropical lower stratosphere.

The effect of molecular diffusion may be enhanced by shallow patches of three-dimensional turbulence, triggered by breaking inertia-gravity waves (Dewan, 1981). Dewan argued that the transport due to encounters of fluid elements with such turbulent patches may be represented by an eddy diffusivity. Using Dewan's ideas, Woodman and Rastogi (1984) have estimated the relevant

vertical diffusivity to be about $0.2 \text{ m}^2 \text{ s}^{-1}$ from radar observations of turbulence. More conventionally, radar observations are used to deduce eddy diffusivities appropriate to turbulent transport within the patches. For example, Fukao *et al.* (1994) estimated such diffusivities to take annual average values of about $0.5 \text{ m}^2 \text{ s}^{-1}$ at 20 km.

Waugh *et al.* (1997a) used aircraft measurements of two different tracers to identify filaments of partially mixed air. They used a simple advective-diffusive model together with information on horizontal stretching rates to infer an effective horizontal diffusivity of about $10^3 \text{ m}^2 \text{ s}^{-1}$. Taking an aspect ratio of 250 then implies a vertical diffusivity of about $0.015 \text{ m}^2 \text{ s}^{-1}$. Balluch and Haynes (1997) deduced a vertical diffusivity more directly from the Waugh *et al.* case and obtained a similar value. The disagreement between these tracer-based estimates of vertical diffusivity and the estimates from radar observations quoted earlier suggests that the radar estimates are not directly relevant to net vertical mixing of tracers. Any meaningful comparison between the values inferred by the two methods must involve a calculation that properly takes account of the spatial and temporal intermittency of the turbulent patches.

The tracer-based diffusivities suggest that air is well mixed on vertical scales of about 50 m and horizontal scales of about 10 km. Taking account of typical stretching rates calculated for the surf zone, this suggests that filaments of polar or tropical air starting, say, at horizontal scales of a few thousand km would survive for about 20-25 days before they become mixed with their surroundings.

The hypothesis that small-scale tracer structure arises from advection by the large-scale flow can be tested by its consistency with various quantitative diagnostics of the small-scale structure. One such diagnostic, the horizontal spatial power spectrum, has been calculated from aircraft data by Strahan and Mahlman (1994) and Bacmeister *et al.* (1996). Both calculations show evidence of a power-law scaling down to the smallest horizontal scales resolved by the data (a few km). There is no evidence of a diffusive cut-off and this by itself is an indication of the limitations of representing mixing by an effective horizontal diffusivity. Ngan and Shepherd (1997) have argued that the approximately inverse-square power-law scaling found in the data is consistent with the existence of a small number of isolated sharp transitions such as those associated with a filamented vortex edge.

The effects of mixing processes in the tropics have also been quantified to some extent. Using estimates of the amplitude and propagation of the H_2O cycle together with estimates of the mean age, Hall and Waugh (1997b) obtained a best estimate of $0.01 \text{ m}^2 \text{ s}^{-1}$ for the vertical diffusivity in the tropical lower stratosphere. Using a different analysis technique, Mote *et al.* (1998) solved for a vertical profile of diffusivity and found large vertical variations, with the estimated diffusivity being larger above 24 km ($\sim 0.1 \text{ m}^2 \text{ s}^{-1}$) than below (~ 0.02 to $0.04 \text{ m}^2 \text{ s}^{-1}$). Whilst the inferred diffusivities may result from large-scale diabatic dispersion (Sparling *et al.*, 1997), as well as from small-scale vertical mixing processes such as gravity-wave induced turbulence, they certainly give upper bounds on the strength of the latter.

7.3.4 Stratosphere-Troposphere Transport and Exchange

The distribution of ozone and other tracers in the lowermost stratosphere, below about the 380 K isentropic surface, is affected by descent from the part of the stratosphere directly above and by quasi-horizontal mixing in of air from the troposphere. Chemical measurements in the lowermost stratosphere have confirmed the importance of the latter process. In a time average, transport from the lowermost stratosphere to the troposphere is equal to the diabatic transport across the upper boundary of the lowermost stratosphere and is hence controlled by wave driving in the stratosphere. However, there are significant differences between the seasonal variation of the transport into the lowermost stratosphere from above and the transport across the tropopause, with the former, in the NH, maximizing in midwinter and the latter maximizing in late spring.

The transport of tropospheric air into the stratosphere through the cold tropical tropopause may, in principle, involve small-scale processes such as penetrative cumulus convection. However, the transport may well be dominated by large-scale upwelling. Tropical dehydration depends on the minimum temperature experienced by air parcels and how ice crystals fall out. Cloud-scale processes, including microphysics, may be particularly important here.

There are strong chemical contrasts between the troposphere and the stratosphere, e.g., in values of mixing ratios of water vapor or ozone. The troposphere and stratosphere have often therefore been regarded as

LOWER STRATOSPHERIC PROCESSES

distinct air masses. The subject of transport and exchange between the stratosphere and troposphere, often abbreviated to stratosphere-troposphere exchange (STE), has been reviewed recently by Holton *et al.* (1995). As emphasized there, STE processes in the extratropical lowermost stratosphere and in the tropics are quite distinct, essentially because of the different character of the tropopause in the two regions (Figure 7-6).

7.3.4.1 LOWERMOST STRATOSPHERE

STE has important implications for chemical distributions, including that of ozone, in the lowermost stratosphere. It has also historically been regarded as a major source of ozone for the upper troposphere.

The extratropical tropopause slopes upward and equatorward relative to isentropic surfaces. Exchange between troposphere and lowermost stratosphere can therefore occur through adiabatic advection along isentropic surfaces, as well as through diabatic advection across isentropic surfaces. Indeed some exchange may be viewed as resulting from filamentation of the tropopause, in much the same way that exchange in the winter stratosphere between polar vortex and surf zone results from filamentation of the vortex edge.

Studies of midlatitude STE have traditionally focused on the exchange from lowermost stratosphere to troposphere associated with "tropopause fold" structures (see Holton *et al.* (1995) and references therein). However there is also significant midlatitude exchange from troposphere to stratosphere. Appenzeller *et al.* (1996a) emphasize filaments of stratospheric air being drawn into the troposphere in their study based on Meteosat water vapor and PV together with high-resolution transport calculations, but also note the possibility of engulfment of tropospheric air into the stratosphere (see also Peters and Waugh, 1996). Vaughan and Timmis (1998) use a combination of PV fields, ozonesonde data, and trajectory studies to argue for a substantial troposphere-to-stratosphere exchange event in the NH in January. Troposphere-to-stratosphere exchange has also been considered by Chen (1995) using a transport model driven by observed winds on isentropic surfaces. Chen showed that such exchange occurs through filamentary structures being drawn poleward, e.g., in association with anticyclonic circulations in the upper troposphere.

Irreversible exchange of filaments of tropospheric air into the stratosphere is likely to be a two-stage process.

Dobson (1973) noted that filaments of air moved poleward from the subtropical troposphere would lose memory of their tropospheric temperature structure (and, we would now say, their tropospheric PV) before losing memory of, e.g., their tropospheric values of ozone mixing ratio, and gave observational evidence to support this idea. Haynes and Ward (1993) provided theoretical support for this idea by showing that radiative processes will generally erase the PV signature of a stretching filament before chemical mixing occurs. One might therefore expect to see filaments of "fossil" tropospheric air, with stratospheric PV but tropospheric values of tracer mixing ratios, in the lowermost stratosphere. Folkens and Appenzeller (1996) noted the occurrence of filaments in the lowermost stratosphere that were stratospheric in their PV values, but had values of ozone and N₂O that were consistent with direct transport from the troposphere. Ultimately, of course, these tracer filaments will be mixed into the lowermost stratosphere by the sort of processes described in Section 7.3.3.3.

There have also been studies based purely on observed chemical tracers that argue for direct exchange from troposphere to stratosphere. Kritz *et al.* (1991) showed evidence for such exchange using relatively low values of Be⁷ as an indicator of tropospheric air. Dessler *et al.* (1995b) inferred indirectly from aircraft water vapor observations that some air must enter the lowermost stratosphere directly from the troposphere, rather than passing through the tropical "cold trap" (see also Tuck *et al.*, 1997). A larger-scale picture of the water vapor distribution in the lowermost stratosphere has been obtained from satellite data by Pan *et al.* (1997), confirming that the mixing ratios are too large for all air in this region to have descended from the stratospheric overworld. Pan *et al.* also show that the lowermost stratosphere in both hemispheres is moister in the summer than in the winter and that the NH is moister than the SH. This is consistent with the seasonal behavior of exchange, and the interhemispheric differences between exchange, found by Chen (1995).

The rate of exchange from lowermost stratosphere to troposphere depends at first sight on small-scale processes such as tropopause folding occurring at the tropopause itself. However, in the time average, the mass flux across the extratropical tropopause must be equal to that across the upper boundary of the lowermost stratosphere, i.e., to the diabatic descent and, hence, as noted in Section 7.3.1, to the wave driving in the stratosphere (e.g., Haynes *et al.*, 1991; Holton *et al.*,

1995). The same must be true of the corresponding fluxes of chemical tracers that are conservative in the lowermost stratosphere. This fact was used by Gettelman *et al.* (1997) to estimate the annual average flux of ozone from the stratosphere into the troposphere. They utilized monthly mean satellite observed ozone mixing ratios and diabatic vertical velocities deduced from satellite data to compute the net ozone flux across the upper boundary of the lowermost stratosphere. In the annual mean this must approximately equal the net flux of ozone from the stratosphere into the troposphere since the chemical lifetime of ozone is very long in the lowermost stratosphere. The estimated flux of 510 Tg ozone per year agrees well with several independent estimates (e.g., Murphy and Fahey, 1994).

Although the mass fluxes into and out of the lowermost stratosphere must balance in a time average, there is no reason why the seasonal variation of the two mass fluxes should be the same, since any difference can be taken up as a temporary change in the mass of the lowermost stratosphere. Appenzeller *et al.* (1996b) have inferred the time series of mass flux across the extratropical tropopause by calculating the difference between the mass flux through the upper boundary of the lowermost stratosphere and the rate of change of the mass of the lowermost stratosphere. They find that the flux across the upper boundary of the lowermost stratosphere in the NH maximizes in midwinter (consistent with the expected variation of the wave driving), but the flux across the extratropical tropopause maximizes five months or so later, in agreement with observations made in the 1970s of the seasonal variation in tropospheric Sr⁹⁰. In the SH, the seasonal variation of the fluxes is smaller and the lag is less marked. This seasonal variation in the flux across the tropopause almost certainly explains part of the observed seasonal variation in ozone in the upper troposphere (e.g., Beekman *et al.*, 1994). However there may be some aspects of upper tropospheric photochemistry that depend sensitively on the details of exchange on small space and time scales. In such cases consideration of large-scale mass fluxes is unlikely to give a satisfactory quantification of exchange.

7.3.4.2 WATER VAPOR AND THE TROPICAL TROPOPAUSE

Water vapor mixing ratios in the stratosphere are much smaller than those in the troposphere. It is

generally agreed that the process leading to this dryness is freeze drying (Brewer, 1949), in which air passing through the tropical tropopause has its water vapor mixing ratio reduced to the ice saturation value in the region of the lowest temperatures. The stratospheric water vapor distribution, therefore, is not determined by transport alone, but also by a combination of temperature history following air parcels and microphysical mechanisms involved in freeze drying. Variability and changes in stratospheric water vapor would have implications for ozone, e.g., through changing distributions of PSCs and composition of stratospheric sulfate aerosols (SSAs) and, hence, the amount of chlorine activation, or through changing concentrations of species such as OH that play a role in gas phase ozone chemistry.

Recent satellite and aircraft measurements and theoretical progress have allowed further insight into the freeze-drying process and its interaction with the large-scale circulation. Zonal-mean temperatures are at no latitude cold enough to account for water vapor mixing ratios even as low as 3 ppmv, but NH winter temperatures over the Indonesian subcontinent (Newell and Gould-Stewart, 1981) and over northern Australia (Selkirk, 1993) are low enough to account for observed stratospheric mixing ratios. It has usually been argued that if large-scale upwelling alone were acting, thick large-scale cirrus cloud decks would be observed in the dehydration regions, which is not the case (Robinson, 1980). However recent satellite observations (Prabhakara *et al.*, 1993; Wang *et al.*, 1994) show that there is widespread subvisible cirrus cloud over substantial regions of the tropics, particularly in the western Pacific. One possible mechanism for formation is through cirrus outflow associated with convection, in which case large particles would be present initially, but would fall out leaving behind the smaller (sub-visible) particles; another is through in situ nucleation associated with either turbulent mixing or large-scale vertical motion (Jensen *et al.*, 1996). The latter possibility revives the idea that substantial condensation may be taking place on large scales.

There are observations of cumulus clouds penetrating the stratosphere, using radon (Kritz *et al.*, 1993) and water vapor (Kelly *et al.*, 1993) as indicators of tropospheric air. However, such penetration may be relatively limited (Highwood and Hoskins, 1998). What can be said is that cumulus convection almost certainly dominates the vertical transport in most of the

LOWER STRATOSPHERIC PROCESSES

troposphere, with larger scale upwelling playing an increasingly important role as one moves upward through the tropical tropopause layer. In the lower stratosphere above 70 mb or so, the flux is almost certainly dominated by the large-scale upwelling, which may be thought of as taking upwards whatever water vapor mixing ratios are imposed in the dehydration regions. Because, as noted in Section 7.3.1, temperatures in the tropical lower stratosphere exhibit an annual cycle, the imposed water vapor mixing ratios are also expected to show an annual cycle, with minimum values in NH winter when the temperatures are lowest. This cycle is recorded on each layer of air moving upward through the tropical tropopause, just as a signal is recorded on a magnetic tape as it passes the head of a tape recorder (Holton *et al.*, 1995; Mote *et al.*, 1996). The upward moving signal is observed in water vapor mixing ratios (see Figure 7-7). This “tape recorder” hypothesis explains why observations of water vapor at Panama in NH summer show a minimum value considerably less than saturation values associated with NH summer temperatures and at a level about 3 km above the local tropopause (Holton *et al.*, 1995).

In the simplest form of the freeze-drying hypothesis, the water vapor mixing ratio is set by the ice saturation mixing ratio at the minimum temperature experienced by an air parcel. Even assuming that ice particles form immediately upon supersaturation, this neglects the possibility that ice particles may be carried along with the air parcel and simply re-evaporate (and hence re-moisten the air) when the temperature of the parcel increases. Cloud-scale processes, including microphysics, may therefore be important in allowing effective dehydration. Observations from the Stratosphere-Troposphere Exchange Project (STEP) campaign showed examples of a cumulus anvil where it appeared that excess ice had fallen out, leaving air that contained water vapor mixing ratios close to local ice saturation values (of 1.7 ppmv) (Holton *et al.*, 1995). However other observations showed that in anvil regions of high ice crystal content (200 ppmv or more of water vapor as ice), about 2% of the mass was in particles of size less than 10 microns (Knollenberg *et al.*, 1993), which would take over a day to fall 1 km. Re-evaporation, which would increase water vapor mixing ratios by 4 ppmv or more, is therefore a real possibility.

Various mechanisms have been suggested that might lead to larger particle sizes and therefore to decreased probability of re-evaporation. Because

particles that form over several days rather than several hours tend to be somewhat larger (Jensen and Toon, 1994; see Section 7.2.2), variations in temperatures experienced by air parcels on longer time scales may lead to more effective dehydration. Such variations might arise through tropical Kelvin wave propagation (Tsuda *et al.*, 1994) or through large-scale advection. Another possibility is growth of ice crystals in turbulent mixing taking place in radiatively destabilized anvils (Danielsen, 1982). It is also the case that if an air parcel experiences many freezing events, then even if particle fall rates are small the net effect of many such events may be to reduce water vapor mixing ratios to stratospheric values. Potter and Holton (1995) noted this possibility in association with freezing events associated with small-scale gravity waves.

Notwithstanding the above questions, it should be noted that although minimum large-scale temperatures in NH winter seem to be consistent with the minimum water vapor mixing ratios, minimum large-scale temperatures in NH summer seem too high to account for the maximum water vapor mixing ratios observed in the lower stratosphere as part of the “tape recorder” signal (Mote *et al.*, 1996). There is evidence for lower temperatures on small scales in radiosonde observations (e.g., Atticks and Robinson, 1983), but whether this can account for the maximum mixing ratios is not yet clear.

7.4 COUPLED PROCESSES

7.4.1 Mesoscale Structure and Its Impact

Mesoscale structure (i.e., horizontal scales between a few km and a few hundred km), which is well below the resolution of current global models, may have a systematic impact on chemical evolution. Gravity waves, particularly mountain waves, can cause mesoscale temperature fluctuations of up to 10 K about the mean. During the lower excursions of such temperature fluctuations, ice PSCs can form and are observed as mother-of-pearl clouds. Despite their short lifetimes, the large surface areas of these particles make them highly efficient processors of chlorine species. Also, there is evidence that acid hydrates might nucleate on these ice particles, which continue to exist downstream of the waves. Such phenomena have been shown to yield chemical processing rates substantially enhanced above the synoptic mean values that would be predicted in global models. A second potentially important source

of error in prediction of chemical evolution is inaccurate representation of the process of mixing. Studies of the ClO-dimer formation reaction in polar ozone destruction and the deactivation of PSC-processed air have confirmed sensitivity to mixing, or equivalently model resolution, in certain locations. However, the quantitative extent to which mesoscale temperature fluctuations and filamentary structures influence ozone loss cannot be answered now.

Rates of chemical and microphysical processes often have nonlinear dependencies on temperature or concentration. Accurate predictions of the large-scale effects of these processes therefore require the effects of smaller-scale variations in temperature and concentration fields to be taken into account. At the present resolution of global chemical models (see Section 7.5.4), important unresolved structure, due to gravity waves and filaments (see Section 7.3.3.3), lies in the mesoscale.

7.4.1.1 TEMPERATURE FLUCTUATIONS

There is substantial observational evidence of mesoscale temperature fluctuations in the lower stratosphere caused by internal gravity waves (e.g., Bacmeister *et al.*, 1996). Peak-to-peak amplitudes of 2 K (corresponding to vertical displacements of about 200 m) are typical (Murphy and Gary, 1995). Given the strong temperature dependence of heterogeneous reactions like $\text{HCl} + \text{ClONO}_2$ (Ravishankara and Hanson, 1996), the reactive uptake coefficient is underestimated when synoptic-scale temperatures are used instead of the realistic mesoscale temperature field. Murphy and Ravishankara (1994) showed that the neglect of mesoscale fluctuations could underpredict the effective reactive uptake coefficient of the $\text{ClONO}_2 + \text{HCl}$ reaction by a factor of 2.

Mountain-forced gravity waves, in particular, often have large amplitudes and, in extreme cases, can cause deviations from the synoptic average of more than 10 K (e.g., Gary, 1989), leading to PSCs and rapid chemical processing. Such topographically induced Type-2 PSCs are well known as mother-of-pearl clouds. An example is shown in Figure 7-11. The filamentary structure in the backscatter ratio of the cloud (panel a) is interpreted as particle streaks and used to construct air parcel trajectories. The observation can be interpreted as quasi-Lagrangian with air moving from left to right. The trajectory indicated by the white line reveals temperature fluctuations of up to 13 K peak-to-peak with cooling/

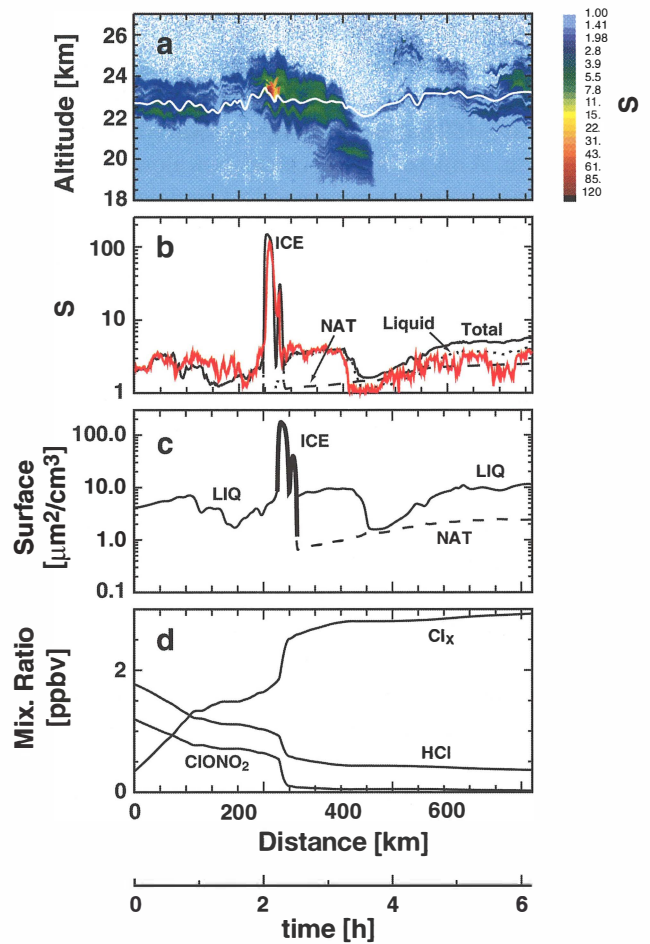


Figure 7-11. Lidar measurements of 15 January 1995 along a flight across the Scandinavian Alps by the German DLR Falcon. (a) Backscatter ratio at 532-nm laser wavelength, S . Lower panels refer to trajectory marked as white curve. (b) Black curves: backscatter calculated by a microphysical model coupled to a non-spherical particle backscatter code; red curve: measurement. (c) Calculated particle surface area. (d) Chemical box model results with $\text{Cl}_x = (2 \times \text{Cl}_2) + (2 \times \text{Cl}_2\text{O}_2) + \text{ClO}$ based on the surface areas given in (c). Adapted from Carlsaw *et al.* (1998).

heating rates of more than 100 K/h. The spot at 250 km (~ 2 h) with very high backscatter indicates the formation of ice particles, which means that the minimum temperature was more than 10 K below the synoptic temperature based on the European Centre for Medium-Range Weather Forecasts (ECMWF) analysis.

LOWER STRATOSPHERIC PROCESSES

Simultaneous depolarization measurements (see Figure 3-13 of Chapter 3 of this Assessment) reveal the ice cloud to be directly surrounded by an STS cloud (dark regions at 0-450 km) with no sign of solid HNO_3 hydrate formation. A microphysical calculation along the shown trajectory coupled to a non-spherical particle backscatter code allows the observed backscatter ratio (panel b) and depolarization ratio to be simulated. Very large ice surface areas are revealed (panel c). A chemical simulation utilizing the particle distributions calculated by the microphysical model indicates practically complete chlorine processing in less than 3 h (panel d). After the ice and liquid particles evaporate almost fully at 450 km (~3h), subsequent cooling leads to the slow growth of depolarizing particles at >600 km. Microphysical calculations indicate that although more than 50% of all particles became activated as ice particles, only the smallest 2% of them served as nuclei for NAT or other solid HNO_3 hydrates (Carslaw *et al.*, 1998).

While this sort of observation and calculation suggests that mountain wave clouds can be a very efficient chemical processor, their large-scale importance is yet to be assessed.

7.4.1.2 FILAMENTARY STRUCTURE

Inaccurate representation of the process of mixing is potentially an important source of quantitative error in the predictions of stratospheric chemical transport models. The possibility of such errors was first pointed out in the context of 1-D and 2-D models (Tuck, 1979; Pyle and Zavody, 1990), but remains relevant even to the 3-D models currently used for prediction purposes. Sensitivity to mixing will obviously be greatest in regions where abundances of chemical species vary on small spatial scales. In the lower stratosphere, small-scale variation is most likely in the neighborhood of the vortex edge and in the surf zone (see Section 7.3.3.3). Small-scale variation is also expected near the tropopause, as a result of stratosphere-troposphere exchange events (see Section 7.3.4.1).

Mixing can either decrease or increase reaction rates, depending on the situation. For example, the reaction $\text{ClO} + \text{ClO} + \text{M}$, which is the rate-limiting step in the dominant ozone destruction cycle in the polar regions, will be slowed down if small-scale structure in ClO is mixed away. On the other hand, the reaction $\text{ClO} + \text{NO}_2 + \text{M}$, which removes ClO, will be speeded up if ClO and NO_2 are brought into contact through mixing.

Both sets of reactions have been studied in some detail in this context.

The quantitative implications for ozone depletion of the effects of mixing on the $\text{ClO} + \text{ClO} + \text{M}$ reaction were assessed by Edouard *et al.* (1996) using a single-level transport model (forced by analyzed winds and temperatures), coupled with a simple, idealized chemistry scheme. They found a very strong dependence of the calculated ozone loss in the Arctic polar vortex on the model resolution, which ranged from 15 km to 200 km. Their calculated ozone loss varied by up to a factor of 2.5, which they attributed to differing filamental ClO_x distributions acting through the nonlinear ClO-ClO cycle. Searle *et al.* (1998a,b) carried out a similar study with both an idealized and a full chemistry scheme. Their results showed much less sensitivity to resolution and were demonstrated to be consistent with simple theoretical estimates derived from the modeled ClO distribution. Further evidence for only a moderate resolution dependence came from Sparling *et al.* (1998), who used in situ aircraft ClO measurements to infer the corresponding resolution dependence of the associated ozone destruction due to $\text{ClO} + \text{ClO} + \text{M}$. They concluded that the small-scale spatial structure in the ClO observations could not lead to resolution dependence of the magnitude predicted by Edouard *et al.* (1996).

The effect of mixing on the deactivating $\text{ClO} + \text{NO}_2 + \text{M}$ reaction was first examined by Prather and Jaffe (1990), who considered the chemical evolution of a filament of polar air with anomalous composition (e.g., high ClO) being transported to midlatitudes. Mixing in “chemical-diffusion fronts” at the edges of the filament deactivates the high ClO air and leads to high mixing ratios of species such as ClONO_2 in these regions. Prather and Jaffe’s results are suggestive of the “collar” region of high ClONO_2 observed at the edge of the polar vortex (Toon *et al.*, 1989a). However, Chipperfield *et al.* (1997) showed that such a “collar” region can arise purely through photochemical recovery. Tan *et al.* (1998) investigated the effect of mixing on the rate of ClO_x decay in the same context, using an isentropic transport model for the lower stratosphere driven by observed winds and incorporating a simplified reaction scheme. Tan *et al.* concluded that, under conditions relevant to filamentation at the edge of the NH vortex, deactivation by mixing dominated that due to HNO_3 photolysis at resolutions of 500 km or so used in current models. However, depending on ambient NO_x values, the two processes would still be competitive if the resolution was

sufficiently fine to represent realistic mixing. Tan *et al.* also concluded that predicted ozone loss rates are sensitive to model resolution in the regime relevant to current models (i.e., 100 km or more), but that the sensitivity decreases considerably once the resolution is finer than 100 km.

If chemical model results do give evidence of sensitivity to resolution, and if it is not practical to use resolution at which the representation of mixing is quantitatively realistic, then some method of parameterizing the effect of small scales on chemistry will be needed. One such parameterization has been developed by Thuburn and Tan (1997) for the ClO + NO₂ reaction. However, much further work would be needed to develop a parameterization for a multiple set of reactions whose rates could be either enhanced or suppressed by mixing.

7.4.2 Seasonal Evolution of Inorganic Chlorine

The processes affecting chlorine activation are qualitatively understood in the polar regions. Measurements and models suggest that if the temperatures are cold enough, a large fraction of available chlorine is converted into active forms. Model-derived chlorine activation under Antarctic conditions does not appear to be sensitive to the physical states of the particles. It also appears that model-calculated chlorine activation and ozone depletion are not very sensitive to dehydration and/or denitrification in the Antarctic. This is due to the importance of continued chlorine activation after sunlight has returned to the vortex. Overall the finding that stratospheric liquid aerosols can cause chlorine activation similar to solid PSCs simplifies our understanding of polar ozone depletion. The details of the phase of the particles may be important for prediction of the Antarctic ozone hole recovery and the extent of Arctic ozone depletion, but temperature and water vapor are the crucial factors.

Inorganic chlorine only destroys ozone if it is in active forms (such as ClO) as opposed to inactive forms (primarily HCl and ClONO₂). The balance between active and inactive forms is altered by heterogeneous/multiphase reactions (see Section 7.2.3). The degree of ozone depletion is ultimately tied to the amount of activated chlorine, its lifetime after activation, and its competition with other factors affecting ozone (such as

transport). While current knowledge is incomplete, recent advances have in some ways simplified our understanding of polar ozone depletion.

ANTARCTIC

Perturbed chlorine partitioning due to heterogeneous reactions is the primary cause of the Antarctic ozone hole. Earlier WMO Assessments contain extensive discussions on why the Antarctic region experiences the most perturbed chlorine partitioning and the largest ozone losses. Briefly, the relatively stable southern polar vortex causes very cold temperatures to be pervasive in this region during winter and spring. This allows PSCs to form, and reactions (especially HCl + ClONO₂) on these PSCs convert chlorine from inactive into more active forms. Furthermore, solid-PSC sedimentation (especially by Type-2 PSCs) can cause extensive denitrification and dehydration. The denitrification along with the isolation of the vortex allows chlorine to remain active during the springtime when sunlight returns to the vortex and induces large ozone loss.

This conceptual picture has been altered by new information in recent years, including the role of liquid aerosols, the role of denitrification and dehydration, the influence of volcanic perturbations, and the role of temperature variations. These effects all, either directly or indirectly, alter the partitioning of inorganic chlorine and thus influence chemical ozone loss. However, the overall effect remains that reactions on condensed matter cause a large increase in active chlorine inside the vortex, which leads to extensive ozone depletion.

Observations, especially those from aircraft, have shown that both solid and liquid aerosols are present in the Antarctic region (Fahey *et al.*, 1989; Del Negro *et al.*, 1997). Presently, it is not known as to which conditions lead to which type of aerosol (see Section 7.2.2). However, as discussed in Section 7.2.3, chlorine-activating reactions occur on both liquid and solid aerosols at temperatures approaching the frost point. Since sulfate aerosols are ubiquitous in the lower stratosphere, chlorine activation is not limited to isolated solid-PSC events, which could have significant nucleation barriers. Only cold temperatures are needed. Indeed, both two- and three-dimensional model simulations show that models assuming only liquid aerosols or only NAT aerosols both produce realistic Antarctic ozone holes (Portmann *et al.*, 1996; Brasseur *et al.*, 1997). The discovery that liquid sulfate aerosols

LOWER STRATOSPHERIC PROCESSES

(and ternary solutions) can activate chlorine comparably to NAT PSCs simplifies our understanding (of chlorine activation) because the complex phase transformations of solid PSCs may not have to be understood (this may not be true for short-term events, see Section 7.2.2).

Recent modeling studies show that denitrification is not a prerequisite for extensive ozone loss (Portmann *et al.*, 1996; Brasseur *et al.*, 1997). This is due to heterogeneous/multiphase activation of chlorine on condensed matter during springtime, either on NAT PSCs, ternary solutions, or sulfate aerosols. In addition to reforming active chlorine, reactions such as $\text{ClONO}_2 + \text{HCl}$ and $\text{ClONO}_2 + \text{H}_2\text{O}$ also reform nitric acid and thus chemically limit the release of NO_x . Furthermore, even in the absence of NO_x , active chlorine can be lost to HCl due to its gas phase reformation by $\text{Cl} + \text{CH}_4$. The presence of Cl is assured during springtime, even in the absence of NO, by the photolysis of chlorine-containing molecules. Figure 7-12 shows the sensitivity of the Garcia-Solomon two-dimensional model (Solomon *et al.*, 1996), assuming only liquid aerosols, to denitrification and dehydration. This shows that although somewhat larger loss is found with a 90% denitrification, the difference is relatively small. Also, relatively smaller changes in the amount of dehydration (less than 40% removal of water vapor) cause a comparable change in the ozone loss as the 90% denitrification. This is due to the strong dependence of the reaction rates on the water content of SSAs. Similar behavior is found in simulations assuming only NAT is present, although in this case the availability of NAT is also directly influenced by the amount of water and nitric acid.

Taken together, these studies suggest that solid PSC events are not essential for Antarctic ozone hole formation (i.e., heterogeneous activation of chlorine, followed by sustainment of active chlorine through springtime due to denitrification), but instead all that is needed are aerosols (whether liquid or solid) and cold temperatures. Portmann *et al.* (1996) show that even a 2 K change in mean temperature has as much effect as denitrification in the model simulation, while a 5 K increase in mean temperature can nearly eliminate the ozone hole. Carslaw and Peter (1997) have recently suggested that reactions such as $\text{HCl} + \text{ClONO}_2$ may be up to a factor of 100 times slower on NAT compared with liquid aerosols; in this case, it would be difficult to produce an ozone hole with NAT PSCs and the dominance of liquid aerosols will be indicated.

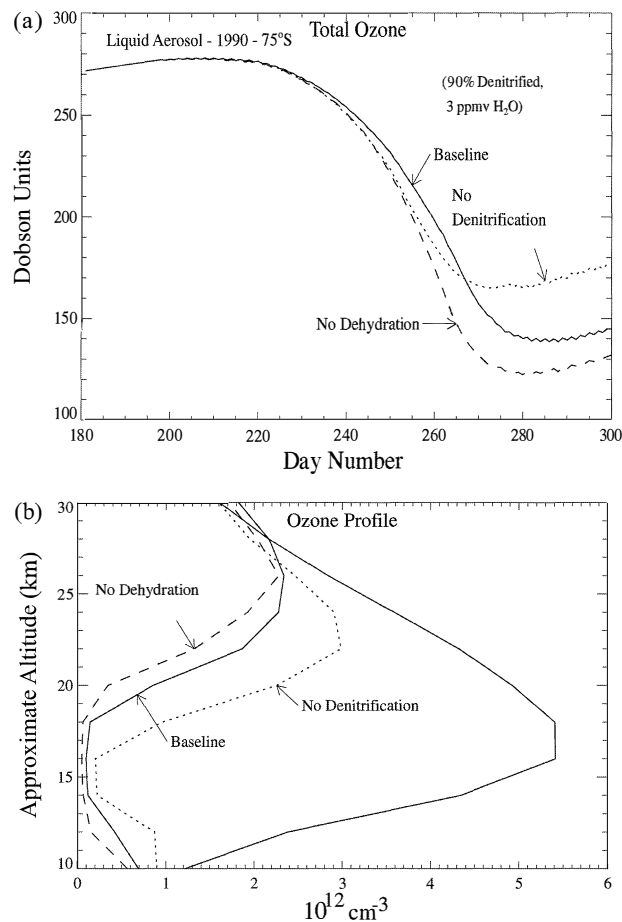


Figure 7-12. Sensitivity of the Garcia-Solomon two-dimensional model to denitrification and dehydration at 75°S during springtime (figure 12 of Portmann *et al.* (1996)). The total ozone time series and the profiles corresponding to the minimum total ozone are shown. The unmarked line in (b) is the ozone profile before depletion.

ARCTIC

The Arctic vortex is considerably more dynamically active than the Antarctic vortex. This causes the Arctic vortex to break up much earlier than in the south and, even while the vortex is present, temperatures are much warmer than in the southern vortex. See WMO (1995) for an extensive discussion on the difference between the northern and southern vortices.

Chemical ozone loss is more difficult to detect in the Northern Hemisphere due to its smaller extent and the increased variability of ozone. However, the strong correlation between cold temperatures (i.e., those below

about 195 K) and large abundances of ClO has been extensively documented (e.g., Waters *et al.*, 1995; Santee *et al.*, 1995). In fact, ClO values inside the northern vortex during winter can sometimes be as large as those in the southern vortex. However, the amount of ozone depletion caused by the ClO depends also on the amount of sunlight experienced by the chlorinated radicals. Thus activation later in the winter and in spring causes more extensive ozone depletion than earlier activation. However, even activation that occurs during polar night can cause ozone depletion if the vortex is sufficiently asymmetric to allow parcels to intersect sunlight during part of their trajectories.

There is increasing evidence that liquid aerosols play a dominant role in chlorine activation in the Arctic. Bregman *et al.* (1997) show that reactions on liquid aerosol are necessary to explain aircraft observations during the Stratosphere-Troposphere Exchange Experiment by Aircraft Measurement (STREAM) mission in 1993 in the lowermost stratosphere at isentropic surfaces below about 375 K. Tie *et al.* (1997) show that the colder temperatures in spring 1993 compared with 1992 caused greater activation due to enhanced reactions on liquid aerosols.

The potential importance of dehydration and denitrification in the Arctic region has not been quantitatively addressed. Earlier studies suggested that denitrification would be necessary to cause large ozone losses in the Arctic region (Brune *et al.*, 1991; Salawitch *et al.*, 1993) but these studies did not include the recently measured reactions on liquid aerosols, and thus are potentially overly sensitive to denitrification as a means of maintaining active chlorine. Dehydration would likely reduce Arctic ozone loss due to the reduction in the liquid aerosol reaction rates, as in the Antarctic.

7.4.3 Lessons from Mt. Pinatubo

The eruption of Mt. Pinatubo was an atmospheric dynamics and chemistry "experiment" on a global scale. Considerable evidence shows that the enhanced aerosol levels caused a reduction in total ozone during winter and spring in the extratropics. It is possible that volcanic influences since 1979 may be confused with solar cycle variations due to the roughly 10-year spacing of the El Chichón and Mt. Pinatubo eruptions, which both occurred near the transition from solar maximum to minimum. The Mt. Pinatubo eruption shows that future ozone recovery could be strongly affected by volcanic eruptions.

The eruption of Mt. Pinatubo in June 1991 injected a very large amount of sulfur dioxide into the tropical lower stratosphere, which was quickly transformed into a sulfate aerosol. This is probably the largest natural stratospheric perturbation of the century. It was an episodic perturbation, however, and differs from the major anthropogenic stratospheric perturbations, which are long-lived. Thus, other stratospheric forcing agents, such as chlorine loading, were essentially constant during the volcanic perturbation, allowing the possible separation of the volcanic effects. Large changes in stratospheric dynamics, radiative transfer, and trace gases occurred and they provided a valuable test of our ability to quantify and model the changes. (See WMO (1995) for an extensive discussion on the detection, transport, and modeling of the changes, and Chapter 3 of this Assessment for a discussion of the aerosol properties and morphology.) The longer persistence of the aerosol allowed higher chlorine activation beyond the period of perturbed dynamics and provided evidence for chlorine-catalyzed ozone destruction during that period.

Record-low ozone abundances were observed after the Mt. Pinatubo eruption, and model calculations indicate that these depletions were related to multiphase chemistry in the sulfate aerosols (WMO, 1995). Most early studies only included reaction (7-1) (Section 7.2.3), which is efficient at nearly all temperatures, and reaction (7-2), which is only efficient at cold temperatures. At midlatitudes, the reduction of NO_x due to reaction (7-1) causes an increase in ClO due to a shift in the partitioning of ClO and ClONO₂. HO_x radicals are also generally increased by the reduction in NO₂. These effects both increased the chemical ozone loss rates in the lower stratosphere. Figure 7-13 shows two-dimensional model calculations of the ozone anomaly compared with those computed from the Total Ozone Mapping Spectrometer (TOMS) measurements (Tie *et al.*, 1994). Dynamical variations related to the QBO (which the model does not include) have been removed from the TOMS data using regression (Randel *et al.*, 1995). The model reproduces the general shape and magnitude of the anomalies quite well, suggesting that much of the anomaly is indeed chemical.

Due to improved understanding of processes in or on condensed matter (see Section 7.2.3) it is now recognized that reactions directly involving HCl are efficient in sulfate aerosol at cold temperatures, especially reactions (7-3) and (7-4). This implies that volcanically perturbed aerosol could have an enhanced role at

LOWER STRATOSPHERIC PROCESSES

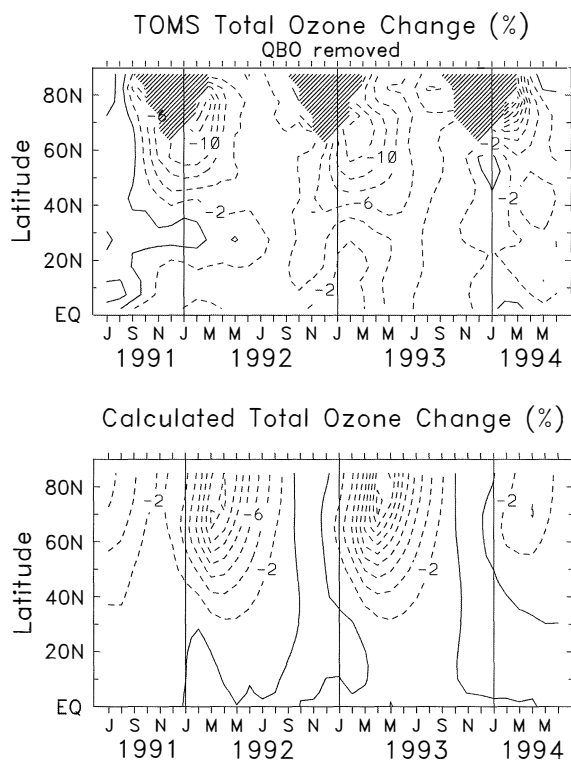


Figure 7-13. Total ozone anomalies from a two-dimensional model compared with those computed from TOMS V6 data. Note that the effect of the QBO has been removed from the TOMS data (the model has no QBO). The model includes both chemical and radiative effects due to sulfate aerosols. Adapted from Tiedje *et al.* (1994) and Randel *et al.* (1995). Contour interval is 2%.

midlatitudes (Solomon *et al.*, 1996; Solomon *et al.*, 1998) and high latitudes (Portmann *et al.*, 1996; Tiedje *et al.*, 1997), because these reactions greatly enhance the effectiveness of sulfate aerosol at activating chlorine when temperatures are cold. This could explain why the Northern Hemisphere ozone anomaly is larger in 1993 (when it was colder) than in 1992, even though the aerosol loading was higher in 1992 (Tiedje *et al.*, 1997). Bromine nitrate hydrolysis, reaction (7-5), also adds to the enhancement of free radicals due to the volcanic aerosols, causing increased potential for ozone loss.

Enhanced Antarctic ozone losses were well documented after the eruption of Mt. Pinatubo, especially in the lowermost stratosphere (Hofmann and Oltmans, 1993; Hofmann *et al.*, 1995). These enhanced losses

were due to the high efficiency of reactions (7-3) and (7-4) at cold temperatures and the likely presence of sulfate aerosol (or ternary solutions) inside the vortex. Portmann *et al.* (1996) also have suggested that the eruption of El Chichón in 1982 accelerated the severity of the ozone hole in the early 1980s due to this mechanism.

Hofmann and Solomon (1989) suggested that the El Chichón eruption had caused ozone losses at midlatitudes in the early and mid-1980s, and predicted that an eruption occurring later with higher Cl_y would lead to larger depletions. The Mt. Pinatubo eruption and recent laboratory measurements have strengthened this view. Model calculations now show that aerosol perturbations have influenced stratospheric ozone at midlatitudes since at least 1980 (Solomon *et al.*, 1996; Jackman *et al.*, 1996; Callis *et al.*, 1997). In addition, the reduction of model NO_x in the lower stratosphere due to reactions on sulfate aerosols (even during background conditions) has been partially responsible for increasing model-based ozone trends around 20 km, bringing better agreement between models and measurements (although significant discrepancies remain below approximately 16 km; see Section 7.6.2). Solomon *et al.* (1996) have suggested that the roughly ten-year separation of the El Chichón and Mt. Pinatubo eruptions, which both occurred before solar minimum, could confuse efforts to remove the solar cycle from the long-term ozone record by statistical methods (see Figure 7-14), especially at mid and high latitudes.

7.5 QUANTIFICATION AND PREDICTION OF OZONE CHANGES

To understand the cause of ozone changes requires a quantitative accounting for those changes in terms of known processes. Ozone in the lower stratosphere is directly affected by both chemistry and transport. In general, the chemical ozone loss rates cannot be measured directly because they are slow compared to the transport and mixing time scales. (One exception is when the ozone loss rates are relatively large, as in the Arctic springtime vortex; depletion under these circumstances has been measured by the “Match” method; see Section 7.6.1). Therefore, one needs to calculate, rather than measure, the ozone changes. This requirement leads to a hierarchy of models, which are distinguished by the extent to which they are constrained. The more constrained models give more reliable results,

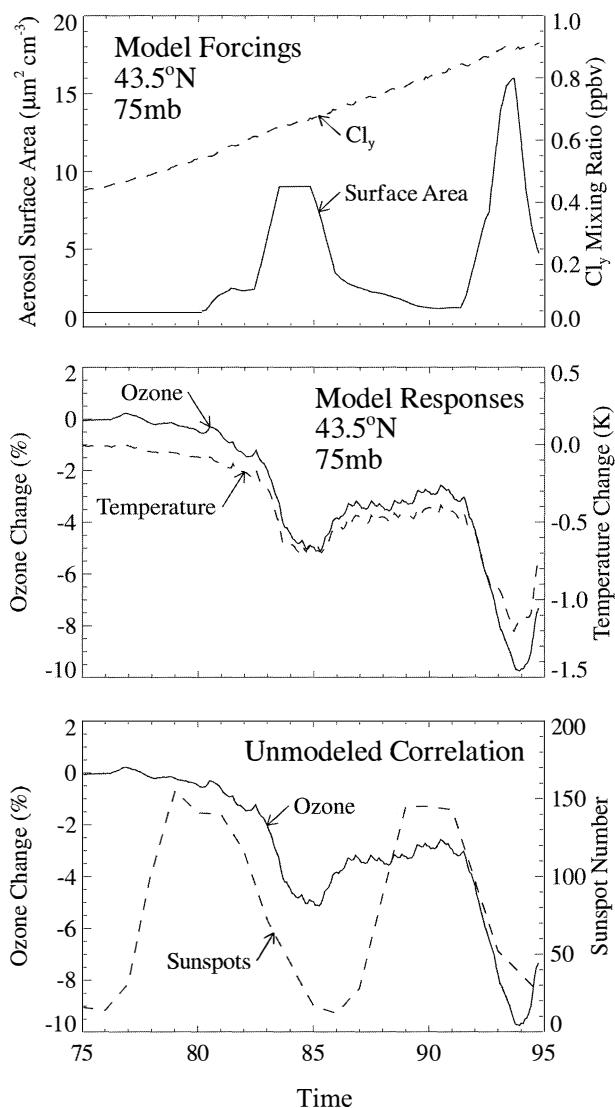


Figure 7-14. Two-dimensional model results suggesting that volcanic and solar cycle variations in ozone could be highly correlated since approximately 1980. The model is forced with chlorine (Cl_y) and volcanic (surface area) changes since 1975, resulting in the ozone and temperature variations shown in the middle panel. The similarity between the model ozone field (which includes no solar cycle effects) and a proxy for the solar cycle (sunspot number) is shown in the bottom panel. Adapted from Solomon *et al.* (1996).

but they address only a piece of the problem; hence, they are not useful for making predictions. In the most constrained case, local chemical ozone loss rates can be quantified at a fixed location or by following a moving air parcel, using observed temperature and measured chemical composition (especially of the involved free radicals). In the least constrained case, a general circulation model with fully interactive ozone chemistry can, in principle, predict future ozone changes under a specified anthropogenic forcing scenario. In this section, we briefly examine the status of these methods.

7.5.1 Local Chemical Ozone Loss

Available field observations are generally consistent with our theoretical and laboratory-derived understanding of chemical ozone loss rates. Uncertainties in some processes that impact ozone are significant. Observations in the lowest part of the extratropical stratosphere within a few km above the tropopause remain very limited. Partitioning of reactive families at midlatitudes is fairly well understood qualitatively. The diurnal dependence of HO_x species indicates a new source of HO_x , now thought to be photolysis of HOBr formed in BrONO_2 hydrolysis. Calculations that use the total and relative contributions to chemical loss rates of midlatitude ozone continue to support the view that HO_x is the major catalyst that chemically controls the extrapolar lower stratospheric ozone abundance, although the NO_x , Cl_x , and Br_x species compete effectively with HO_x .

Comparisons with atmospheric observations form an important test of the accuracy of our theoretical and laboratory-derived understanding of chemical processes as implemented in models. Measurements also constrain the abundance of species for which our knowledge of controlling processes is inadequate. Observations of chemical constituents above 20 km have improved notably in coverage and accuracy since the last Assessment (WMO, 1995); but observations in the lowest few km of the extratropical stratosphere remain very limited. Constraints placed by some of the field observations on chemistry have been noted in Section 7.2. A few others are discussed below with the aim to use field measurements to constrain the ozone loss rates.

Measured distributions of total NO_y from aircraft in the lower stratosphere extend from 70°S to 70°N in spring and fall seasons (see, e.g., Fahey *et al.*, 1996). Profiles of NO_y measured from balloon (Kondo *et al.*,

LOWER STRATOSPHERIC PROCESSES

1994, 1996) are very consistent with the aircraft results. NO_y is also estimated from the sum of components measured by space-based spectrometers (e.g., Russell *et al.*, 1988). NO_y distributions from UARS (Morris *et al.*, 1997) and ATMOS (Rinsland *et al.*, 1996b) satellite measurements are very similar to those from aircraft. The accuracy of NO_y measurements in the lower stratosphere is estimated to be less than roughly 20%. Thus, the overall abundance of NO_y is reasonably well defined in the lower stratosphere.

Cl_y is not measured as a total, but deduced from other observations, as discussed in Chapter 1 of this Assessment. The deduced Cl_y is accurate to within several hundred pptv, which becomes a large fraction of the mean Cl_y at altitudes near the tropopause but is sufficiently good for higher altitudes. These deduced amounts may be in error because of the nonlinear changes in total chlorine with time (see Section 7.3.3.1).

The unexpectedly low values of HCl reported by Webster *et al.* (1994) and attributed by them to volcanically enhanced sulfate surface area were discussed in the previous Assessment; these low values have yet to be resolved theoretically or experimentally. Cl_y partitioning from ATMOS (Michelsen *et al.*, 1996; Chang *et al.*, 1996) and balloon (Chance *et al.*, 1996) measurements is consistent with model results within noted uncertainties below about 25 km. HCl measurements from ATMOS exceed those from the ER-2 by 10 to 40% for nearly identical locations; the cause of the difference is not clear (Chang *et al.*, 1996). UARS measurements of HCl and ClONO_2 (Dessler *et al.*, 1995a) suggest that models do underpredict ClONO_2 relative to HCl near 20 km, but not as much as that inferred from Webster *et al.* (1994). The increase in HCl/ Cl_y with decreasing sulfate loading following Mt. Pinatubo as measured from UARS (Dessler *et al.*, 1997) is about 16% from July 1992 to June 1996.

Determination of inorganic bromine (Br_y) is discussed in Chapter 1. There are discrepancies in values of stratospheric BrO derived from different estimates and measurements. One estimate of Br_y is obtained from summing the bromine content of organic bromine compounds measured in the lower stratosphere and the troposphere and adjusting for slight trends in their abundances (Schauffler *et al.*, 1993; Fabian *et al.*, 1994; Wamsley *et al.*, 1998). Uncertainty in Br_y derived by this method is estimated to be ± 2 pptv (Wamsley *et al.*, 1998). Alternatively, Br_y has been estimated from the abundances of BrO measured, in situ, around 20 km and

deriving the abundances of other bromine compounds (BrONO_2 , HOBr, HBr, etc.). The value of Br_y that is deduced by this method (~ 20 pptv) agrees, with an uncertainty of about $\pm 50\%$ at those altitudes, with the Br_y abundances derived from organic bromine measurements. The large uncertainty of $\sim 50\%$ is mainly due to uncertainties in the in situ observations of BrO (Wamsley *et al.*, 1998). (It should be noted, however, that the larger reported values for BrO are inconsistent with the lower values of estimated CBr_y .) Values of Br_y derived from ground-based measurements of BrO appear to be somewhat better defined (e.g., Fish *et al.*, 1997), yielding around 20 pptv of Br_y . The values of Br_y estimated by the above two methods agree within the large uncertainties associated with them. However, there are a few possible inconsistencies. The Br_y estimated from some in situ BrO observations may be 30 to 40% higher than that derived from organic bromine (CBr_y). If true, short-lived organics may be contributing to the stratospheric bromine budget, or there are inadequacies in our understanding of bromine chemistry. Also, some of the in situ observations of Avallone *et al.* (1995) yield BrO values lower than those used by Wamsley *et al.* (1998). If the lower values are correct, the calculated Br_y would be in better agreement with the values shown in Figure 1-18b of this Assessment. Thus, given the uncertainty in the partitioning between BrO and other constituents within the bromine family and the uncertainties in measured abundances, there is still a significant range in the estimates of total inorganic bromine, varying between ~ 15 and 25 pptv.

Recent ground-based measurements (e.g., Arpag *et al.*, 1994; Richter *et al.*, 1998; Aliwell *et al.*, 1997) using zenith-viewing UV absorption spectroscopy provide a reasonably consistent picture of stratospheric BrO column amounts, with largest column amounts at high latitudes in winter, decreasing in spring and at lower latitudes. The slant column measurements imply BrO concentrations maximize near and below 20 km, with mixing ratios of 5-10 pptv. Height-resolved observations of BrO, both by in situ resonance fluorescence (Avallone *et al.*, 1995; McKinney *et al.*, 1997) and more recently by balloonborne solar occultation (Pundt *et al.*, 1998; Harder *et al.*, 1998), show BrO mixing ratios increasing from about 5 to 15 pptv in the height range 20-30 km; the observations are also consistent with ground-based observations noted above.

Inside the denoxified chemically activated vortex, where BrCl is thought to be the principal nighttime

reservoir, both remote sensing (ground-based and balloonborne) and in situ measurements show BrO abundances that are broadly consistent with photochemical simulations. The seasonal variation in midlatitude BrO total column abundances, measured by ground-based methods, suggests that BrO amounts are governed by seasonal variations in NO₂ abundances (Fish *et al.*, 1997; Richter *et al.*, 1998). However, balloonborne solar occultation measurements in less denoxified air (outside the polar vortex, or in late spring inside the vortex) indicate that in the presence of large amounts of NO₂, absolute concentrations of BrO in the 15-25 km range exceed those expected based on current chemistry understanding (Pundt *et al.*, 1998; Harder *et al.*, 1998). Therefore, the current understanding of the BrONO₂ reservoir may not be adequate. The implication of this possible inadequacy for the Ozone Depletion Potentials (ODPs) of bromine compounds is as yet unknown.

The measurements of BrO (see above), HBr (Nolt *et al.*, 1997) and references therein, and upper limits for HOBr (Johnson *et al.*, 1995) are broadly consistent with Br_y partitioning from models. The effectiveness of the BrONO₂ + H₂O reaction on atmospheric sulfate aerosol is difficult to diagnose from atmospheric observations of bromine; however, there are indications based on observations of column BrO that it does occur (Slusser *et al.*, 1997) (see below about early morning OH production). Recently, large nighttime concentrations (~20 pptv) of a new bromine species, symmetric bromine dioxide (OBrO), have been inferred via remote sensing (Renard *et al.*, 1997). Accounting for OBrO in such a large abundance, if present, awaits further work.

The significant components of HO_x in the lower stratosphere, OH and HO₂, are measured directly from the ER-2 (Figure 7-15) (Wennberg *et al.*, 1994; Wennberg *et al.*, 1995). OH mixing ratios at the same altitude and solar zenith angle do not vary much with latitude and, hence, temperature, ozone, or other constituent mixing ratios within the sampled conditions. Measurements of HO_x generally seem to be slightly higher than those expected from models (Wennberg *et al.*, 1995; Salawitch *et al.*, 1994) and suggest possible missing processes. The OH/HO₂ ratio, however, is consistent with theory, reaction rate coefficients, and measured abundances of reactant species that control HO_x partitioning (Cohen *et al.*, 1994). Diurnal measurements of HO_x species (Salawitch *et al.*, 1994) have shown that a (photolytic) source of HO_x, in addition to the O(¹D) source, is

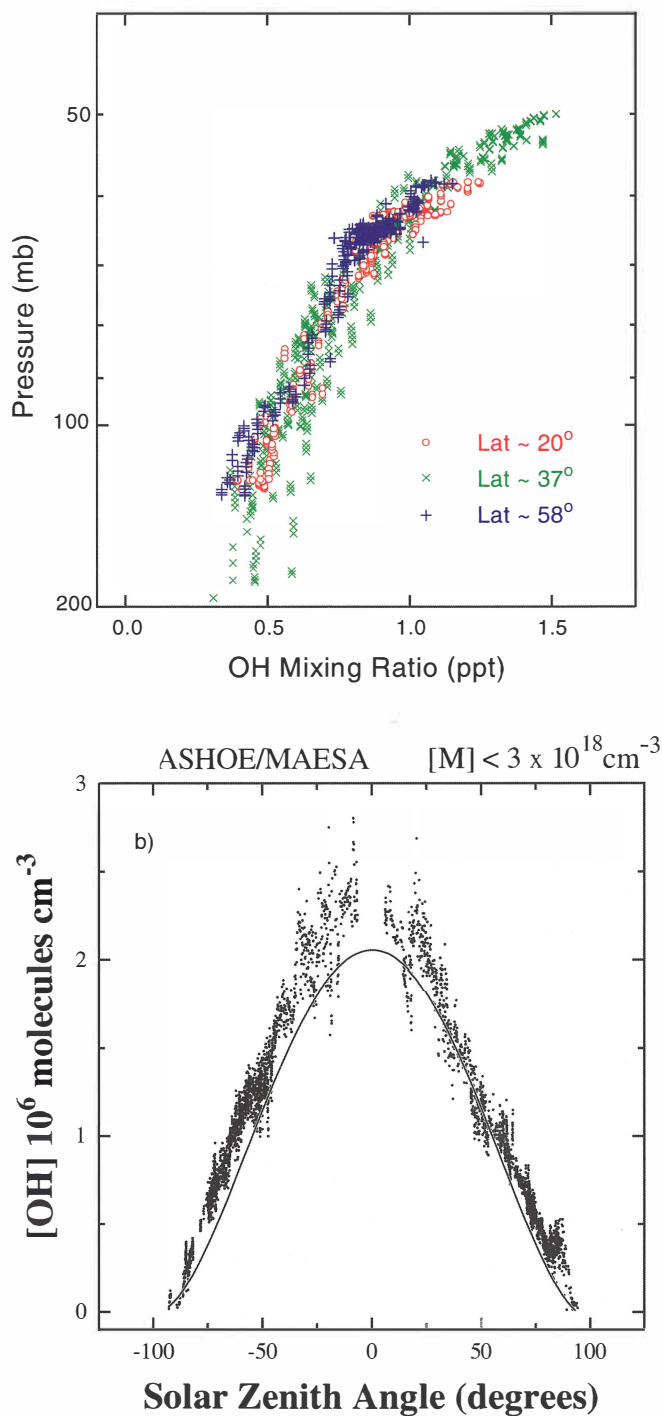


Figure 7-15. (a) OH mixing ratio versus altitude and (b) OH concentration as a function of solar zenith angle, adapted from Wennberg *et al.* (1994) with additional data from recent campaigns. The solid curve is a model prediction from Wennberg *et al.* (1994).

LOWER STRATOSPHERIC PROCESSES

significant at high solar zenith angles. The morning rise in HO_x (Wennberg *et al.*, 1994) is now believed to be consistent with photolysis of HOBr produced by reaction of $\text{BrONO}_2 + \text{H}_2\text{O}$ on sulfate aerosol (Hanson and Ravishankara, 1995; Hanson *et al.*, 1996; Lary *et al.*, 1996) rather than photolysis of HONO .

To evaluate the chemical processes that influence ozone, the abundances and partitioning of key families of reactive species (HO_x , NO_y , Cl_y , and Br_y) must be known and the current status of this knowledge has been discussed above. Radical species, which are catalysts in ozone loss in the lower stratosphere, are now sufficiently well measured to constrain the rate of ozone loss via catalytic cycles of all the major families, at least for a limited set of conditions, e.g., Figure 7-16. HO_x is the dominant catalyst for ozone loss in much of the lower stratosphere (Wennberg *et al.*, 1994) while NO_x predominates above ~ 25 km (Jucks *et al.*, 1996; Osterman *et al.* (1997) and references therein). The relative contributions depend on conditions such as sunlight, temperature, and aerosol loading as well as abundances (discussed above) and partitioning of the other constituent families that are linked chemically. Radical measurements alone are not sufficient to define the total O_3 loss if missing mechanisms exist, but ozone loss rates derived from observed radicals constrain calculations from global predictive models. Observations over a wider range of locations, times, and other conditions would better constrain the ozone loss rates.

7.5.2 2-D Models

Two-dimensional models are presently highly developed and include detailed representations of chemistry and zonal mean dynamics. Current 2-D models can, to varying degrees, reproduce the mean seasonal cycle of ozone. The representation of the chemical effects of planetary waves has been improved in several models, which helps to bridge the gap between 2-D and 3-D models. The representation of aerosol processes (sulfate and PSC) varies greatly, from complex microphysical models to a complete reliance on observations. These methods can all produce the large ozone losses observed in the southern vortex. Although not an inherent limitation, interannual dynamical variability has not been incorporated in most 2-D models. Also, the diffusive approximation used to represent planetary wave mixing cannot represent some inherently three-dimensional processes (e.g., filamentation), and

may be of limited utility in the lowermost stratosphere where the parcel motion is not quasi-zonal (i.e., well confined latitudinally). The highly parameterized nature of 2-D models may limit their ability to represent feedbacks due to possible future changes in the climate system. Yet, two-dimensional models remain useful tools for characterizing chemical/radiative effects in the present climate system.

Two-dimensional (2-D) models (latitude-altitude) are relatively computationally efficient, which allows them to incorporate detailed representations of chemistry and radiative transfer. They are capable of long (decadal) integrations using current computers and thus have been widely used for assessment studies. The use of zonal means is a limitation on the representation of transport processes and localized chemical processes, particularly in light of the high degree of nonlinearity of heterogeneous chemistry (Murphy and Ravishankara, 1994). However, some models partially overcome the latter problem by using parameterizations that allow them to incorporate some effects of zonal asymmetries and nonlinearities with chemical reaction rates.

The simulation of the ozone seasonal cycle is an important indicator of model performance because it critically depends on chemical, dynamical, and radiative aspects of the model. Chapter 6 in WMO (1995) compares the seasonal cycles of many 2-D models and finds that, while most perform reasonably well, some have discrepancies of up to 30% at high latitudes in summer. To illustrate the capabilities of 2-D models, Figure 7-17 shows the seasonal amplitude of ozone computed with the Garcia-Solomon 2-D model (Solomon *et al.* (1996) and references therein) together with TOMS observations. Overall the features are well reproduced, including the large amplitude of the seasonal cycle at high northern latitudes. However, the Southern Hemisphere spring maximum is too small.

Many three-dimensional processes are presently impossible to represent in 2-D models (e.g., filamentation). Also, the specification of the planetary wave forcing as a lower boundary condition in the troposphere, which is the usual practice, produces less interannual variability than is observed, although there have been attempts to incorporate this interannual variability into 2-D models (Callis *et al.*, 1997). The representation of breaking planetary waves, which are necessary to produce a realistic surf zone, has improved. Several models solve the self-consistent planetary wave equations for low zonal wavenumber waves and estimate

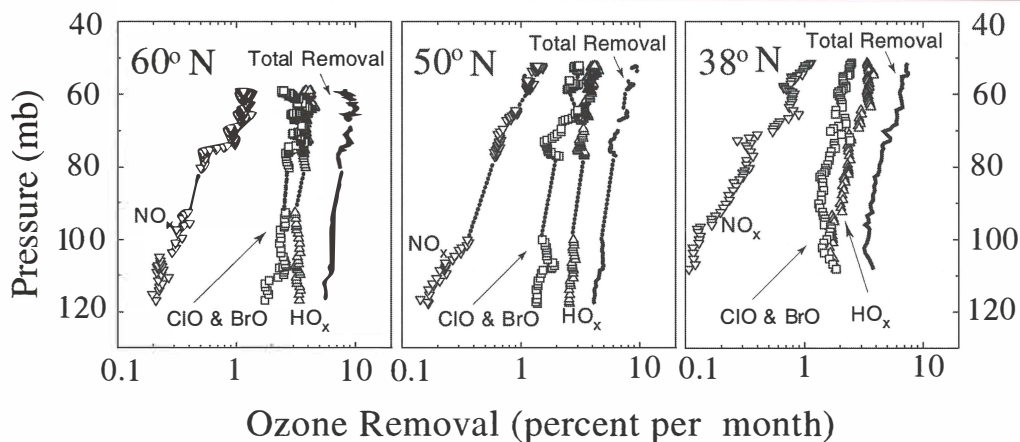


Figure 7-16. Photochemical loss rates of ozone for the major chemical cycles in the lower stratosphere from ER-2 measurements in May 1993. Adapted from Wennberg *et al.* (1994).

the momentum transfer (wave drag) and meridional mixing induced by breaking planetary waves (Garcia and Boville, 1994; Rosenfield *et al.*, 1997). This representation produces mixing that is highly seasonally varying and that responds to model winds, and is probably a reasonable representation of 3-D reality in the surf zone (see Section 7.3.2) where mixing is fairly rapid. These methods partially bridge the gap between 2-D and 3-D models and produce more realistic tracer distributions. However, diffusive representations of mixing are problematic in the neighborhood of transport barriers such as the edges of the surf zone and in the lowermost stratosphere. The planetary wave amplitudes can also be used to generate waves in the temperature fields and variations in the solar zenith angle and length of day (Solomon *et al.*, 1996). In this way, the effects of an asymmetric polar vortex on chemistry are represented, albeit in a highly parameterized way. This approach assumes that parcel motion is quasi-zonal and confined within a well-defined latitude band, which is reasonable either in regions where there is no large-scale wave breaking (e.g., within the polar vortex) or in the surf zone itself.

The representation of chemistry on condensed matter varies considerably between models. The most common method is to model all PSCs as NAT and compute the surface area based on NAT supersaturation for the available nitric acid (e.g., Tie *et al.*, 1994; Considine *et al.*, 1995). Implementation in models varies depending on how the size distribution is handled. This method has the weakness that it strongly depends on the model nitric acid field, which is not well predicted because the processes affecting denitrification are presently poorly

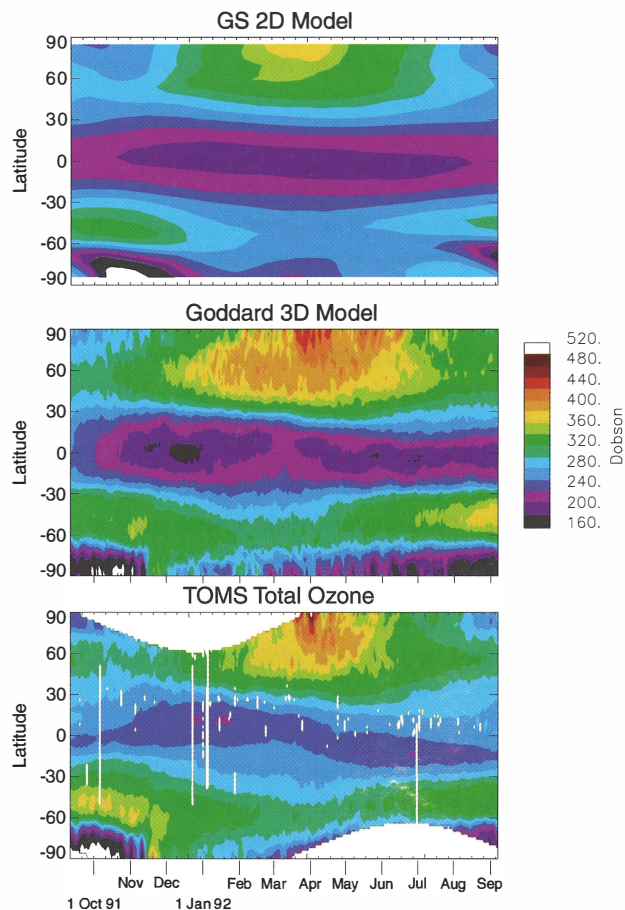


Figure 7-17. Comparison of the annual cycle in ozone derived from TOMS V7 with the Garcia-Solomon 2-D model (Solomon *et al.*, 1996), and a 3-D chemical transport model (Douglass *et al.*, 1996). See Sections 7.5.2 and 7.5.4.

LOWER STRATOSPHERIC PROCESSES

known. Detailed microphysical models have been incorporated into a few models (e.g., De Rudder *et al.*, 1996). However, this method is limited by the uncertainty in many of the key processes affecting aerosol transformation (see Section 7.2.2). PSC processes have also been modeled assuming they are always liquid using aerosol surface areas inferred from observations (Portmann *et al.*, 1996). Temperature and water vapor effectively determine whether a PSC is formed, even though the aerosol is always present. This is because the multiphase reaction efficiencies depend strongly on temperature and water vapor pressure. These methods can generally all reproduce the large ozone losses found over Antarctica, in part because of the very cold temperatures during Antarctic winter, which cause a large degree of activation by all representations. Differences in the Arctic are more apparent because conditions there are often marginal for PSC formation. The growing consensus that aerosols usually remain liquid in the Arctic could simplify PSC representation there.

7.5.3 General Circulation Models

There has been considerable progress in middle atmosphere general circulation modeling over the last few years. Gravity wave momentum forcing is now believed to be considerably more important in determining the circulation of the winter stratosphere than was recognized a few years ago. This effect is thought to be primarily caused by the downward meridional circulations forced by gravity waves that propagate upward from the troposphere and break in the mesosphere. The gravity wave parameterizations in most general circulation models (GCMs) remain crude, with Rayleigh friction still being commonly used. Including the feedbacks between ozone and dynamics in GCMs is now an active research area, although only limited results are available to date.

General circulation models (GCMs) are three-dimensional models that attempt to simulate the global atmospheric circulation from “first principles.” They explicitly represent the large-scale flow and parameterize the effects of unresolved scales. The horizontal truncation scale in current GCMs is typically in the range of 2000-500 km. In principle, the large-scale simulation given by a GCM should be insensitive to the resolution of the model, except perhaps near the truncation scale. Unfortunately, it is typically found that the simulation, even on the largest scales, changes significantly with

resolution (e.g., Boer and Lazare, 1988; Boville, 1995; Hamilton *et al.*, 1995).

There are now many GCMs in use for middle atmosphere applications; they have vertical domains extending from the surface through the stratosphere (and in most cases well into the mesosphere). These models include all of the numerical approximations and physical parameterizations found in tropospheric GCMs and are principally distinguished by more vertical levels and modest changes to the physical parameterizations.

The representation of wave drag arising from unresolved gravity waves (typical horizontal wavelengths of 10-200 km) is probably the single largest problem in middle atmosphere GCMs. All current GCMs either employ an arbitrarily tuned gravity wave parameterization or suffer from excessively cold polar temperatures in the winter stratosphere, together with an excessively strong polar night jet. This “cold pole” problem is especially notable in the Southern Hemisphere, where the wintertime cold temperature bias can reach 40 K in the upper stratosphere (Boville, 1995). Rather surprisingly, gravity wave drag has also been found to be crucial for obtaining realistic simulations of the Northern Hemisphere winter (Boville, 1995; Beagley *et al.*, 1997).

Following the “downward control” principle (Haynes *et al.*, 1991), Garcia and Boville (1994) used a 2-D model with parameterized planetary and gravity waves to show that the descending motion over the pole caused by gravity wave drag in the mesosphere can provide enough dynamical heating to eliminate the cold pole problem in the SH. Recently, several GCMs (e.g., Manzini and Bengtsson, 1996; Butchart and Austin, 1998) have eliminated most of the cold pole problem by including a strong Rayleigh friction in the upper stratosphere or lower mesosphere. Although Rayleigh friction is effective in obtaining reasonable mean states, it can produce erroneous meridional circulations (Shepherd *et al.*, 1996), which may influence both the temperature and transport properties of the model.

Most gravity wave parameterizations included in GCMs (or in 2-D models) have been based on the formulation of Lindzen (1981) for a single gravity wave of specified horizontal wavelength and phase speed. Observations suggest that a spectrum of gravity waves is usually present with a range of wavelengths and phase speeds (e.g., Fritts and VanZandt, 1993). This spectrum can be represented by applying the Lindzen parameterization with several phase speeds. Param-

eterizations that allow the waves in the spectrum to interact have recently been proposed (Medvedev and Klaassen, 1995; Hines, 1997). In all these schemes the initial amplitude and shape of the gravity wave spectrum must be determined empirically; unfortunately, current observations provide little information on either of these quantities, although the work of Allen and Vincent (1995) is a beginning in this respect.

SH winter simulations with the "SKYHI" GCM (Hamilton *et al.*, 1995; Jones *et al.*, 1997) improve significantly with increasing resolution, apparently due to resolving more of the gravity wave drag. Such calculations are extremely computationally challenging, yet even at 0.6 degree resolution (which can resolve gravity waves longer than about 100 km), a cold bias of up to 20 K remains in the upper stratosphere.

A consistent failing of GCMs has been their inability to simulate the QBO. Recently, Takahashi (1996) and Horinouchi and Yoden (1998) have obtained QBO-like oscillations in highly simplified GCMs with better than 1-km vertical resolution and very little horizontal dissipation. The oscillation in the latter model is forced by a broad spectrum of waves, including equatorial waves and large-scale (greater than 100 km) inertia-gravity waves. However, none of the published simulations from full GCMs have used high enough resolution in both the horizontal and vertical dimensions to reproduce these results.

A seasonally varying zonal mean ozone distribution is normally specified to determine the radiative heating in GCMs, with no feedback from the modeled chemistry. Extended simulations with fully interactive chemistry require that both the radiative-dynamical and chemical aspects be simulated accurately, or the model state will differ so much from the real atmosphere as to make the simulation useless. Rasch *et al.* (1995) obtained a reasonably realistic simulation of ozone when they incorporated a fairly comprehensive stratospheric chemistry model into a middle atmosphere GCM, but only so long as the simulated ozone was not allowed to feed back onto the radiation and dynamics.

Ozone transport with parameterized chemistry has been successfully used for several years (e.g., Cariolle *et al.*, 1992). The chemistry parameterization is linearized about a reference state with rates that depend on the local temperature and ozone mixing ratio and the overhead ozone column. This approach has recently been used by Shindell *et al.* (1998a) to determine the ozone response in an atmosphere with doubled CO₂ concentration.

7.5.4 3-D Chemical Models

Three-dimensional chemical models have advanced considerably in recent years and currently have the ability to run seasonal to multi-year simulations. Three-dimensional chemical transport models (3-D CTMs) using analyzed winds produce simulations of horizontal transport in good agreement with observations (with the exception of the tropics because of inaccuracies in the winds). Because of their ability to include "full" chemistry and to capture the interaction of chemistry and transport on comparable time scales, these models produce good simulations of reactive species measurements and are useful tools for testing our current understanding. Prediction of future atmospheric change requires the coupling of these CTMs with GCM winds and temperatures, or direct inclusion of chemistry in GCMs. Although the 3-D models do give realistic simulations of the midlatitude ozone seasonal cycle, the use of these models for annual or longer simulations is currently limited by uncertainties in the diabatic circulation from both the GCMs and the analyses. Computational cost currently precludes the inclusion of detailed microphysical parameterizations in "full" chemistry models.

The ability to model stratospheric chemistry in three dimensions has evolved considerably over the past few years. Due to rapidly increasing computer power, detailed chemical schemes can now be included in 3-D models, and, at present, these models can typically be integrated for simulations of a few months to years. Another significant factor in the improvement in 3-D modeling has been the provision of meteorological fields derived from observational analyses throughout the stratosphere.

Early attempts at 3-D chemical modeling involved adding chemistry schemes to GCMs (e.g., Grose *et al.*, 1987). Because of computer limitations these schemes were necessarily simplified, containing only a small subset of the important stratospheric reactions. This approach of including chemistry interactively in a full GCM produces a fully coupled model, which can include feedbacks between chemistry, radiation and dynamics. Ultimately, when computer resources allow and the GCM formulation is adequate (see Section 7.5.3), these will be the preferred 3-D tool for assessment and prediction. However, other 3-D approaches currently offer significant advantages and will continue to do so over the next few years.

LOWER STRATOSPHERIC PROCESSES

In recent years, “off-line” chemical transport models (CTMs) have become widely used (e.g., Rood *et al.*, 1991; Chipperfield *et al.*, 1993, 1994a, 1995; Lefèvre *et al.*, 1994). In these CTMs the wind and temperature fields (from global meteorological analyses or GCM output) are input to the model, which then advects the trace species and updates the chemistry. CTMs therefore do not treat the feedback between chemistry and dynamics. These models have a number of advantages over GCMs. CTMs are cheaper to run, as the dynamics and radiation are not calculated. Also, if the CTM is forced by meteorological analyses the model is then “constrained” and can be used for direct comparison with a range of observations, thereby testing our current understanding of atmospheric chemistry. Finally, for processes where a realistic temperature field is essential, such as PSC processing, the meteorological analyses are superior to current GCM simulations.

Because of the large computational cost, many 3-D model studies have concentrated on simulations of a few months for situations where the 3-D formulation has definite advantages over 2-D (latitude-height) models. Therefore a number of workers have studied the seasonal evolution of chlorine activation and ozone loss in the polar regions. Lefèvre *et al.* (1994) used an off-line CTM, forced by ECMWF analyses, to study the chemical evolution of the 1991/92 Arctic winter. The model gave good agreement with Microwave Limb Sounder (MLS) satellite observations of enhanced polar ClO, especially in terms of location. The Arctic winter of 1994/95 has been studied by Chipperfield (1998) using a model formulated with an isentropic vertical coordinate. As the quasi-horizontal motion in the stratosphere occurs on isentropic surfaces, this coordinate reduces the spurious vertical mixing associated with isobaric levels (Chipperfield *et al.*, 1996). Figure 7-18 (top panel) shows a comparison of column ozone observations at Sodankyla (68°N, 27°E) with calculations from a 3-D CTM forced by United Kingdom Meteorological Office (UKMO) analyses. Note that the CTM captures the large day-to-day variability in column ozone seen at this site. This variability is due to rapid, horizontal motion associated with the movement of the polar vortex. As the CTM is forced by meteorological analyses, it captures this motion well. Figure 7-18 (top panel) also shows results from a model simulation in which the initial ozone field is advected as a passive tracer. This quantifies the chemical ozone destruction that has occurred and is around 50 DU by late March in the model.

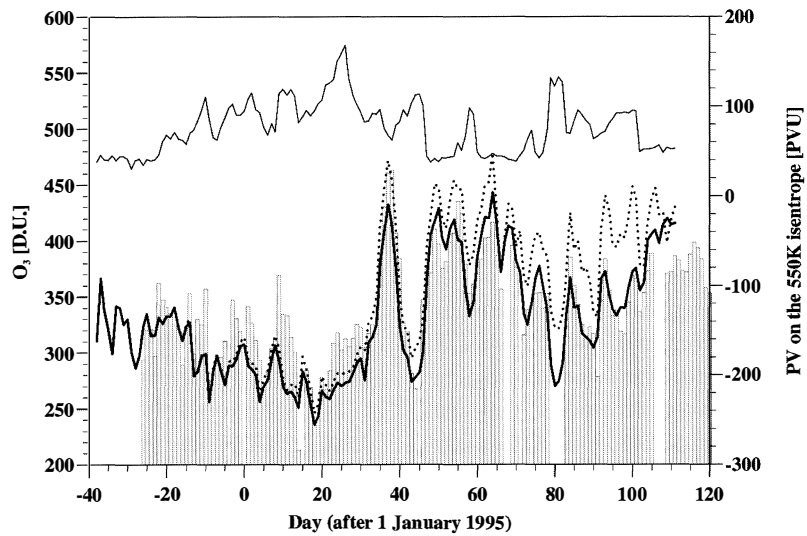
Despite the great success of CTMs in reproducing many features of the observed ozone distribution, there is evidence that the models underestimate the winter/spring depletion at high latitudes. Edouard *et al.* (1996) reported results from the “REPROBUS” chemical transport model of Météo-France for the Arctic winter 1994/95, which indicated that the model underestimated the chemical loss derived from ground-based observations by 40%. Hansen *et al.* (1997) compared observations from Ny Ålesund (78°N, 12°E) during the 1995/96 Arctic winter with 3-D CTM calculations using UKMO analyses. They found that the model gave good quantitative agreement with the observations in January, but by late March the model overestimated the observed ozone by around 50% near 18 km, suggesting that the model either underpredicted the chemical destruction or overpredicted the poleward transport of ozone.

There are several possible reasons why 3-D CTMs may underestimate the observed depletion. First the model transport (and/or initialization) needs to be realistic so that, for example, the model produces sufficient descent at high latitudes leading to large concentrations of inorganic chlorine and bromine in the polar lower stratosphere similar to observations.

Following this dynamical “priming,” the model chemistry then needs to activate sufficient ClO_x to destroy ozone mainly through the ClO/BrO and ClO/ClO cycles. The large-scale temperature analyses used to force CTMs tend to smooth out low temperatures. For example, Knudsen (1996) found that ECMWF temperatures were on average 1.4 K too warm compared with sondes near the NAT point at 50 hPa, while Pullen and Jones (1997) found a similar bias of 1.7 K with UKMO analyses. This implies that models forced by these analyses will underestimate chlorine activation, especially where the temperatures are close to the onset temperature of PSCs. The large-scale temperature fields will also miss the mesoscale activation effects described in Section 7.4.1.1.

Following the activation of chlorine, uncertainties in the laboratory data pertinent to the key catalytic cycles limit the accuracy of model predictions. Fish and Burton (1997) used a trajectory model to perform a Monte-Carlo-type study for Arctic (and midlatitude) ozone depletion. They found that these kinetic uncertainties alone place an uncertainty (1σ) of $\pm 25\%$ on model calculations of polar ozone loss. As expected, given the principal polar catalytic ozone loss cycles, this uncertainty was dominated by uncertainties in the rate

O₃ column above Sodankyla
(SAOZ, 68°N 27°E)



Sodankyla (68N, 27E)

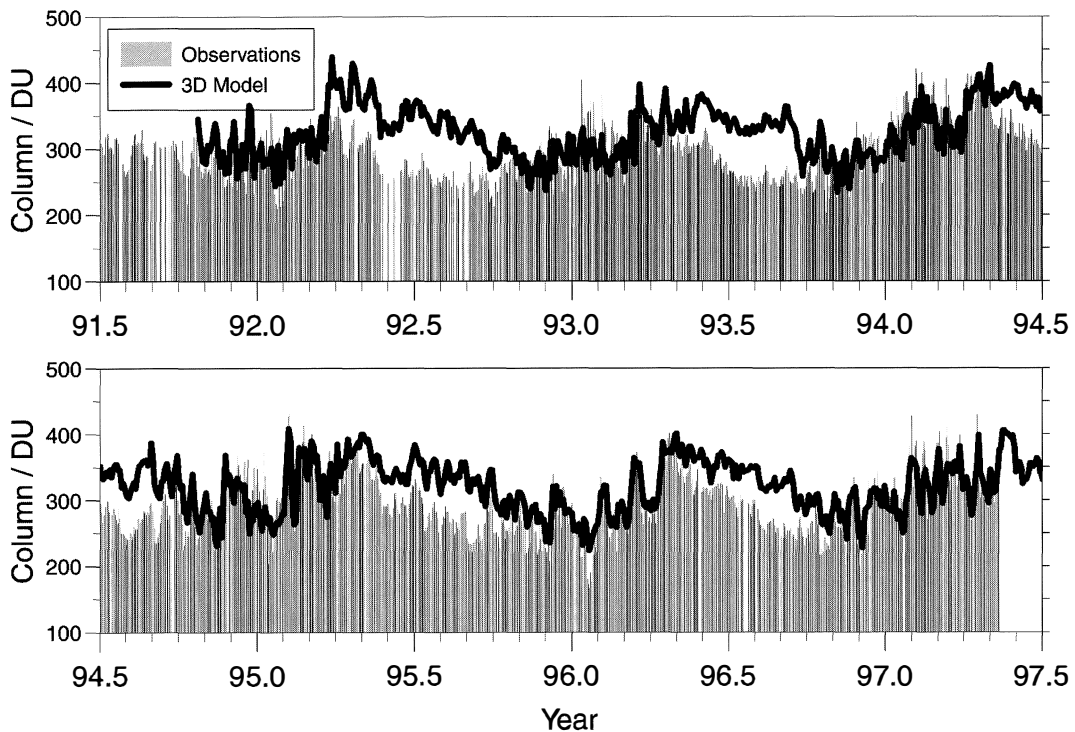


Figure 7-18. Observed ozone column at Sodankyla (68°N) with results from two simulations using the Cambridge University SLIMCAT chemical transport model. Top panel: horizontal resolution of 2.5° latitude × 5.6° longitude. The potential vorticity is shown in the top curve. The dotted line is obtained when O₃ is advected as a passive tracer. Bottom panels: with multi-year integration with horizontal resolution of 7.5° latitude × 7.5° longitude. Figures adapted from Chipperfield (1998).

LOWER STRATOSPHERIC PROCESSES

coefficient for the ClO + BrO reaction and the photolysis rate of Cl₂O₂ (see Section 7.2.1).

The additional potential problem with coarse resolution in global models leading to excessive mixing and rapid deactivation of chlorine is discussed in Section 7.4.1.2. Yet another uncertainty in simulation of polar winter ozone loss is that treatment of heterogeneous or multiphase chemistry in 3-D models, like all other models, is limited by our incomplete understanding (Section 7.2.3). In addition, detailed microphysical treatments are generally too expensive to include in 3-D codes.

The coupling of polar regions and midlatitudes has also been studied with seasonal, and longer, 3-D CTM runs. When off-line CTMs use the same meteorological analyses as used in contour advection studies, they too will capture filamentary structure if run at sufficiently high resolution. For example, Pyle *et al.* (1995) showed that a CTM integrated for June and October 1994 with a horizontal resolution of about 1.5 × 1.5 degrees reproduced well midlatitude filaments of polar air observed in situ by the NASA ER-2 aircraft. Eckman *et al.* (1996) and Brasseur *et al.* (1997) used moderate resolution CTMs (7.5 × 7.5 and 2.8 × 5.6 degrees, respectively) to investigate the evolution of the Antarctic ozone hole and the export of ozone-poor air into midlatitudes. After the polar vortex breakdown in December, the transport and dilution of this air resulted in a column ozone decrease of about 2 to 4% at midlatitudes. Brasseur *et al.* (1997) also noted a 1% decrease in the tropics and a decrease in upper tropospheric ozone.

Because 3-D CTM simulations using analyzed winds are able to simulate horizontal transport well at time and spatial scales in the range of planetary to synoptic waves, they are able to simulate ozone in the lower stratosphere well over time scales up to several weeks, given an initialization from observations. Early simulations diverged from observations after several weeks because of systematic biases in the diabatic circulation (Rood *et al.*, 1991). Improvements in meteorological analysis methods have produced more consistent circulations (e.g., Weaver *et al.*, 1993), which allow longer successful integrations. CTMs using winds from GCMs also have difficulty getting a proper balance between wave-driven and diabatic transport (see Section 7.5.3). Ozone abundances in the lower stratosphere, where most of the overhead column resides, are the result of a balance between transport and chemistry on time scales of several weeks to months. This balance has a distinct annual cycle. Thus a test of the accuracy of the

representation of these processes requires calculations over seasonal to annual time scales.

In general, 3-D seasonal to multi-year simulations of ozone show many similarities to observed variations. An off-line simulation using winds from the National Center for Atmospheric Research (NCAR) Community Climate Model-2 (CCM2) with “full” gas phase chemistry (Rasch *et al.*, 1995) showed good correspondence with observations for the mean and seasonal variations of tropical lower stratospheric ozone and tropical-midlatitude gradients of column ozone. The model did not simulate the vortex breakup well nor the springtime build-up of ozone at high latitudes, but the summertime decrease was similar to that observed.

A multi-year CTM run with winds from the NASA Langley GCM and gas phase chemistry (Eckman *et al.*, 1995) simulated the observed seasonal shift in the tropical minimum of column ozone; however, the calculated mean tropical ozone was significantly lower than that observed and the tropical midlatitude gradient too strong, suggesting excessively strong ascent in the tropics. The high-latitude maximum in the Northern Hemisphere was slightly overestimated and the summertime decline was too slow, while the Southern Hemisphere maximum was underestimated, leading to questions on the balance between mixing and the diabatic circulation. An auxiliary run including heterogeneous chemistry and PSCs improved the representation of total ozone in the southern winter vortex but had little effect elsewhere.

An annual simulation using winds from the Goddard data assimilation system (GEOS-DAS) and linearized ozone chemistry (Douglass *et al.*, 1996) produced a generally good seasonal cycle for total ozone compared with observations, although with some biases in the mean, especially in the tropics and high latitudes (Figure 7-17). The improvement in ability of their 3-D CTM versus a 2-D model to simulate the ozone annual cycle at midlatitudes was found to be largely the result of the explicit three-dimensional representation of seasonal variations in tropopause height. The source of the bias was diagnosed to be the result of an inaccurate balance between horizontal wave and vertical mean transport, which varies with altitude in the upper troposphere and lower stratosphere. A more recent simulation with GEOS-DAS winds and full chemistry (Douglass *et al.*, 1997) shows that ozone gradients may be reasonably well-simulated, even when transport of longer-lived tracers is poor, because of the influence of photochemistry on ozone. Over a longer (multi-year) simulation even this agreement could diverge as the tracer

fields controlling the production of reactive species become distorted.

Steil *et al.* (1998) have reported results of a 15-year integration of a troposphere/lower stratosphere GCM coupled with a detailed chemistry scheme. The model gave a generally good simulation of the ozone seasonal cycle, and interhemispheric asymmetry in chlorine activation. However, the dynamical fields from the GCM were a limiting factor, notably, the GCM did not produce realistic (downward) transport in the polar regions.

To date, 3-D chemistry and transport models have not been used to calculate interannual changes in ozone resulting from trends in CFCs. The potential model problems regarding diabatic circulations uncovered in shorter simulations remain to be solved. However, the apparent lack of climate drift found in annual and multi-year ozone simulations (Douglass *et al.*, 1996; Chipperfield, 1998) suggests that trend calculations may be possible soon with increasing computer power. Note that 3-D CTMs driven by analyzed winds will be able to simulate interannual ozone changes due to dynamical variations as well as ozone changes from trace gas trends. Figure 7-18 (bottom panel) shows results from a multi-year CTM integration (Chipperfield, 1998) compared with column observations at Sodankyla indicating that the CTM does indeed capture some of the observed interannual variability, e.g., the relatively low values during winter 1992/93.

7.6 CURRENT UNDERSTANDING OF OZONE DEPLETION IN THE LOWER STRATOSPHERE

7.6.1 Polar Seasonal Depletion

Late-winter/springtime ozone levels in the Arctic have decreased substantially over the past decade. Within the Arctic vortex, local ozone destruction has been measured and, during the past few years, attributed to halogen-induced ozone destruction. Because of natural variability and difficulty in quantification, uncertainties remain in the partitioning of the observed column depletion between chemical and transport-related factors. Ozone destruction is highly dependent on temperature: the colder the temperature, the larger the ozone destruction (all else being equal). The expected levels of ozone for colder polar temperatures are also lower because of reduced transport of ozone into the polar vortex associated with a weaker diabatic circulation and a stronger vortex. Several of the past years in the Arctic have been particularly cold. It appears that local ozone destruction in the Arctic stratosphere contributes to the observed levels being lower than what would be expected for a pre-CFC atmosphere. This is consistent with our understanding of the mechanisms for ozone destruction based on studies of the Antarctic, where seasonal ozone loss continues unabated.

Large springtime ozone depletion has continued in the Antarctic polar region throughout the 1990s (Figure 7-19). This seasonal column depletion first became visible in the late 1970s, grew through the 1980s, and has changed little during the 1990s. The depletions in the 1990s have been fairly constant because the polar seasonal ozone loss has been essentially complete (nearly 100%) over a deep layer of the Antarctic stratosphere (Figure 7-20). The further depletion seen in 1993 was probably due to increased aerosol from the Mt. Pinatubo eruption, which depleted ozone at altitudes lower than in previous years (Hofmann *et al.*, 1997).

Our observational knowledge and basic understanding of Antarctic depletion has not changed greatly since the last Assessment (WMO, 1995). However, there have been some important advances. The first-order picture that the Antarctic ozone depletion is due to stratospheric chlorine and bromine compounds, activated by heterogeneous or multiphase reactions at

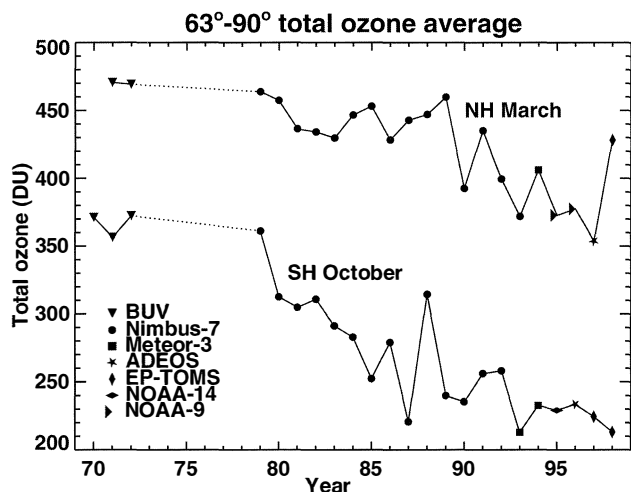


Figure 7-19. Spring average total ozone values in the latitude range 63 to 90 degrees in both hemispheres. Update of the figure presented by Newman *et al.* (1997).

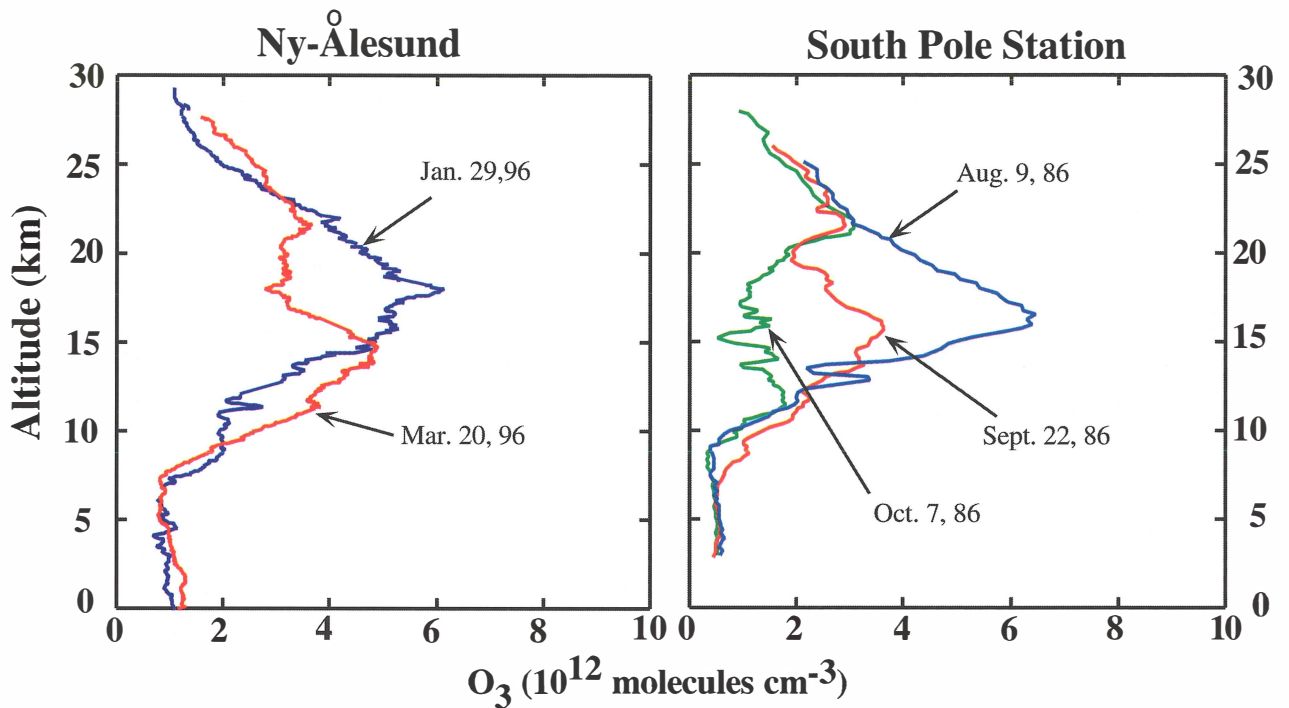


Figure 7-20. Ozone abundance as a function of altitude obtained from balloonborne ozonesondes at Ny-Ålesund in the Arctic region for 1995/96 winter (left panel) (Hartwig Gernandt, Alfred-Wegener Institute for Polar and Marine Research, Potsdam, Germany, personal communication, 1998) and at the South Pole station in the Antarctic for 1986 winter (right panel) (Hofmann *et al.*, 1997). The blue curves show ozone levels before its depletion is initiated. The red curves show the depletion of ozone. The depletion of ozone in the 15-20 km region observed in the mid-1990s in the Arctic is reminiscent of that observed in the Antarctic a decade earlier. Ozone depletion continues into late spring in the Antarctic (green curve), unlike the case in the Arctic. Single profiles may not really represent chemical ozone depletion because of dynamical factors. The shown profile is not due to dynamics and care has been taken to identify dynamical effects.

cold temperatures, is well established by direct observations and by recent model studies (see Section 7.4.2). The model studies have also shown that the details of denitrification, wintertime activation, or even the existence of solid PSCs are not essential (although they are observed) for estimating the overall O₃ loss. This is because chlorine activation is rapid at cold temperatures on all forms of stratospheric condensed matter, and cold temperatures together with vortex isolation persist into springtime, when sunlight can act to destroy ozone. In contrast, as discussed below, the rates of dynamical supply and chemical removal compete in the Arctic and they need to be well quantified to estimate the overall ozone loss.

Figure 7-19 shows a marked decrease in springtime total ozone in the Arctic since the late 1980s, reminiscent

of that seen in the Antarctic ten years earlier. The development of the vertical structure of ozone mixing ratios within the recent Arctic vortex during winter and early spring is also somewhat reminiscent of the Antarctic (Figure 7-20). Yet, one cannot immediately conclude that the Arctic springtime ozone decrease seen in Figure 7-19 has occurred for exactly the same set of reasons as in the Antarctic. First, the Arctic decrease has occurred during a time when the stratospheric chlorine loading, though already high, was not changing rapidly. Second, the Arctic and Antarctic are quite different in certain respects.

One important difference is that the Arctic vortex is much smaller and more distorted than the Antarctic vortex. Thus, although 63-90°S coincides reasonably well with the Antarctic vortex, the changes in March

March total ozone

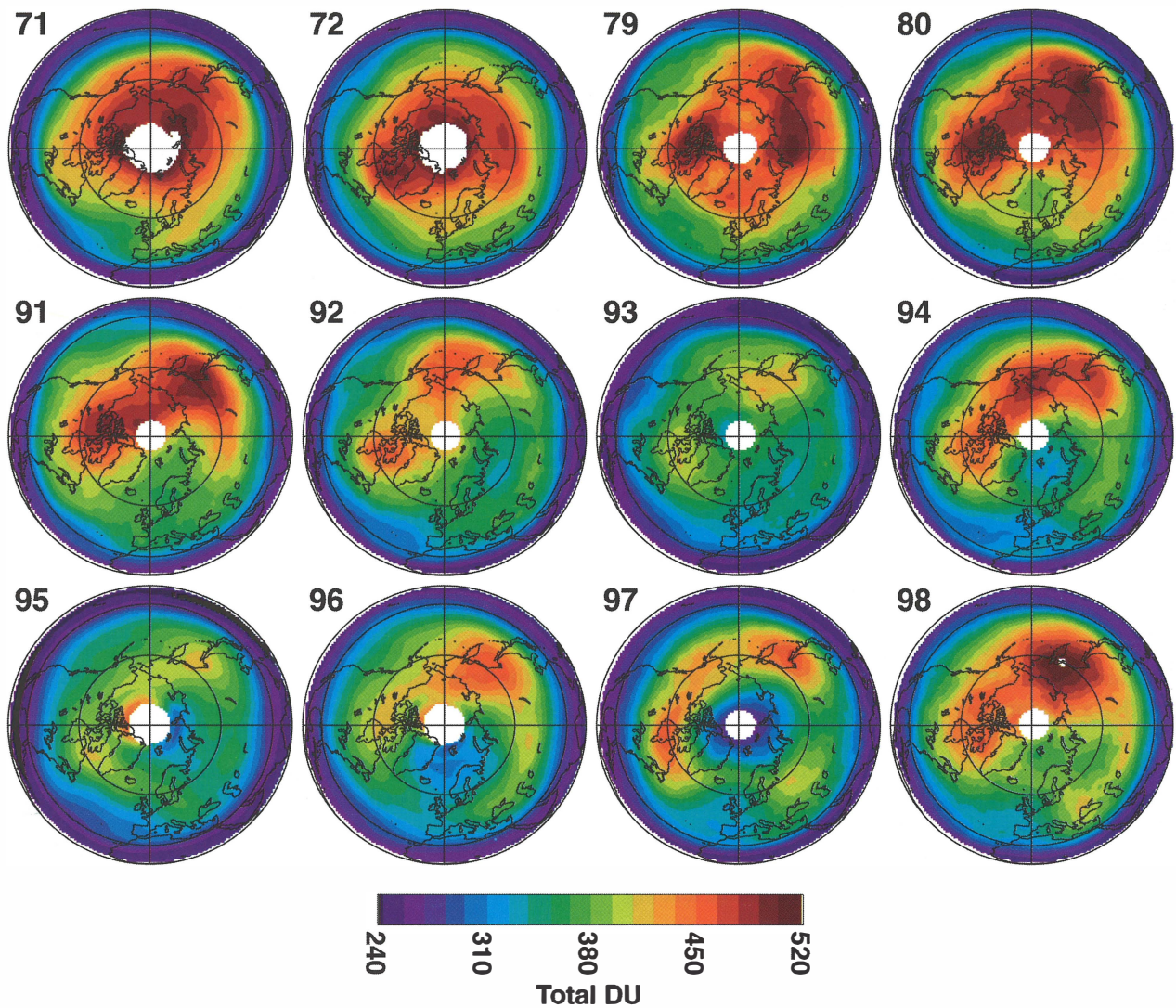


Figure 7-21. March monthly average total ozone polar stereographic images for the Arctic. The 1971 and 1972 data are from Nimbus 4 BUUV, the 1979-1993 data are from Nimbus 7 TOMS, the 1994 data are from Meteor 3 TOMS, the 1995 and 1996 data are from NOAA-9 SBUV/2, and the 1997 and 1998 data are from Earth Probe TOMS.

average 63-90°N total ozone values seen in Figure 7-19 combine changes both within and outside the Arctic polar vortex. While total ozone amounts measured by satellite instruments since 1970 are very large over the entire polar cap during the early years of observations, a distinct minimum in the Arctic region is usually apparent during the 1990s (Figure 7-21). These satellite observations are supported by ground-based observations, which report extremely low ozone column amounts in recent

years, significantly below long-term means (Chapter 4). There is also a significant reduction during the 1990s in the relatively large values that form a croissant structure just outside the vortex. Thus, one must be careful when interpreting Figure 7-19, because the geographical areas in the two hemispheres do not represent the same dynamical regions.

Another important difference between the Arctic and Antarctic is that there is significant interannual

LOWER STRATOSPHERIC PROCESSES

variability in the spatial distribution of Arctic ozone (Figure 7-21). Generally speaking, the springtime Arctic ozone distribution during the 1990s has been more Antarctic in character, with a relative minimum inside the vortex. However, the Arctic vortex is generally centered further off the pole (associated with larger planetary-wave forcing), which means that air parcels can be exposed to sunlight earlier in the season than in the Antarctic, even if the vortex is smaller. Thus the conditions for Arctic depletion are considerably more complex than in the Antarctic, because the potential for ozone loss is not limited to springtime and not all of the Arctic region is conducive to ozone depletion.

Given our present understanding of Antarctic ozone depletion, to produce significant chemical loss in the Arctic requires cold enough temperatures for rapid chlorine activation, exposure to sunlight, and sufficient vortex isolation to allow time for these chemical processes to act. Indeed, meteorological conditions in the Arctic during the 1990s have, generally speaking, been more Antarctic in character, with the vortex being colder and more persistent than in the recent past, especially in 1996/97 (e.g., Coy *et al.*, 1997). But because these meteorological conditions necessarily involve a concomitant reduction in ozone transport into the polar region, it is clear that dynamical and chemical signals are strongly intertwined. Conversely, we would also expect any dynamical signal in ozone associated with a stronger vortex and less transport to involve a concomitant reduction of Arctic temperatures which, in the presence of the current high level of chlorine loading, would lead to enhanced chemical loss.

The decadal trend in the seasonal ozone depletion is difficult to quantify in the Arctic because of the great interannual variability of meteorological conditions, which produces variability in ozone transport as well as in chemical loss (via variability in temperatures and degree of vortex isolation). The recent years of low Arctic ozone are characterized by relatively low planetary wave activity, producing less diabatic descent; thus, as noted above, temperatures inside the Arctic vortex have been colder and more persistent in the recent past (Figure 7-22). This points to a decadal shift in Arctic meteorological conditions, which could well be due to decadal variability in the tropospheric circulation and hence in planetary wave forcing (e.g., Thompson and Wallace, 1998), or even to a long-term change in climate (see Chapter 12). However the reasons for this particular shift are not understood, nor are we able to predict its

persistence. For example, the winter of 1997/98 did not exhibit a cold, persistent Arctic vortex. Note that the enhanced chemical ozone loss expected under these more Antarctic-like meteorological conditions would also produce a radiative feedback, leading to still colder temperatures (see Randel and Wu, 1998; also see Chapter 5).

Because of the above reasons, it is best to look on shorter time scales to quantify chemical loss. In the Arctic, even diagnosing seasonal chemical ozone loss requires a careful separation of changes due to chemistry from those due to dynamics. A number of methods have been developed in recent years for this purpose.

One method, known as Match (von der Gathen *et al.*, 1995; Rex *et al.*, 1998), makes use of pairs of ozonesonde profiles, around five days apart in time, which are matched through Lagrangian trajectory calculations so that they sample the same air mass. By sampling the same air mass, the observed ozone changes can be ascribed to chemistry. von der Gathen *et al.* (1995) calculated ozone loss rates of up to 0.25% per sunlit hour on the 475 K isentropic surface (~18 km altitude), which integrated to give a roughly 40% local loss inside the vortex during January and February of 1992. Confidence in the technique was obtained because the observed depletion only occurred during sunlit times, as would be expected from our understanding of chemical ozone depletion. Chemical ozone depletions have subsequently been evaluated with this method for other Arctic winters (e.g., Rex *et al.*, 1998), with much more extensive spatial and temporal coverage of the vortex. Figure 7-23 shows results from the colder winter of 1994/95. Ozone loss was calculated from about 370 K to 600 K during January through March. The maximum deduced loss rates were over 1.5×10^{11} molecule $\text{cm}^{-3} \text{day}^{-1}$ (~3.3% day^{-1}) at 425 K (about 18 km) in March, and the accumulated total chemical loss in this altitude range through January-March was calculated to be about 125 DU.

The Match technique has the advantage of providing direct quantification of local chemical ozone loss, because it considers ozone changes over short periods for which air masses retain their integrity. Its disadvantage is that it is difficult to quantify total ozone loss over the vortex using only the ozonesonde matches and it does not work when ozone losses are small. Two alternative techniques use satellite measurements to provide vortex-averaged estimates, but must consider changes over longer time periods for which the concept of an air mass is more questionable. Thus the strengths and weaknesses of the Match technique and these two

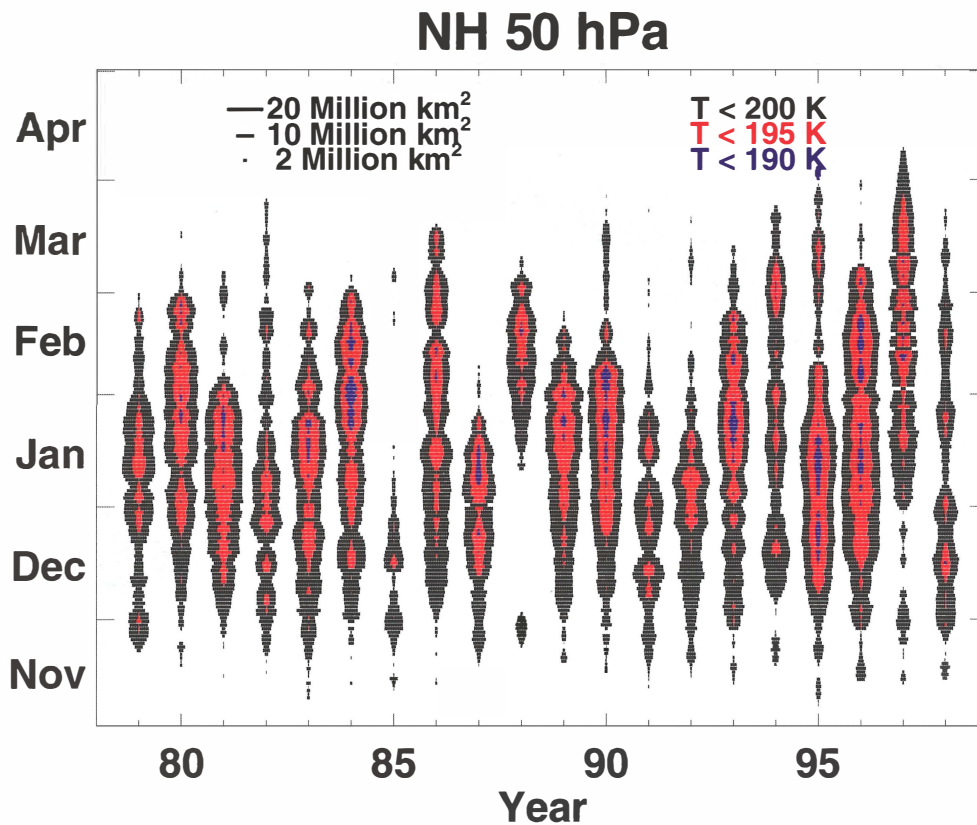


Figure 7-22. Time evolution of the areal coverage of cold 50 hPa temperatures in the Arctic polar region for each winter from 1979 to 1998. The width of each line is proportional to the temperature surface area coverage (see top left key), while the line color represents a particular temperature (see top right key). For example, in early November, there are no observed temperatures below 200 K in the polar region, while the 200 K areal coverage during January oftentimes exceeds 20 million km². Note also that 190 K temperatures (blue) are infrequent, and typically cover only a few million km². (Supplied by Paul Newman, NASA Goddard Space Flight Center, U.S.).

techniques, described below, are complementary.

The first alternative technique (e.g., Manney *et al.*, 1995b, 1997) uses MLS satellite observations of O₃ in the lower and middle stratosphere together with calculated three-dimensional trajectories to estimate the effect of transport in compensating for in situ chemical loss. Because this technique does not explicitly include mixing, a large number of closely associated trajectories are used. The results indicate that a considerable fraction of the chemical loss that occurs during late-winter/spring is masked by transport, to the extent that there is often little relation between local chemical loss and observed changes in column ozone. The calculated O₃ losses tend to follow periods of activated chlorine, provided there is sunlight. For example, in 1996/97 the greatest

abundances of ClO at 465 K (~18 km) were observed in late February, and a vortex-averaged chemical depletion of 0.6 ppmv (20%) was estimated to occur at this altitude during March and early April (Manney *et al.*, 1997).

The second alternative technique (Müller *et al.*, 1996, 1997) uses simultaneous HALOE satellite observations of O₃ and CH₄ within the vortex to construct equivalent vertical profiles of O₃ that factor out the effects of diabatic descent by treating CH₄ as an air mass label. Changes in O₃ for each value of CH₄ are then summed to provide an estimate of total chemical ozone loss within the vortex. Such a calculation should give a reasonable estimate of the vortex-averaged chemical ozone loss if the air within the vortex is isolated during the period of analysis and subject only to unmixed descent. The effects

LOWER STRATOSPHERIC PROCESSES

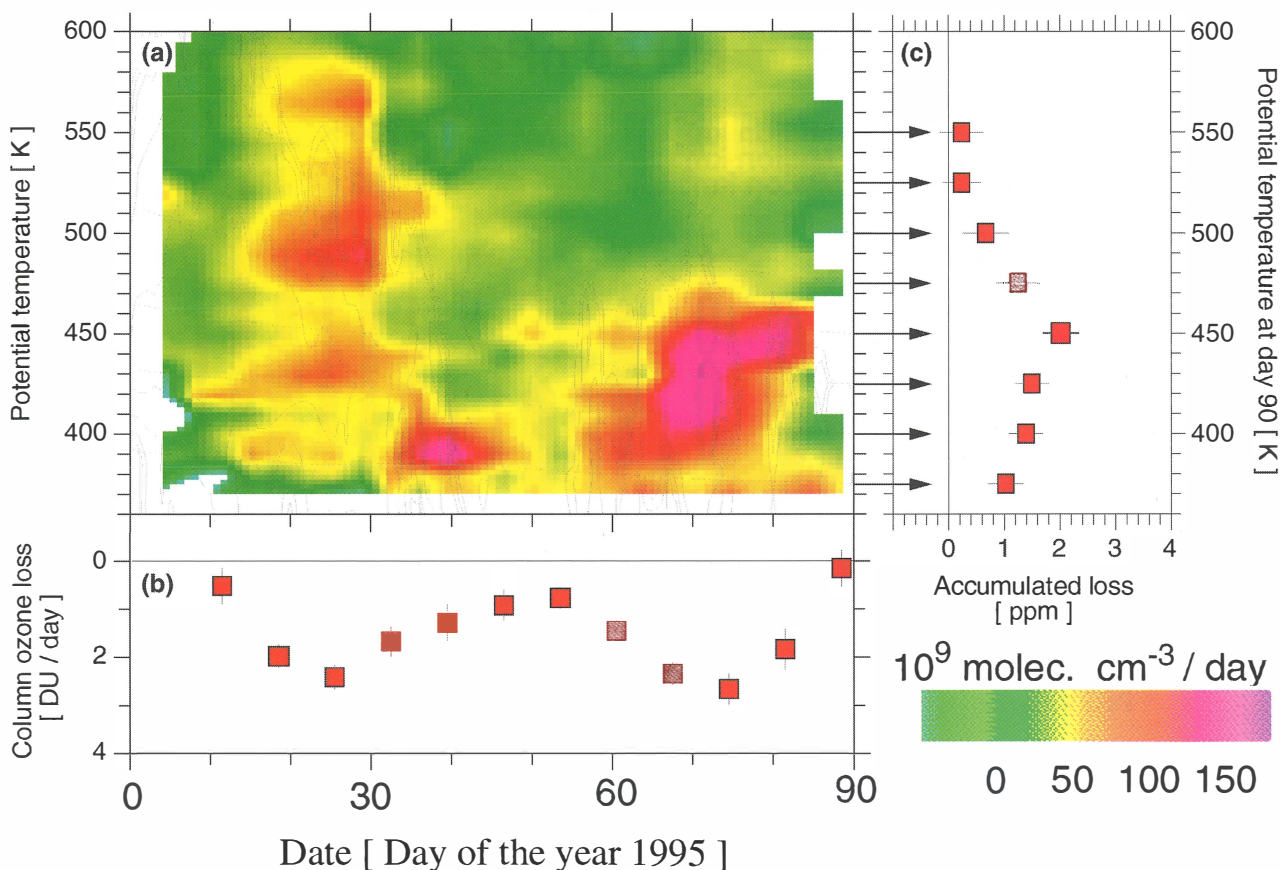


Figure 7-23. (a) Contour plot showing the ozone loss rate as a function of date and potential temperature. A total of 1470 matches contributed to this plot. There was significant ozone loss when the temperatures were cold enough for PSCs to form (see Rex *et al.*, 1998). (b) Ozone column loss rates obtained by integrating the local loss rates from 370 K to 600 K. The accumulated column loss over the winter is 127 ± 14 DU (corresponding to $36 \pm 4\%$, with 350 DU as the vortex-averaged ozone column at day one). (c) The accumulated ozone loss integrated over time between day 1 and day 90 (day 20-90, day 40-90, day 50-90 for the upper most levels, respectively) in the air masses subsiding to indicated levels. All error bars show 1σ uncertainties. (Adapted from Rex *et al.*, 1998).

of mixing on the accuracy of the estimate are yet to be determined. This technique has been used to estimate chemical ozone losses between November/December and March/April during the Arctic winters of 1991/92 through 1996/97 (Müller *et al.*, 1997). The losses range from 50 DU (1996/97) to 120-160 DU (1995/96), with more than 50% local loss in the lower stratosphere in the latter.

The above studies, taken together, clearly show that significant chemical ozone depletion has occurred inside the polar vortex in recent Arctic winters, and is, therefore, an important component of the observed reduction in column O₃ seen in Figure 7-19. These studies also show that enhanced ozone depletion inside the Arctic vortex is due to a combination of cold temperatures, high active

chlorine, and exposure to sunlight, consistent with our theoretical expectations. Significantly, although cold Arctic winters before the build-up of anthropogenic chlorine, such as that in 1967, were characterized (as we would expect) by low ozone, the ozone abundances were never as low as those seen recently (Fioletov *et al.*, 1997).

Chemical ozone depletion in the Arctic has been simulated by constraining models, to various degrees, with observations. Models that use measured ClO amounts and isentropic transport derived from analyzed winds have succeeded in broadly reproducing the observed ozone losses (Mackenzie *et al.*, 1996). Such studies provide strong evidence that the qualitative picture of chemical ozone loss is correct. However, they

are only valid for short time periods (less than seasonal) and thus cannot directly model the long-term ozone trend. Models that predict both the ozone and chlorine fields over longer time periods have been less successful (Chipperfield *et al.*, 1996; Hansen *et al.*, 1997). These models tend to underpredict the ClO fields, possibly due to unresolved mesoscale structure (see Section 7.4.1) or other model deficiencies (see Section 7.5.4). In addition, even these model simulations have not been run over long enough time periods to calculate the long-term trend, i.e., the possible contribution of a transport-induced change to the trend has not been directly estimated.

The croissant shaped region in the Arctic, referred to earlier, bridges the high-latitude vortex region with the midlatitudes. While less dramatic than the ozone depletions inside the vortex, the ozone losses in this region are still quite large and mostly seasonal, exhibiting a maximum during March (Figure 7-21 and Chapter 4). Unfortunately, the Lagrangian-based methods that have been successfully used inside the vortex to identify chemical ozone depletion cannot be used here because the time scales for ozone loss are too long. In this respect, the problem of attribution is similar to that encountered with midlatitude decadal trends (see Section 7.6.2 below). Based on our present understanding of ozone chemistry, we expect in situ chemical loss driven by direct chlorine activation on sulfate aerosol during cold temperature excursions. Two-dimensional model results including this effect can indeed reproduce the trend and some of the variability in ozone in this region (50-60°N) when constrained by observed zonal-mean temperatures together with the effects of temperature fluctuations driven by observed planetary-wave amplitudes (Solomon *et al.*, 1998). However, it has not been possible to quantify the possible role of transport changes in this region, or the influence of within-Arctic ozone loss (2-D models do not represent transport within the vortex edge region very well; see Section 7.5.2).

Thus, while a large body of evidence supports the conclusion that chemical ozone loss is occurring seasonally in the Arctic, uncertainties remain in the partitioning of the long-term trend between purely local chemical loss and other factors. Despite their differences, the physical and chemical environment in the Arctic has many similarities to the Antarctic. The conceptual picture that cold temperatures activate chlorine, and that the chlorine available for ozone depletion thus depends on total chlorine as well as on temperature, is valid in both hemispheres. The primary complications in quantifying

and attributing the ozone depletion in the Arctic are the difficulties in estimating the transport and containment in the vortex, and difficulty in predicting the temperatures. Temperatures are especially important because they are in a regime where very small decreases cause very large increases in activation of chlorine. Yet, it is clear that the depletions in the Arctic during the 1990s are due to colder temperatures in the presence of chlorine loading that was already high. In contrast, the increased depletions observed in the Antarctic during the 1980s were the result of increased chlorine loading in the presence of temperatures that were already cold. The extent of late-winter/spring ozone depletion in the Arctic during the next few years will depend on meteorological conditions.

7.6.2 Midlatitude Trends

There is a large body of evidence that shows that the increased chlorine and bromine loading has contributed to the observed midlatitude ozone depletion (with the chemical loss principally occurring via midlatitude chemical processes). However, quantification of the processes contributing to this depletion is not complete. In particular, the balance between changes due to chlorine-related chemical processes and the (likely smaller) decadal variations in the circulation is not known. Obtaining such a quantitative understanding will probably require models that accurately represent chemistry, aerosol loading, temperature, and transport (including interannual and decadal variations). Recent laboratory and field studies suggest that iodine compounds from the troposphere do not contribute more than about 10% of the local observed depletion of ozone in the lowest part of the stratosphere. The role of cirrus clouds is unclear and could be a significant contributor to the ozone depletion in the lowest part of the stratosphere.

Ground-based and satellite observations both show decadal decreases in column ozone in the midlatitudes of both hemispheres (see Chapter 4). The major contributor to the column loss is the decrease in the lower stratosphere around 20 km, even though the fractional local depletion in the upper stratosphere is comparable to that in the lower stratosphere. In contrast to the polar seasonal depletion discussed in Section 7.6.1, the decadal trend in ozone at midlatitudes is markedly smaller than the seasonal cycle and is comparable in magnitude to the natural interannual variability. The decadal trend in

LOWER STRATOSPHERIC PROCESSES

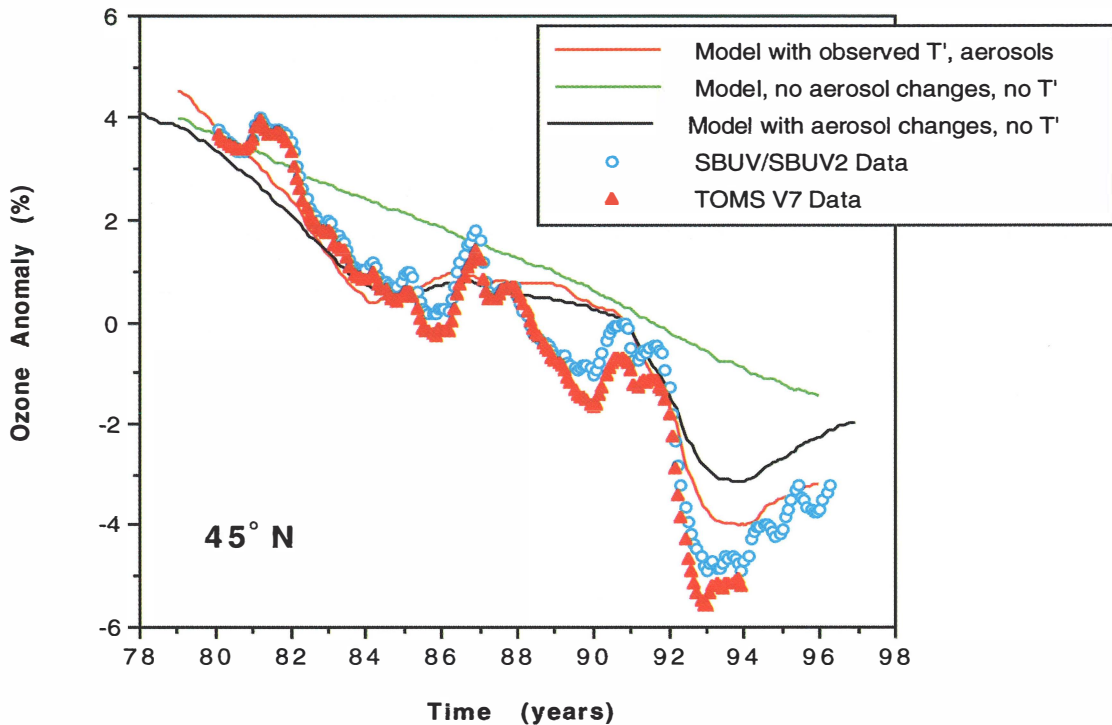


Figure 7-24. Observed and calculated total ozone anomalies from 1979 to 1997 at 45°N. All cases shown are smoothed by a 25-month running mean to average over both the annual cycle and the QBO. Red triangles show the zonally averaged TOMS V7 data and the blue circles show the combined SBUV/SBUV2 data. All model results shown include chlorine and bromine increases. In addition, the red line shows the model results including observed aerosol variations and zonal mean temperature and planetary wave temperature amplitudes (T') estimated from National Centers for Environmental Prediction (NCEP) observations. The black line is similar to the red line except the planetary wave temperature amplitudes are not used in the model. The green line shows model results with constant 1979 aerosol observation used throughout the calculation. (Adapted from Plate 1 of Solomon *et al.* (1996) using TOMS V7 data and model results from Solomon *et al.*, 1998).

the monthly mean values at high latitudes also shows a clear downward trend. The magnitude of the column ozone decadal trend and the vertical variation in the fractional depletion have been revised in this Assessment. This revision shows that significant uncertainty still remains in the quantification of the trend, especially in the last few years (see Chapter 4).

Because of the difficulty in obtaining the quantitative trend estimates from data, it is critical that we use the pattern of the ozone changes in time and space and attempt to attribute the patterns, rather than the precise magnitudes, of the changes to causes. Important signatures are provided by the latitudinal, vertical, and seasonal dependence of the trends, as well as by the

effects of volcanic eruptions.

The Mt. Pinatubo eruption, in particular, had a major impact on midlatitude ozone (see Section 7.4.3). The direct radiative-dynamical effects due to the aerosol cloud were mostly confined to the first year after the eruption, but the ozone perturbation lasted for several years (see Figure 7-24), suggesting that chemical effects from the increased aerosol played a significant role. Based on laboratory studies of heterogeneous/multiphase processes and analysis of in situ measurements, increased volcanic aerosol is expected to enhance ozone depletion in midlatitudes in the presence of current chlorine loading because the amount of reactive chlorine species would be greatly enhanced in such situations. Note that without

chlorine, stratospheric ozone would, in contrast, be expected to increase with an increase in volcanic aerosol because enhanced volcanic aerosol will decrease the levels of nitrogen oxides and thereby reduce ozone loss by NO_x catalytic cycles (Solomon *et al.*, 1998; Tie and Brasseur, 1995). Indeed, increases in ozone abundances in the middle stratosphere, where NO_x is the dominant catalyst (see Section 7.5.1), are visible in HALOE data following the Mt. Pinatubo eruption (Mickley *et al.*, 1998). Figure 7-24 shows the smoothed anomalies from satellite measurements of ozone for the 1979-1995 period compared with a two-dimensional model simulation (Solomon *et al.*, 1996; Solomon *et al.*, 1998). The model ozone variation is dominated by the trend in chlorine (and a smaller trend in bromine) along with the volcanic perturbation of the aerosols. The dramatic decreases observed after the Mt. Pinatubo eruption are reproduced, together with the ozone decrease after the El Chichón eruption in 1982 and the relatively flat period during the late 1980s.

The Mt. Pinatubo eruption illustrates the strong nonlinear coupling that exists between natural (volcanic) and anthropogenic (halogen) effects. Statistical regression techniques, based on an assumption of linear superposition, cannot be expected to separate natural from anthropogenic parts of this signal.

While the pattern of the model-based ozone anomalies shown in Figure 7-24 and those derived by Jackman *et al.* (1996) is similar in many respects to that of the observations, the magnitude is not exactly the same. The differences in magnitude could be due to various shortcomings of the 2-D models (see Section 7.5.2) or due to uncertainties in the derived trend (see Chapter 4). Note also that existing 2-D model results have used a fixed dynamical forcing, and changes in dynamical forcing could well be an important contributor to the signal (see further discussion below). Yet regardless of the differences in magnitude, the agreement in the timing of changes in midlatitude ozone between model and observations provides strong evidence for the dominant role of chlorine (and bromine) in causing the observed ozone changes following the Mt. Pinatubo eruption.

The vertical profile of the trends provides a second important signature for the cause of the ozone depletion. Chemical effects of increasing chlorine and bromine, largely due to multiphase chemistry in aerosols, give an ozone depletion with a vertical dependence consistent with that observed, namely, with greater depletion in the lower stratosphere than in the middle stratosphere

(Chapter 4). This vertical dependence arises because while chlorine is a major contributor to ozone loss in the lower stratosphere, its relative contribution decreases with altitude before increasing again in the upper stratosphere. However there are quantitative differences between observations and the results from 2-D models, which are likely related both to uncertainties in the trends and to deficiencies in the models. For example, 2-D models are not expected to accurately represent the transport in the lowermost stratosphere (below about 16 km) (see Section 7.5.2). Possible chlorine activation on cirrus clouds (see below) is also not explicitly included in some of the above models. Because of the above reasons, uncertainties in simulations of ozone depletion in 2-D models, especially at altitudes just above the tropopause, are not surprising.

Other signatures of the ozone change include the latitudinal variation and seasonal cycle of the trend in total ozone. These can be summarized as enhanced depletion at higher latitudes, larger depletion in northern midlatitudes than in southern midlatitudes, and with the largest effect (in both hemispheres) in winter and spring (Chapter 4). These features are qualitatively consistent with the impact and temperature dependence of heterogeneous/multiphase reactions. Possible factors that contribute to the NH/SH asymmetry are the colder temperature and lower water abundances in the SH, differences in the amplitude of longitudinal asymmetries, and differences in the rate of ozone transport. It does not appear that the asymmetry between North Pole and South Pole directly affects midlatitudes, at least not above 16 km (see further discussion below). While a detailed understanding of these patterns is not well characterized, the overall trends in time and space are consistent with the hypothesis that chlorine and bromine are the primary cause of the lower stratospheric ozone depletion in the midlatitudes.

Our understanding and modeling of midlatitude chemistry is based to some extent on analyses of photochemistry over the Antarctic and the Arctic, where temperatures are cold enough to extensively activate chlorine and subsequently deplete ozone. In the lower stratosphere, hydrolysis of N_2O_5 on sulfate aerosol indirectly enhances active chlorine and direct activation of Cl_y at cold temperatures also impacts radical speciation. HO_x and NO_x catalytic cycles dominate midlatitude ozone loss, but the ClO_x catalytic cycle is a significant ozone loss mechanism at altitudes below 25 km (see Section 7.5.1). Increasing chlorine then leads

LOWER STRATOSPHERIC PROCESSES

to enhanced ozone loss in this region. Midlatitude ozone depletion in the lower stratosphere is thus more like that in the polar regions than that in the upper stratosphere: in the lower stratosphere temperatures are low enough for chlorine activation, and ozone production regions are far away; thus, significant ozone depletion can occur even for significantly slower ozone loss rates than those found in polar regions or in the upper stratosphere.

In view of the polar (high latitude) ozone depletion, an important question is how much of the midlatitude ozone trend might be due to polar effects. This is related to basic questions of how well we understand the stratospheric circulation. Observational and 3-D modeling studies indicate that above 16 km only a small amount of polar processed air is transported into midlatitudes before the vortex breaks up, and that this process will not have a large impact on midlatitude ozone (see Section 7.3.3.2). However, there are indications that there is greater transport of polar processed air below 16 km, and that this process may play a role in midlatitude low altitude ozone depletion. Also, 3-D modeling studies suggest that post-vortex ozone dilution has an impact on midlatitude ozone in both the Southern (e.g., Brasseur *et al.*, 1997; Eckman *et al.*, 1996) and Northern (Hadjinicolaou *et al.*, 1997) Hemispheres. There is also a clear springtime signature of Antarctic vortex dilution in NO_y and H_2O poleward of 50°S (Nevison *et al.*, 1997; Rosenlof *et al.*, 1997).

Although natural interannual variability cannot account for the large ozone depletion following the volcanic eruptions, it cannot be conclusively eliminated as a cause of the observed decadal midlatitude ozone decline. Simulations with both 2-D (e.g., Callis *et al.*, 1997; Jackman *et al.*, 1996; Schneider *et al.*, 1991) and 3-D (Hadjinicolaou *et al.*, 1997) models indicate that interannual variability in the stratospheric circulation may be a significant contributor to interannual changes in midlatitude ozone. For example, Hadjinicolaou *et al.* (1997) reproduce many of the changes in column ozone in northern midlatitudes during 1992 to 1994 (in particular, the recovery in 1993) in a model that includes interannual variability in the meteorology but no heterogeneous/multiphase chemistry. Furthermore, a statistical link has been found between the observed decadal changes in stratospheric ozone and the observed changes in lower stratospheric circulation (Hood *et al.*, 1997), as well as between ozone changes and changes in the wave forcing that drives the stratospheric circulation (Fusco and Salby, 1998). Fusco and Salby point to the

striking observed anticorrelation between interannual variations of extratropical and tropical total ozone as providing further evidence for the role of variations in the Brewer-Dobson circulation. While this anticorrelation clearly holds on time scales of a few years, it does not necessarily apply on longer time scales; indeed, there is no statistically significant decadal trend in total ozone in the tropics (Chapter 4). Note also that a decadal trend in the strength of the Brewer-Dobson circulation should be reflected in compensating trends in tropical and extratropical temperatures (see Section 7.3.1), and such a trend is not seen in Figure 7-5.

Interpreting the statistical relationships referred to above is not, in any case, straightforward. Because of the synergy that exists between dynamics and chemistry, a trend in chemical ozone loss driven by a change in dynamical conditions, such as has occurred in the Arctic late-winter/spring over the last decade (see Section 7.6.1), would in the context of a statistical regression analysis be explained by the dynamical proxy. In fact, dynamical and chemical effects interact strongly and it is not simply a case of one effect or the other (see further discussion in Section 7.7).

Future trends in ozone at midlatitudes (i.e., ozone recovery as chlorine and bromine loading decreases in the future) are dependent on any trends in stratospheric circulation. Trends in lower stratospheric temperature will also be critical because activation of chlorine on condensed matter is highly temperature dependent. These effects make lower stratospheric ozone particularly sensitive to future climate change.

In addition to the chemical processes discussed above, other processes have been invoked to account for the observed ozone depletion in the lowermost stratosphere: (a) activation of chlorine via heterogeneous/multiphase reactions on condensed matter in the tropopause region and (b) iodine-catalyzed ozone destruction.

The same heterogeneous/multiphase reactions that occur in the polar regions can also take place in the tropopause region. It is well known that the altitude where the ozone starts to increase toward stratospheric values is generally about 1 km below the thermal tropopause. If the elevated ozone is due to stratospheric air, non-zero Cl_y should also be present in this region. Additionally, the water vapor mixing ratios are much higher in this altitude region compared to higher altitudes (Oltmans and Hofmann, 1995; Holton *et al.*, 1995) and, thus, many key heterogeneous reactions (Hanson and

Ravishankara, 1994) must be rapid. Based on in situ ER-2 data for aerosol and chemical composition and 2-D model calculations for the concentrations of the chlorine-containing gas phase species, Borrmann *et al.* (1997) showed that heterogeneous chlorine activation could be close to or exceed that from the gas phase OH + HCl reaction. Solomon *et al.* (1997, 1998) showed that multiphase reactions on the aerosol of the tropopause region could enhance ClO sufficiently to make a significant contribution to the ozone depletion in northern midlatitudes.

Some field data suggest that ClO increases are due to chlorine activation in the tropopause region. Solomon *et al.* estimated an average ClO enhancement of about 50% at the tropical tropopause because of the nearly continuous presence of cirrus clouds there as indicated by the satellite observations. Borrmann *et al.* (1997) showed that up to 2.7 parts per trillion by volume (pptv) of ClO could be formed in a single cirrus cloud event, albeit with considerable uncertainties. Their model calculations also indicate that it will take several days for the enhanced ClO to return to "clear sky" levels. Thus the impact of the heterogeneous chemistry may last longer than a specific cloud event itself. Other evidence for this process comes from observations of unusually low ozone concentrations inside cirrus clouds (Reichardt *et al.*, 1996) and the reduced NO/NO_y ratio and ClO abundances near 90 pptv observed by Keim *et al.* (1996) in a layer of volcanic aerosol 500 m above the midlatitude tropopause.

Ozone trends in the lowermost stratosphere may also be affected by iodine-chlorine chemistry. Based on the observed abundance of natural iodine compounds in the troposphere, Solomon *et al.* (1994) assumed that up to 1 pptv of iodine could be present in the lower stratosphere. If such an abundance of iodine was present in the lower stratosphere, they suggested that a large fraction of the decadal trend of ozone in the lowermost stratosphere could be due to the reaction between IO and ClO; the abundance of IO remained constant while that of ClO increased due to the increasing chlorine loading, i.e., the trend in ozone arises because of the trend in chlorine. They assumed a rate coefficient for the reaction of ClO with IO of $1 \times 10^{-10} \text{ cm}^3 \text{ molecule}^{-1} \text{ s}^{-1}$, based on analogy with known reactions of IO with IO and of ClO with BrO. The rate coefficient for this reaction has now been measured to be 5 times slower at lower stratospheric temperatures (Turnipseed *et al.*, 1997). In addition, long-path atmospheric ultraviolet (UV) absorption

measurements have placed limits of <0.2 pptv for IO in the lower stratosphere (Pundt *et al.*, 1998; Wennberg *et al.*, 1997). Based on these two sets of findings, it appears that iodine may not contribute very significantly to the observed lower stratospheric ozone depletion (Gilles *et al.*, 1997). However, Solomon *et al.* (1997) show that cirrus enhancement of ClO could lead to an increased efficiency of iodine such that even 0.1 pptv of IO could lead to a 10% increase of the ozone loss rate. Thus, contributions of iodine to the lower stratospheric ozone depletion cannot be ruled out, but their contribution to the column ozone decreases should be small. Yet, it appears that injection of iodine to the stratosphere would be detrimental to the ozone in this region.

7.7 SYNTHESIS

Chemical, microphysical, and dynamical processes each play critical roles in determining the abundance of ozone in the lower stratosphere. (N.B. In this section, for brevity, "dynamics" is understood to include radiation as well as wave forcing and transport.) Often, these processes can reinforce each other with regard to changing ozone levels, while in other situations they tend to cancel or reduce the effect of one another. In situations where the dynamical processes are separable in time and space from the chemical processes, it is possible to detect, quantify, and, even, attribute the ozone changes to certain causes. However, it is never possible to truly separate microphysics from either chemistry or dynamics; dynamics forces temperature changes, while chemistry controls the concentration of the many constituents such as HNO₃ that make up the various types of condensed matter. Our understanding is not yet sufficient to quantitatively deal with a situation where the effects of all three kinds of processes are not separable.

Given this situation, can we answer the question: What is causing lower stratospheric ozone depletion? In other words, in what way is the lower stratosphere of today different from that of the 1970s? What agents that force alterations in ozone abundance have changed during this period? What caused their changes?

Over the last few decades there has been a definite increase in the abundance of stratospheric halogens, which chemically forces a change in the system. Our current understanding of stratospheric chemistry implies that, if all other things remained the same, the chlorine increase should lead to ozone depletion. However, this does not mean that we can therefore attribute the changes

LOWER STRATOSPHERIC PROCESSES

in observed ozone abundances to halogens and halogens alone. At the same time as chlorine changed, there was natural variability in dynamics (arising from dynamical variability on many different time scales and perhaps including some kind of climate drift effect), as well as in the rates of heterogeneous/multiphase processes (arising principally from volcanic eruptions). Because chemical, dynamical, and microphysical processes are strongly coupled in the lower stratosphere, the chemical forcing interacts with the natural variability and, thereby, prevents a straightforward attribution of any perceived correlation between ozone changes and chlorine increases to the effects of halogens alone.

Therefore, an understanding of the causes of ozone depletion in the lower stratosphere must be based not only on the observed trends but also on an understanding of how chemical, microphysical, and dynamical processes interact, and when they lead to ozone depletion. The way in which these processes work together is quite different in the different regions of the lower stratosphere, and our level of understanding and predictive ability vary accordingly. For example, in polar regions, where the depletion is seasonal, the separation between dynamics and chemistry is easier. Further, there is a synergism between dynamics and chemistry that produces much greater ozone depletion than would be the case from either effect (isolated cold vortex or halogens) alone. In midlatitudes, the transport and chemical lifetimes are very similar and dynamical and chemical processes are inseparable. However, the synergism between the two processes is much weaker. On a different temporal and spatial scale, there is a synergism between microphysics and chemistry subsequent to aerosol loading from volcanic eruptions that, again, produces much greater ozone depletion than would be the case from either effect (halogens or aerosol loading) alone.

Quantitative understanding of the overall, coupled effects of these processes is limited by our current understanding of the processes themselves. In a few cases, this understanding is incomplete at a fundamental level. One example is the rates of reactions on condensed matter (see Section 7.2.3), which remain uncertain in large measure due to an insufficient understanding of the microphysical processes that determine the nature of the condensed matter in the stratosphere (see Section 7.2.2). A second example is the impact of mesoscale microphysical and chemical structure on ozone loss rates (see Section 7.4.1). A third example is the impact of gravity wave drag on winter stratospheric polar temperatures

(see Section 7.5.3). These limitations in our basic understanding are also present inherently in stratospheric models. In addition to these fundamental deficiencies, there are other deficiencies in models of a more quantitative nature, such as the ability to represent dynamics adequately, that provide a significant uncertainty in the prediction of ozone changes (see Section 7.5). However, very useful and reliable information can nevertheless be obtained for certain questions from models that either do not represent or do not represent accurately all the processes discussed above.

The problem of identification, quantification, and attribution of ozone depletion depends very much on the level of the above uncertainties, as well as on the nature of the coupling between chemical forcing and natural variability. Broadly speaking, the problem is progressively more difficult in today's Antarctic, Arctic, and midlatitudes, for reasons discussed earlier.

In today's Antarctic, we have a "cause-and-effect" relationship between halogens and ozone. Dynamics provide a setting for cold temperatures and the consequent heterogeneous chemical processing to act for long periods of time on a nearly isolated air mass. Compositional changes in this region can thus be quantified from direct observations. We can account for the observed seasonal ozone loss, and we can confidently state that chlorine and bromine are responsible. Details of the microphysics do not matter much, because the time scales for chlorine activation and ozone destruction (in a given layer of the polar stratosphere) are less than the duration of the vortex. Thus, uncertainties in ozone destruction rates do not, at present, affect the calculated total extent of ozone depletion. On the other hand, as chlorine levels decrease in the future, the ozone destruction time will become comparable to dynamical time scales; in that case, given present uncertainties, it will become difficult to quantify and, at some point, perhaps difficult even to attribute ozone depletion to chlorine and bromine.

In today's Arctic, we almost have a "cause-and-effect" relationship. Dynamics does not provide the same setting for complete ozone destruction as in the Antarctic, because the vortex does not provide as much isolation, and there is much more interannual variability. This means that we cannot quantify the extent of ozone depletion without accounting for dynamics. At present, this is achieved by removing the purely dynamical effects (see Section 7.6.1) using various techniques. We conclude that the large springtime ozone depletion

observed in the Arctic in recent years is due to more “Antarctic-like” meteorological conditions (i.e., a colder, more isolated Arctic vortex), leading to reduced transport of ozone as well as increased chemical loss due to chlorine and bromine. If the Arctic reverts to characteristics of the 1980s in future years, we would expect reduced chemical loss even while chlorine remains at present-day high values. However, it is not obvious that this level of attribution will continue to be possible in the future, as chlorine levels decrease. An additional point is that because the ozone destruction in the Arctic is not complete, time scales matter, and so the uncertainties discussed above mean that we cannot now quantitatively account for the extent and the rate of ozone depletion in that region.

The midlatitude lower stratosphere has many features in common with the polar regions: it is far away from the ozone production region, has low temperatures and condensed matter (sulfuric acid aerosols) that can activate chlorine and bromine, and is characterized by relatively slow ozone loss rates (compared with those in the upper stratosphere or the tropics). In contrast to the polar regions, however, the observed decadal ozone depletion in midlatitudes cannot be well quantified. Even the ozone depletion that has been quantified cannot be unambiguously identified as an “enhanced chemical loss.” By chemical loss we mean that ozone was removed chemically from the lower stratosphere at midlatitudes after it was transported to this region. This uncertainty arises partly because the depletion is much smaller than in the polar regions; it is only a small trend compared with the seasonal cycle, which must be extracted by statistical means. It is also partly because there is not sufficient integrity, or coherence, of air masses over the time scale of chemical loss to use the currently available methods, which have been used in polar regions, for isolating compositional changes from dynamical variations (see Section 7.6.1).

Given this situation, we attempt to explain the decadal midlatitude lower-stratospheric ozone depletion by examining the patterns of this depletion in space and time. The variations of ozone depletion with altitude, latitude, season, and volcanic forcing all hold clues to the causes of ozone depletion. The space-time pattern of the depletion is consistent with it being due to chlorine and bromine. The strongest of these connections arises from the impact of the eruption of Mt. Pinatubo and the clearly visible short-term (a few years) rapid decrease in the ozone abundance. This decline can be demonstrably

connected to the effect of chlorine and bromine loading at midlatitudes, and linked to chemical loss as opposed to natural dynamical variability. The vertical distribution of the ozone depletion is also semi-quantitatively consistent with chlorine and bromine being responsible for the decadal ozone trend. Such vertical variations in the contributions of various chemical catalysts have been determined not only from models but also directly in some locations by field measurements of the reactive radicals. The patterns in ozone change with latitude and season are not inconsistent with halogens being responsible. Based on this evidence, there is increasing evidence that a significant fraction of the lower-stratospheric ozone depletion in midlatitudes is driven by anthropogenic halogens, although a significant influence of natural variability in transport cannot be ruled out.

REFERENCES

- Abbatt, J.P.D., Heterogeneous reaction of HOBr with HBr and HCl on ice surfaces at 228 K, *Geophys. Res. Lett.*, *21*, 665-668, 1994.
- Abbatt, J.P.D., Interaction of HNO₃ with water-ice surfaces at temperatures of free troposphere, *Geophys. Res. Lett.*, *24*, 1479-1482, 1997.
- Abbatt, J.P.D., and M.J. Molina, Heterogeneous interactions of ClONO₂ and HCl on nitric acid trihydrate at 202 K, *J. Phys. Chem.*, *96*, 7674-7679, 1992.
- Aliwell, S.R., D.J. Fish, and R.L. Jones, Midlatitude observations of the seasonal variation of BrO: 1, Zenith sky measurements, *Geophys. Res. Lett.*, *24*, 1195-1198, 1997.
- Allanic, A., R. Oppliger, and M.J. Rossi, Real-time kinetics of the uptake of HOBr and BrONO₂ on ice and in the presence of HCl in the temperature range 190 to 200 K, *J. Geophys. Res.*, *102*, 23529-23541, 1997.
- Allen, S.J., and R.A. Vincent, Gravity wave activity in the lower atmosphere: Seasonal and latitudinal variations, *J. Geophys. Res.*, *100*, 1327-1350, 1995.
- Andrews, D.G., J.R. Holton, and C.B. Leovy, *Middle Atmospheric Dynamics*, 489 pp., Academic Press, New York, 1987.
- Appenzeller, C., and J.R. Holton, Tracer lamination in the stratosphere: A global climatology, *J. Geophys. Res.*, *102*, 13555-13569, 1997.
- Appenzeller, C., H.C. Davies, and W.A. Norton, Fragmentation of stratospheric intrusions, *J. Geophys. Res.*, *101*, 1435-1456, 1996a.

LOWER STRATOSPHERIC PROCESSES

- Appenzeller, C., J.R. Holton, and K.H. Rosenlof, Seasonal variation of mass transport across the tropopause, *J. Geophys. Res.*, *101*, 15071-15078, 1996b.
- Arnold, F., V. Burger, K. Gollinger, M. Roncossek, J. Schneider, and S. Spreng, Observations of nitric acid perturbations in the winter Arctic stratosphere: Evidence for PSC-sedimentation, *J. Atmos. Chem.*, *30*, 49-59, 1998.
- Arpag, K.H., P.V. Johnston, H.L. Miller, R.W. Sanders, and S. Solomon, Observations of the stratospheric BrO column over Colorado, 40N, *J. Geophys. Res.*, *99*, 8175-8181, 1994.
- Atkinson, R., D.L. Baulch, R.A. Cox, R.F. Hampson, J.A. Kerr, M.J. Rossi, and J. Troe, Evaluated kinetic and photochemical data for atmospheric chemistry: Supplement V, IUPAC subcommittee on gas kinetic data evaluation for atmospheric chemistry, *J. Phys. Chem. Ref. Data*, *26*, 521-1011, 1997.
- Atticks, M.G., and G.D. Robinson, Some features of the structure of the tropical tropopause, *Quart. J. Roy Meteorol. Soc.*, *109*, 295-308, 1983.
- Avallone, L.M., and M.J. Prather, Photochemical evolution of ozone in the lower tropical stratosphere, *J. Geophys. Res.*, *101*, 1457-1461, 1996.
- Avallone, L.M., S.M. Schauffler, W.H. Pollock, L.E. Heidt, E.L. Atlas, and K.R. Chan, In situ measurements of BrO during AASE II, *Geophys. Res. Lett.*, *22*, 831-834, 1995.
- Bacmeister, J.T., S.D. Eckermann, P.A. Newman, L. Lait, K.R. Chan, M. Loewenstein, M.H. Proffitt, and B.L. Gary, Stratospheric horizontal wavenumber spectra of winds, potential temperature, and atmospheric tracers observed by high-altitude aircraft, *J. Geophys. Res.*, *101*, 9441-9470, 1996.
- Ball, S.M., G. Hancock, S.E. Martin, and J.C.P.D. Moira, A direct measurement of the O(¹D) quantum yields from the photodissociation of ozone between 300 and 328 nm, *Chem. Phys. Lett.*, *264*, 531-538, 1997.
- Balluch, M.G., and P.H. Haynes, Quantification of lower stratospheric mixing processes using aircraft data, *J. Geophys. Res.*, *102*, 23487-23504, 1997.
- Banham, S.F., A.B. Horn, T.G. Koch, and J.R. Sodeau, Ionisation and solvation of stratospherically relevant molecules on ice films, *Faraday Discuss. Chem. Soc.*, *100*, 321-332, 1995.
- Beagley, S.R., J. de Grandpré, J.N. Koshyk, N.A. McFarlane, and T.G. Shepherd, Radiative-dynamical climatology of the first generation Canadian middle atmosphere model, *Atmos.-Ocean*, *35*, 293-331, 1997.
- Beekman, M., G. Ancellet, and G. Mégie, Climatology of tropospheric ozone in southern Europe and its relation to potential vorticity, *J. Geophys. Res.*, *99*, 12841-12854, 1994.
- Bekki, S., On the possible role of aircraft-generated soot in the middle latitude ozone depletion, *J. Geophys. Res.*, *102*, 10751-10758, 1997.
- Bischof, W., R. Borchers, P. Fabian, and B.C. Kruger, Increased concentration and vertical distribution of carbon dioxide in the stratosphere, *Nature*, *316*, 708-710, 1985.
- Boer, G.J., and M. Lazare, Some results concerning the effect of horizontal resolution and gravity wave drag on simulated climate, *J. Climate*, *1*, 789-806, 1988.
- Boering, K.A., B.C. Daube, S.C. Wofsy, M. Loewenstein, J.R. Podolske, and E.R. Keim, Tracer-tracer relationships and lower stratospheric dynamics: CO₂ and N₂O correlations during SPADE, *Geophys. Res. Lett.*, *21*, 2567-2571, 1994.
- Boering, K.A., S.C. Wofsy, B.C. Daube, H.R. Schneider, M. Loewenstein, J.R. Podolske, and T.J. Conway, Stratospheric mean ages and transport rates from observations of carbon dioxide and nitrous oxide, *Science*, *274*, 1340-1343, 1996.
- Bojkov, R.D., and V.E. Fioletov, Estimating the global ozone characteristics during the last 30 years, *J. Geophys. Res.*, *100*, 16537-16551, 1995.
- Borrmann, S., S. Solomon, L. Avallone, D. Toohey, and D. Baumgardner, On the occurrence of ClO in cirrus clouds and volcanic aerosol in the tropopause region, *Geophys. Res. Lett.*, *24*, 2011-2014, 1997.
- Boville, B.A., Middle atmosphere version of CCM2 (MACCM2): Annual cycle and interannual variability, *J. Geophys. Res.*, *100*, 9017-9039, 1995.
- Bowman, K.P., Global patterns of the quasi-biennial oscillation in total ozone, *J. Atmos. Sci.*, *46*, 3328-3343, 1989.
- Bowman, K.P., Barotropic simulation of large-scale mixing in the Antarctic polar vortex, *J. Atmos. Sci.*, *50*, 2901-2914, 1993.
- Bowman, K.P., and A.J. Kruger, A global climatology of total ozone from the Nimbus 7 total ozone mapping spectrometer, *J. Geophys. Res.*, *90*, 7967-7976, 1985.
- Brasseur, G.P., X.X. Tie, P.J. Rasch, and F. Lefèvre, A three-dimensional simulation of the Antarctic ozone hole: Impact of anthropogenic chlorine on the lower stratosphere and upper troposphere, *J. Geophys. Res.*, *102*, 8909-8930, 1997.

- Bregman, A., M. van den Broek, K.S. Carslaw, R. Müller, T. Peter, M.P. Scheele, and J. Lelieveld, Ozone depletion in the late winter lower Arctic stratosphere: Observations and model results, *J. Geophys. Res.*, *102*, 10815-10828, 1997.
- Brewer, A.W., Evidence for a world circulation provided by the measurements of helium and water vapour distribution in the stratosphere, *Quart. J. Roy. Meteorol. Soc.*, *75*, 351-363, 1949.
- Brune, W.H., J.G. Anderson, D.W. Toohey, D.W. Fahey, S.R. Kawa, R.L. Jones, D.S. McKenna, and L.R. Poole, The potential for ozone depletion in the Arctic polar stratosphere, *Science*, *252*, 1260-1266, 1991.
- Burkholder, J.B., R.L. Mauldin III, R.J. Yokelson, and A.R. Ravishankara, Kinetic, thermochemical, and spectroscopic study of Cl₂O₃, *J. Phys. Chem.*, *97*, 7597-7605, 1993.
- Burkholder, J.B., A.R. Ravishankara, and S. Solomon, UV/visible and IR absorption cross sections of BrONO₂, *J. Geophys. Res.*, *100*, 16793-16800, 1995.
- Butchart, N., and J. Austin, Middle atmosphere climatologies from the troposphere-stratosphere configuration of the UKMO's unified model, *J. Atmos. Sci.*, *55*, 2782-2809, 1998.
- Callis, L.B., M. Natarajan, J.D. Lambeth, and R.E. Boughner, On the origin of midlatitude ozone changes: Data analysis and simulations for 1979-1993, *J. Geophys. Res.*, *102*, 1215-1228, 1997.
- Cariolle, D., M. Amodei, and P. Simon, Dynamics of the ozone distribution in the winter stratosphere: Modelling the interhemispheric differences, *J. Atmos. Terr. Phys.*, *54*, 627-640, 1992.
- Carslaw, K.S., and T. Peter, Uncertainties in reactive uptake coefficients for solid stratospheric particles-1. Surface chemistry, *Geophys. Res. Lett.*, *24*, 1743-1746, 1997.
- Carslaw, K.S., B.P. Luo, S.L. Clegg, T. Peter, P. Brimblecombe, and P.J. Crutzen, Stratospheric aerosol growth and HNO₃ gas phase depletion from coupled HNO₃ and water uptake by liquid particles, *Geophys. Res. Lett.*, *21*, 2479-2482, 1994.
- Carslaw, K.S., S.L. Clegg, and P. Brimblecombe, A thermodynamic model of the system HCl-HNO₃-H₂SO₄-H₂O including solubilities of HBr from < 200 to 328 K, *J. Phys. Chem.*, *99*, 11557-11574, 1995.
- Carslaw, K.S., T. Peter, and S.L. Clegg, Modeling the composition of liquid stratospheric aerosols, *Rev. Geophys.*, *35*, 125-154, 1997.
- Carslaw, K.S., M. Wirth, A. Tsias, B.P. Luo, A. Dörnbrack, M. Leutbecher, H. Volkert, W. Renger, J.T. Bacmeister, and T. Peter, Particle microphysics and chemistry in remotely observed mountain polar stratospheric clouds, *J. Geophys. Res.*, *103*, 5785-5796, 1998.
- Chance, K., W.A. Traub, D.G. Johnson, K.W. Jucks, P. Ciarpallini, R.A. Stachnik, R.J. Salawitch, and H.A. Michelsen, Simultaneous measurements of stratospheric HO_x, NO_x, and Cl_x: Comparison with a photochemical model, *J. Geophys. Res.*, *101*, 9031-9043, 1996.
- Chang, A.Y., R.J. Salawitch, H.A. Michelsen, M.R. Gunson, M.C. Abrams, R. Zander, C.P. Rinsland, J.W. Elkins, G.S. Dutton, C.M. Volk, C.R. Webster, R.D. May, D.W. Fahey, R.S. Gao, M. Loewenstein, J.R. Podolske, R.M. Stimpfle, D.W. Kohn, M.H. Proffitt, J.J. Margitan, K.R. Chan, M.M. Abbas, A. Goldman, F.W. Irion, G. Manney, M.J. Newchurch, and G.P. Stiller, A comparison of measurements from ATMOS and instruments aboard the ER-2 aircraft: Halogenated gases, *Geophys. Res. Lett.*, *23*, 2393-2396, 1996.
- Chatfield, R.B., Anomalous HNO₃/NO_x ratio of remote tropospheric air: Conversion of nitric acid to formic acid and NO_x? *Geophys. Res. Lett.*, *21*, 2705-2708, 1994.
- Chen, P., The permeability of the Antarctic vortex edge, *J. Geophys. Res.*, *99*, 20563-20571, 1994.
- Chen, P., Isentropic cross-tropopause mass exchange in the extratropics, *J. Geophys. Res.*, *100*, 16661-16673, 1995.
- Chen, P., J.R. Holton, A. O'Neill, and R. Swinbank, Isentropic mass exchange between the tropics and extratropics in the stratosphere, *J. Atmos. Sci.*, *51*, 3006-3028, 1994.
- Chipperfield, M.P., Multiannual simulations with a three-dimensional chemical transport model, *J. Geophys. Res.*, in press, 1998.
- Chipperfield, M.P., D. Cariolle, P. Simon, R. Ramarosan, and D.J. Lary, A three-dimensional modeling study of trace species in the Arctic lower stratosphere during winter 1989-90, *J. Geophys. Res.*, *98*, 7199-7218, 1993.
- Chipperfield, M.P., D. Cariolle, and P. Simon, A 3-D chemical transport model study of chlorine activation during EASOE, *Geophys. Res. Lett.*, *21*, 1467-1470, 1994a.

LOWER STRATOSPHERIC PROCESSES

- Chipperfield, M.P., L.J. Gray, J.S. Kinnersley, and J. Zawodny, A two-dimensional model study of the QBO signal in SAGE II NO₂ and O₂, *Geophys. Res. Lett.*, *21*, 589-592, 1994b.
- Chipperfield, M.P., J.A. Pyle, C.E. Blom, N. Glatthor, M. Hopfner, T. Gulde, C. Piesch, and P. Simon, The variability of ClONO₂ in the Arctic polar vortex: Comparison of Transall MIPAS measurements and 3-D model results, *J. Geophys. Res.*, *100*, 9115-9129, 1995.
- Chipperfield, M.P., M.L. Santee, L. Froidevaux, G.L. Manney, W.G. Read, J.W. Waters, A.E. Roche, and J.M. Russell, Analysis of UARS data in the southern polar vortex in September 1992 using a chemical transport model, *J. Geophys. Res.*, *101*, 18861-18881, 1996.
- Chipperfield, M.P., E.R. Lutman, J.A. Kettleborough, J.A. Pyle, and A.E. Roche, Model studies of chlorine deactivation and formation of ClONO₂ collar in the Arctic polar vortex, *J. Geophys. Res.*, *102*, 1467-1478, 1997.
- Chu, L.T., M.T. Leu, and L.F. Keyser, Uptake of HCl in water ice and nitric acid ice films, *J. Phys. Chem.*, *97*, 7779-7785, 1993.
- Clark, J., and J.S. Francisco, Study of the stability of Cl₂O₃ using ab initio methods, *J. Phys. Chem. A.*, *101*, 7145-7153, 1997.
- Cohen, R.C., P.O. Wenneberg, R.M. Stimpfle, J. Koplow, J.G. Anderson, D.W. Fahey, E.L. Woodbridge, E.R. Keim, R. Gao, M.H. Proffitt, M. Loewenstein, and K.R. Chan, Are models of catalytic removal of O₃ by HO_x accurate? Constraints from in situ measurements of the OH to HO₂ ratio, *Geophys. Res. Lett.*, *21*, 2539-2542, 1994.
- Considine, D.B., A.R. Douglass, and C.H. Jackman, Sensitivity of two-dimensional model predictions of ozone response to stratospheric aircraft: An update, *J. Geophys. Res.*, *100*, 3075-3090, 1995.
- Coy, L., and R. Swinbank, Characteristics of stratospheric winds and temperatures produced by data assimilation, *J. Geophys. Res.*, *102*, 25673-25781, 1997.
- Coy, L., E.R. Nash, and P.A. Newman, Meteorology of the polar vortex: Spring 1997, *Geophys. Res. Lett.*, *24*, 2693-2696, 1997.
- Cronkhite, J.M., R.E. Stickel, J.M. Nicovich, and P.H. Wine, Laser flash photolysis studies of radical-radical reaction kinetics: The HO₂ + BrO reaction, *J. Phys. Chem. A.*, *102*, 6651-6658, 1998.
- Dahlberg, S.P., and K.P. Bowman, Isentropic mixing in the Arctic stratosphere during the 1992-1993 and 1993-1994 winters, *Geophys. Res. Lett.*, *22*, 1237-1240, 1995.
- Daniel, J.S., S.M. Schauffler, W.A. Pollock, S. Solomon, A. Weaver, L.E. Heidt, R.R. Garcia, E.L. Atlas, and J.F. Vedder, On the age of stratospheric air and inorganic chlorine and bromine release, *J. Geophys. Res.*, *101*, 16757-16770, 1996.
- Danielsen, E.F., A dehydration mechanism for the stratosphere, *Geophys. Res. Lett.*, *9*, 605-608, 1982.
- De Rudder, A.D., N. Larsen, X. Tie, G.P. Brasseur, and C. Granier, Model study of polar stratospheric clouds and their effect on stratospheric ozone, *J. Geophys. Res.*, *101*, 12567-12574, 1996.
- Del Negro, L.A., D.W. Fahey, S.G. Donnelly, R.S. Gao, E.R. Keim, R.C. Wamsley, E.L. Woodbridge, J.E. Dye, D. Baumgardner, B.W. Gandrud, J.C. Wilson, H.H. Jonsson, M. Loewenstein, J.R. Podolske, C.R. Webster, R.D. May, D.R. Worsnop, A. Tabazadeh, M.A. Tolbert, K.K. Kelly, and K.R. Chan, Evaluating the role of NAT, NAD, and liquid H₂SO₄/H₂O/HNO₃ solutions in Antarctic polar stratospheric cloud aerosol: Observations and implications, *J. Geophys. Res.*, *102*, 13255-13282, 1997.
- DeMore, W.B., S.P. Sander, D.M. Golden, R.F. Hampson, M.J. Kurylo, C.J. Howard, A.R. Ravishankara, C.E. Kolb, and M.J. Molina, *Chemical Kinetics and Photochemical Data for Use in Stratospheric Modeling: Evaluation No. 12*, Jet Propulsion Laboratory, California Institute of Technology, Pasadena, Calif., 1997.
- Dessler, A.E., D.B. Considine, G.A. Morris, M.R. Schoeberl, J.M. Russell III, A.E. Roche, J.B. Kumer, J.L. Mergenthaler, J.W. Waters, J.C. Gille, and G.K. Yue, Correlated observations of HCl and ClONO₂ from UARS and implications for stratospheric chlorine partitioning, *Geophys. Res. Lett.*, *22*, 1721-1724, 1995a.
- Dessler, A.E., E.J. Hints, E.M. Weinstock, J.G. Anderson, and K.R. Chan, Mechanisms controlling water vapor in the lower stratosphere: "A tale of two stratospheres", *J. Geophys. Res.*, *100*, 23167-23172, 1995b.
- Dessler, A.E., S.R. Kawa, A.R. Douglass, D.B. Considine, J.B. Kumer, A.E. Roche, J.L. Mergenthaler, J.W. Waters, J.M. Russell III, and J.C. Gille, A test of the partitioning between ClO and ClONO₂ using simultaneous UARS measurements of ClO, NO₂, and ClONO₂, *J. Geophys. Res.*, *101*, 12515-12521, 1996.

- Dessler, A.E., D.B. Considine, J.E. Rosenfield, S.R. Kawa, A.R. Douglass, and J.M. Russell III, Lower stratospheric chlorine partitioning during the decay of the Mt. Pinatubo aerosol cloud, *Geophys. Res. Lett.*, *24*, 1623-1626, 1997.
- Deters, B., J.P. Burrows, S. Himmelmann, and C. Blindauer, Gas phase spectra of HOBr and Br₂O and their atmospheric significance, *Ann. Geophys.*, *14*, 468-475, 1996.
- Deters, B., J.P. Burrows, and J. Orphal, UV-visible absorption cross sections of bromine nitrate determined by photolysis of BrONO₂/Br₂ mixtures, *J. Geophys. Res.*, *103*, 3563-3570, 1998.
- Dewan, M.E., Turbulent vertical transport due to thin intermittent mixing layers in the stratosphere and other stable fluids, *Science*, *211*, 1041-1042, 1981.
- Disselkamp, R.S., S.E. Anthony, A.J. Prenni, T.B. Onasch, and M.A. Tolbert, Crystallization kinetics of nitric acid dihydrate aerosols, *J. Phys. Chem.*, *100*, 9127-9137, 1996.
- Dobson, G.M.B., The laminated structure of ozone in the atmosphere, *Quart. J. Roy. Meteorol. Soc.*, *99*, 599-607, 1973.
- Donaldson, D.J., A.R. Ravishankara, and D.R. Hanson, Detailed study of HOCl + HCl → Cl₂ + H₂O in sulfuric acid, *J. Phys. Chem. A.*, *101*, 4717-4725, 1997.
- Douglass, A.R., C.J. Weaver, R.B. Rood, and L. Coy, A three dimensional simulation of the ozone annual cycle using winds from a data assimilation system, *J. Geophys. Res.*, *101*, 1463-1474, 1996.
- Douglass, A.R., R.B. Rood, S.R. Kawa, and D.J. Allen, A three dimensional simulation of the evolution of the middle latitude winter ozone in the middle stratosphere, *J. Geophys. Res.*, *102*, 19217-19232, 1997.
- Dunkerton, T.J., The role of gravity waves in the quasi-biennial oscillation, *J. Geophys. Res.*, *102*, 26053-26076, 1997.
- Dyer, A.J., and B. Hicks, Global spread of volcanic dust from the Bali eruption, *Quart. J. Roy. Meteorol. Soc.*, *95*, 545-554, 1968.
- Eckman, R.S., W.L. Grose, R.E. Turner, W.T. Blackshear, and J.M. Russell III, Stratospheric trace constituents simulated by a three-dimensional general circulation model: Comparison with UARS data, *J. Geophys. Res.*, *100*, 13952-13966, 1995.
- Eckman, R.S., W.L. Grose, D.E. Turner, and W.T. Blackshear, Polar ozone depletion: A 3-dimensional chemical modeling study of its long-term global impact, *J. Geophys. Res.*, *101*, 22977-22989, 1996.
- Edouard, S., B. Legras, F. Lefèvre, and R. Eymard, The effect of small-scale inhomogeneities on ozone depletion in the Arctic, *Nature*, *384*, 444-447, 1996.
- Elrod, M.J., R.F. Meads, J.B. Lipson, J.V. Seeley, and M.J. Molina, Temperature dependence of the rate constant for the HO₂ + BrO reaction, *J. Phys. Chem.*, *100*, 5808-5812, 1996.
- Eluszkiewicz, J.E., R. Zurek, L. Elson, E. Fishbein, L. Froidevaux, J. Waters, R. Grainger, A. Lambert, R. Harwood, and G. Peckham, Residual circulation in the stratosphere and lower mesosphere as diagnosed from Microwave Limb Sounder data, *J. Atmos. Sci.*, *53*, 217-240, 1996.
- Fabian, P., R. Borchers, and K. Kourtidis, Bromine-containing source gases during EASOE, *Geophys. Res. Lett.*, *21*, 1219-1222, 1994.
- Fahey, D.W., D.M. Murphy, K.K. Kelly, M.K.W. Ko, M.H. Proffitt, C.S. Eubank, G.V. Ferry, M. Loewenstein, and K.R. Chan, Measurements of nitric oxide and total reactive nitrogen in the Antarctic stratosphere: Observations and chemical implications, *J. Geophys. Res.*, *94*, 16665-16681, 1989.
- Fahey, D.W., K.K. Kelly, S.R. Kawa, A.F. Tuck, M. Loewenstein, K.R. Chan, and L.E. Heidt, Observations of denitrification and dehydration in the winter polar stratospheres, *Nature*, *344*, 321-324, 1990.
- Fahey, D.W., S.G. Donnelly, E.R. Keim, R.S. Gao, R.C. Wamsley, L.A. DelNegro, E.L. Woodbridge, M.H. Proffitt, K.H. Rosenlof, M.K.W. Ko, D.K. Weisenstein, C.J. Scott, C. Nevison, S. Solomon, and K.R. Chan, In situ observations of NO₂, O₃, and the NO₂/O₃ ratio in the lower stratosphere, *Geophys. Res. Lett.*, *23*, 1653-1656, 1996.
- Feely, H.W., and J.S. Spar, Tungsten-185 from nuclear bomb tests as a tracer for stratospheric meteorology, *Nature*, *188*, 1062-1064, 1960.
- Fioletov, V.E., J.B. Kerr, D.I. Wardle, J. Davies, E.W. Hare, C.T. McElroy, and D.W. Tarasick, Long-term ozone decline over the Canadian Arctic to early 1997 from ground-based and balloon observations, *Geophys. Res. Lett.*, *24*, 2705-2708, 1997.
- Fish, D.J., and M.R. Burton, The effect of uncertainties in kinetic and photochemical data on model predictions of stratospheric ozone depletion, *J. Geophys. Res.*, *102*, 25537-25542, 1997.
- Fish, D.J., S.R. Aliwell, and R.L. Jones, Midlatitude observations of the seasonal variation of BrO: 2, Interpretation and modelling study, *Geophys. Res. Lett.*, *24*, 1199-1202, 1997.

LOWER STRATOSPHERIC PROCESSES

- Flesch, R., B. Wassermann, B. Rothmund, and E. Ruhl, Photodissociation of A(²A₂)-Excited OCIO and its aggregates, *J. Phys. Chem.*, *98*, 6263-6271, 1994.
- Folkens, I., and C. Appenzeller, Ozone and potential vorticity at the subtropical tropopause break, *J. Geophys. Res.*, *101*, 18787-18792, 1996.
- Fritts, D.C., and T.E. VanZandt, Spectral estimates of gravity wave energy and momentum fluxes: Part I, Energy dissipation, acceleration, and constraints, *J. Atmos. Sci.*, *50*, 3685-3694, 1993.
- Fukao, S., M.D. Yamanaka, N. Ao, W. Hocking, T. Sato, M.Y. Tamamoto, T. Nakamura, T. Tsuda, and S. Kato, Seasonal variability of vertical eddy diffusivity in the middle atmosphere: 1, Three-year observations by the middle and upper atmosphere radar, *J. Geophys. Res.*, *99*, 18973-18987, 1994.
- Fusco, A.C., and M.L. Salby, Interannual variations of total ozone and their relationship to variations of planetary wave activity, *J. Clim.*, in press, 1998.
- Gao, R.S., D.W. Fahey, R.J. Salawitch, S.A. Lloyd, D.E. Anderson, R. DeMajistre, C.T. McElroy, E.L. Woodbridge, R.C. Wamsley, S.G. Donnelly, L.A. Del Negro, M.H. Proffitt, R.M. Stimpfle, D.W. Kohn, S.R. Kawa, L.R. Lait, M. Loewenstein, J.R. Podolske, E.R. Keim, J.E. Dye, J.C. Wilson, and K.R. Chan, Partitioning of the reactive nitrogen reservoir in the lower atmosphere of the Southern Hemisphere: Observations and modeling, *J. Geophys. Res.*, *102*, 3935-3949, 1997.
- Garcia, R.R., and B.A. Boville, "Downward control" of the mean meridional circulation and temperature distribution of the polar winter stratosphere, *J. Atmos. Sci.*, *51*, 2238-2245, 1994.
- Gary, B.L., Observational results using the microwave temperature profiler during the Airborne Antarctic Ozone Experiment, *J. Geophys. Res.*, *94*, 11223-11231, 1989.
- Gelman, M.E., A.J. Miller, R.M. Nagatani, and C.S. Long, Use of UARS data in the NOAA stratospheric monitoring program, *Adv. Space Res.*, *14* (9), 21-31, 1994.
- Gettelman, A., J.R. Holton, and K.H. Rosenlof, Mass fluxes of O₃, CH₄, N₂O, and CF₂Cl₂ in the lower stratosphere calculated from observational data, *J. Geophys. Res.*, *102*, 19149-19159, 1997.
- Gilles, M.K., A.A. Turnipseed, J.B. Burkholder, A.R. Ravishankara, and S. Solomon, Kinetics of the IO radical: 2, Reaction of IO with BrO, *J. Phys. Chem. A.*, *101*, 5526-5534, 1997.
- Goodman, J., S. Verma, R.F. Pueschel, P. Hamill, G.V. Ferry, and D. Webster, New evidence of size and composition of polar stratospheric cloud particles, *Geophys. Res. Lett.*, *24*, 615-618, 1997.
- Grant, W.B., E.V. Browell, C.S. Long, L.L. Stowe, R.G. Grainger, and A. Lambert, Use of volcanic aerosols to study the tropical stratospheric reservoir, *J. Geophys. Res.*, *101*, 3973-3988, 1996.
- Grose, W.L., J.E. Nealy, R.E. Turner, and W.T. Blackshear, Modeling the transport of chemically active constituents in the stratosphere, in *Transport Processes in the Middle Atmosphere*, pp. 229-250, Reidel, Dordrecht, Holland, 1987.
- Hadjinicolaou, P., J.A. Pyle, M.P. Chipperfield, and J.A. Kettleborough, Effect of interannual meteorological variability on middle latitude ozone, *Geophys. Res. Lett.*, *24*, 2993-2996, 1997.
- Hall, T.M., and R.A. Plumb, Age as a diagnostic of stratospheric transport, *J. Geophys. Res.*, *99*, 1059-1070, 1994.
- Hall, T.M., and M.J. Prather, Seasonal evolutions of N₂O, O₃, and CO₂: Three-dimensional simulations of stratospheric correlations, *J. Geophys. Res.*, *100*, 16699-16720, 1995.
- Hall, T.M., and D.W. Waugh, Timescales for the stratospheric circulation derived from tracers, *J. Geophys. Res.*, *102*, 8991-9001, 1997a.
- Hall, T.M., and D.W. Waugh, Tracer transport in the tropical stratosphere due to vertical diffusion and horizontal mixing, *Geophys. Res. Lett.*, *24*, 1383-1387, 1997b.
- Hamilton, K., Effects of an imposed quasi-biennial oscillation in a comprehensive troposphere-stratosphere-mesosphere general circulation model, *J. Atmos. Sci.*, *55*, 2393-2418, 1998.
- Hamilton, K., R.J. Wilson, J.D. Mahlman, and L.J. Umscheid, Climatology of the SKYHI troposphere-stratosphere-mesosphere general circulation model, *J. Atmos. Sci.*, *52*, 5-43, 1995.
- Hansen, G., T. Svenoe, M. Chipperfield, A. Dahlback, and U.P. Hoppe, Evidence of substantial ozone depletion in winter 1996/97 over northern Norway, *Geophys. Res. Lett.*, *24*, 799-802, 1997.
- Hanson, D.R., The uptake of HNO₃ onto ice, NAT, and frozen sulfuric acid, *Geophys. Res. Lett.*, *19*, 2063-2066, 1992.
- Hanson, D.R., Reaction of N₂O₅ with H₂O on bulk liquids and on particles and the effect of dissolved HNO₃, *Geophys. Res. Lett.*, *24*, 1087-1090, 1997a.

- Hanson, D.R., Surface-specific reactions on liquids, *J. Phys. Chem. B.*, *101*, 4998-5001, 1997b.
- Hanson, D.R., and E.R. Lovejoy, The reaction of ClONO₂ with submicrometer sulfuric acid aerosol, *Science*, *267*, 1326-1328, 1995.
- Hanson, D.R., and E.R. Lovejoy, Heterogeneous reaction in sulfuric acid: HOCl and HCl as a model system, *J. Phys. Chem.*, *100*, 6397-6405, 1996.
- Hanson, D.R., and A.R. Ravishankara, Investigation of the reactive and nonreactive processes involving ClONO₂ and HCl on water and nitric acid doped ice, *J. Phys. Chem.*, *96*, 2682-2691, 1992.
- Hanson, D.R., and A.R. Ravishankara, Uptake of HCl and HOCl onto sulfuric acid: Solubilities, diffusivities and reaction, *J. Phys. Chem.*, *97*, 12309-12319, 1993.
- Hanson, D.R., and A.R. Ravishankara, Reactive uptake of ClONO₂ onto sulfuric acid due to reaction with HCl and H₂O, *J. Phys. Chem.*, *98*, 5728-5735, 1994.
- Hanson, D.R., and A.R. Ravishankara, Heterogeneous chemistry of bromine species in sulfuric acid under stratospheric conditions, *Geophys. Res. Lett.*, *22*, 385-388, 1995.
- Hanson, D.R., A.R. Ravishankara, and S. Solomon, Heterogeneous reactions in sulfuric acid aerosols: A framework for model calculations, *J. Geophys. Res.*, *99*, 3615-3629, 1994.
- Hanson, D.R., A.R. Ravishankara, and E.R. Lovejoy, Reaction of BrONO₂ with H₂O on submicron sulfuric acid aerosol and the implications for the lower stratosphere, *J. Geophys. Res.*, *101*, 9063-9069, 1996.
- Harder, H., C. Camy-Peyret, F. Ferlemann, R. Fitzenberger, T. Hawat, H. Osterkamp, D. Perner, U. Platt, M. Schneider, P. Vradelis, and K. Pfeilsticker, Stratospheric BrO profiles measured at different latitudes and seasons: Atmospheric observations, *Geophys. Res. Lett.*, *25*, 3843-3846, 1998.
- Harnisch, J., R. Borchers, P. Fabian, and M. Maiss, Tropospheric trends for CF₄ and C₂F₆ since 1982 derived from SF₆ dated stratospheric air, *Geophys. Res. Lett.*, *23*, 1009-1102, 1996.
- Harwood, M.H., J.B. Burkholder, and A.R. Ravishankara, Photodissociation of BrONO₂ and N₂O₅: Quantum yields for NO₃ production at 248, 308, and 352.5 nm, *J. Phys. Chem. A.*, *102*, 1309-1317, 1998.
- Hasebe, F., Quasi-biennial oscillations of ozone and diabatic circulation in the equatorial stratosphere, *J. Atmos. Sci.*, *51*, 729-745, 1994.
- Haynes, P.H., and J. Anglade, The vertical-scale cascade of atmospheric tracers due to large-scale differential advection, *J. Atmos. Sci.*, *54*, 1121-1136, 1997.
- Haynes, P.H., and W.E. Ward, The effect of realistic radiative transfer on potential vorticity structures, including influence of background shear and strain, *J. Atmos. Sci.*, *50*, 3431-3453, 1993.
- Haynes, P.H., C.J. Marks, M.E. McIntyre, T.G. Shepherd, and K.P. Shine, On the "downward control" of extratropical diabatic circulations by eddy-induced mean zonal forces, *J. Atmos. Sci.*, *48*, 651-678, 1991.
- Henson, B.F., K.R. Wilson, and J.M. Robinson, A physical absorption model of the dependence of ClONO₂ heterogeneous reactions on relative humidity, *Geophys. Res. Lett.*, *23*, 1021-1024, 1996.
- Hess, P.G., and D. O'Sullivan, A three dimensional modeling study of the extra-tropical quasi-biennial oscillation in ozone, *J. Atmos. Sci.*, *52*, 1539-1554, 1995.
- Highwood, E.J., and B.J. Hoskins, The tropical tropopause, *Quart. J. Roy. Meteorol. Soc.*, *124*, 1579-1604, 1998.
- Hines, C.O., Doppler spread parameterization of gravity-wave momentum deposition in the middle atmosphere: Part I, Broad and quasi monochromatic spectra and implementation, *J. Atmos. Solar Terr. Phys.*, *59*, 387-400, 1997.
- Hints, E.J., E.M. Weinstock, A.E. Dessler, J.G. Anderson, M. Loewenstein, and J.R. Podolske, SPADE H₂O measurements and the seasonal cycle of stratospheric water vapor, *Geophys. Res. Lett.*, *21*, 2559-2562, 1994.
- Hofmann, D.J., and S.J. Oltmans, Anomalous Antarctic ozone during 1992: Evidence for Pinatubo volcanic aerosol effects, *J. Geophys. Res.*, *98*, 18555-18561, 1993.
- Hofmann, D.J., and S. Solomon, Ozone destruction through heterogeneous chemistry following the eruption of El Chichón, *J. Geophys. Res.*, *94*, 5029-5041, 1989.
- Hofmann, D.J., S.J. Oltmans, B.J. Johnson, J.A. Lathrop, J.M. Harris, and H. Vomel, Recovery of ozone in the lower stratosphere at the South Pole during the spring of 1994, *Geophys. Res. Lett.*, *22*, 2493-2496, 1995.
- Hofmann, D.J., S.J. Oltmans, J.M. Harris, B.J. Johnson, and J.A. Lathrop, Ten years of ozonesonde measurements at the South Pole: Implications for recovery of springtime Antarctic ozone, *J. Geophys. Res.*, *102*, 8931-8943, 1997.

LOWER STRATOSPHERIC PROCESSES

- Holton, J.R., A dynamically based transport parameterization for one-dimensional photochemical models of the stratosphere, *J. Geophys. Res.*, *91*, 2681-2686, 1986.
- Holton, J.R., and H.-C. Tan, The influence of the equatorial quasi-biennial oscillation on the global circulation at 50 mb, *J. Atmos. Sci.*, *37*, 2200-2208, 1980.
- Holton, J.R., P.H. Haynes, M.E. McIntyre, A.R. Douglass, R.B. Rood, and L. Pfister, Stratosphere-troposphere exchange, *Rev. Geophys.*, *33*, 403-439, 1995.
- Hood, L.L., J.P. McCormack, and K. Labitzke, An investigation of dynamical contributions to mid-latitude ozone trends in winter, *J. Geophys. Res.*, *102*, 13079-13093, 1997.
- Horinouchi, T., and S. Yoden, Wave-mean flow interaction associated with a QBO like oscillation in a simplified GCM, *J. Atmos. Sci.*, *55*, 502-526, 1998.
- Hu, J.H., and J.P.D. Abbatt, Reaction probabilities for N₂O₅ hydrolysis on sulfuric acid and ammonium sulfate aerosols at room temperature, *J. Phys. Chem. A.*, *101*, 871-878, 1997.
- Hübler, G., D.W. Fahey, K.K. Kelly, D.D. Montzka, M.A. Carroll, A.F. Tuck, L.E. Heidt, W.H. Pollock, G.L. Gregory, and J.F. Vedder, Redistribution of reactive odd nitrogen in the lower Arctic stratosphere, *Geophys. Res. Lett.*, *17*, 453-465, 1990.
- Ingham, T., D. Bauer, J. Landgraf, and J.N. Crowley, The UV-visible absorption cross sections of gaseous HOBr, *J. Phys. Chem. A.*, *102*, 3293-3298, 1998.
- Iraci, L.T., and M.A. Tolbert, Heterogeneous interaction of formaldehyde with cold sulfuric acid: Implications for the upper troposphere and lower stratosphere, *J. Geophys. Res.*, *102*, 16099-16107, 1997.
- Iraci, L.T., T.J. Fortin, and M.A. Tolbert, Dissolution of sulfuric acid tetrahydrate at low temperatures and subsequent growth of nitric acid trihydrate, *J. Geophys. Res.*, *103*, 8491-8498, 1998.
- Jackman, C.H., E.L. Fleming, S. Chandra, D.B. Considine, and J.E. Rosenfield, Past, present, and future modeled ozone trends with comparisons to observed trends, *J. Geophys. Res.*, *101*, 28753-28767, 1996.
- Jaeglé, L., C.R. Webster, R.D. May, D.W. Fahey, E.L. Woodbridge, E.R. Keim, R.S. Gao, M.H. Proffitt, R.M. Stimpfle, R.J. Salawitch, S.C. Wofsy, and L. Pfister, In situ measurements of the NO₂/NO ratio for testing atmospheric photochemical models, *Geophys. Res. Lett.*, *21*, 2555-2558, 1994.
- Jensen, E.J., and O.B. Toon, Ice nucleation in the upper troposphere: Sensitivity to aerosol number density, temperature and cooling rate, *Geophys. Res. Lett.*, *21*, 2019-2022, 1994.
- Jensen, E.J., O.B. Toon, H.B. Selkirk, J.D. Spinhirne, and M.R. Schoeberl, On the formation and persistence of subvisible cirrus clouds near the tropical tropopause, *J. Geophys. Res.*, *101*, 21361-21375, 1996.
- Johnson, D.G., W.A. Traub, K.V. Chance, and K.W. Jucks, Detection of HBr and upper limits for HOBr: Bromine partitioning in the stratosphere, *Geophys. Res. Lett.*, *22*, 1373-1376, 1995.
- Jones, D.B.A., H.R. Schneider, and M.B. McElroy, Effects of the quasi-biennial oscillation on the zonally averaged transport of tracers, *J. Geophys. Res.*, *103*, 11235-11249, 1998.
- Jones, P.W., K. Hamilton, and R.J. Wilson, A very high resolution general circulation model simulation of the global circulation in Austral winter, *J. Atmos. Sci.*, *54*, 1107-1116, 1997.
- Jones, R.L., and J.L. Pyle, Observations of CH₄ and N₂O by the Nimbus-7 SAMS: A comparison with in-situ data and two-dimensional numerical model calculations, *J. Geophys. Res.*, *89*, 5263-5279, 1984.
- Juckes, M.N., and M.E. McIntyre, A high resolution, one-layer model of breaking planetary waves in the stratosphere, *Nature*, *328*, 590-596, 1987.
- Jucks, K.W., D.G. Johnson, K.V. Chance, W.A. Traub, R.J. Salawitch, and R.A. Stachnik, Ozone production and loss rate measurements in the middle stratosphere, *J. Geophys. Res.*, *101*, 28785-28792, 1996.
- Kawa, S.R., P.A. Newman, L.R. Lait, M.R. Schoeberl, R.M. Stimpfle, D.W. Kohn, C.R. Webster, R.D. May, D. Baumgardner, J.E. Dye, J.C. Wilson, K.R. Chan, and M. Loewenstein, Activation of chlorine in sulfate aerosol as inferred from aircraft observations, *J. Geophys. Res.*, *102*, 3921-3933, 1997.
- Keim, E.R., D.W. Fahey, L.A. Del Negro, E.L. Woodbridge, R.S. Gao, P.O. Wennberg, R.C. Cohen, R.M. Stimpfle, K.K. Kelly, E.J. Hints, J.C. Wilson, H.H. Jonsson, J.E. Dye, D. Baumgardner, S.R. Kawa, R.J. Salawitch, M.H. Proffitt, M. Loewenstein, J.R. Podolske, and K.R. Chan, Observations of large reductions in the NO/NO_y ratio near the mid-latitude tropopause and the role of heterogeneous chemistry, *Geophys. Res. Lett.*, *23*, 3223-3226, 1996.

- Kelly, K.K., M.H. Proffitt, K.R. Chan, M. Loewenstein, J.R. Podolske, S.E. Strahan, J.C. Wilson, and D. Kley, Water vapor and cloud water measurements over Darwin during the STEP 1987 tropical mission, *J. Geophys. Res.*, *98*, 8713-8723, 1993.
- Kida, H., General circulation of air parcels and transport characteristics derived from a hemispheric GCM: Part 2, Very long-term motions of air parcels in the troposphere and stratosphere, *J. Meteorol. Soc. Japan*, *61*, 510-522, 1983.
- Klassen, J., Z. Hu, and L.R. Williams, Diffusion coefficients for HCl and HBr in 30 wt % to 72 wt % sulfuric acid at temperatures between 220 and 300 K, *J. Geophys. Res.*, *103*, 16197-16202, 1998.
- Knollenberg, R.G., K. Kelly, and J.C. Wilson, Measurements of high number densities of ice crystals in the tops of tropical cumulonimbus, *J. Geophys. Res.*, *98*, 8639-8664, 1993.
- Knudsen, B.M., Accuracy of Arctic stratospheric temperature analyses and the implications for the prediction of polar stratospheric clouds, *Geophys. Res. Lett.*, *23*, 3747-3750, 1996.
- Kolb, C.E., D.R. Worsnop, M.S. Zahniser, P. Davidovits, L.F. Keyser, M.-T. Leu, M.J. Molina, D.R. Hanson, A.R. Ravishankara, L.R. Williams, and M.A. Tolbert, Laboratory studies of atmospheric heterogeneous chemistry, Chapter 18 in *Progress and Problems in Atmospheric Chemistry*, edited by J.R. Barker, pp. 771-875, World Scientific Publishing, Singapore, 1995.
- Kondo, Y., U. Schmidt, T. Sugita, P. Amedieu, M. Koike, H. Ziereis, and Y. Iwasaka, Total reactive nitrogen, N₂O, and ozone in the winter Arctic stratosphere, *Geophys. Res. Lett.*, *21*, 1247-1250, 1994.
- Kondo, Y., U. Schmidt, T. Sugita, A. Engel, M. Koike, P. Amedieu, M.R. Gunson, and J. Rodriguez, NO₂ correlation with N₂O and CH₄ in the midlatitude stratosphere, *Geophys. Res. Lett.*, *23*, 2369-2372, 1996.
- Kondo, Y., T. Sugita, R.J. Salawitch, M. Koike, and T. Deshler, Effect of Pinatubo aerosols on stratospheric NO, *J. Geophys. Res.*, *102*, 1205-1213, 1997.
- Koop, T., and K.S. Carslaw, Melting of H₂SO₄·4H₂O particles upon cooling: Implications for polar stratospheric clouds, *Science*, *272*, 1638-1641, 1996.
- Koop, T., U.M. Biermann, W. Raber, B.P. Luo, P.J. Crutzen, and T. Peter, Do stratospheric aerosol droplets freeze above the ice frost point? *Geophys. Res. Lett.*, *22*, 917-920, 1995.
- Koop, T., B.P. Luo, U.M. Biermann, P.J. Crutzen, and T. Peter, Freezing of HNO₃/H₂SO₄/H₂O solutions at stratospheric temperatures: Nucleation statistics and experiments, *J. Phys. Chem. A.*, *101*, 1117-1133, 1997a.
- Koop, T., K.S. Carslaw, and T. Peter, Thermodynamic stability of PSC particles, *Geophys. Res. Lett.*, *24*, 2199-2202, 1997b.
- Kritz, M.A., S.W. Rosner, E.F. Danielsen, and H.B. Selkirk, Air mass origins and troposphere-to-stratosphere exchange associated with mid-latitude cyclogenesis and tropopause folding inferred from Be⁷ measurements, *J. Geophys. Res.*, *96*, 17405-17414, 1991.
- Kritz, M.A., S.W. Rosner, K.K. Kelly, M. Loewenstein, and K.R. Chan, Radon measurements in the lower tropical stratosphere: Evidence for rapid vertical transport and dehydration of tropospheric air, *J. Geophys. Res.*, *98*, 8725-8736, 1993.
- Larichev, M., F. Maguin, G. LeBras, and G. Poulet, Kinetics and mechanism of the BrO + HO₂ reaction, *J. Phys. Chem.*, *99*, 15911-15918, 1995.
- Larsen, N., B.M. Knudsen, J.M. Rosen, N.T. Kjome, R. Neuber, and E. Kyrö, Temperature histories in liquid and solid PSC formation, *J. Geophys. Res.*, *102*, 23505-23517, 1997.
- Lary, D.J., M.P. Chipperfield, R. Toumi, and T. Lenton, Heterogeneous atmospheric bromine chemistry, *J. Geophys. Res.*, *101*, 1489-1504, 1996.
- Lary, D.J., A.M. Lee, R. Toumi, M.J. Newchurch, M. Pirre, and J.B. Renard, Carbon aerosols and atmospheric photochemistry, *J. Geophys. Res.*, *102*, 3671-3682, 1997.
- Lefèvre, F., G.P. Brasseur, I. Folkins, A.K. Smith, and P. Simon, Chemistry of the 1991-1992 stratospheric winter: Three-dimensional model simulations, *J. Geophys. Res.*, *99*, 8183-8195, 1994.
- Li, Z., R.R. Friedl, and S.P. Sander, Kinetics of the HO₂ + BrO reaction over the temperature range 233-348 K, *J. Chem. Soc. Faraday Trans.*, *93*, 2683-2691, 1997.
- Lindzen, R.S., Turbulence and stress due to gravity wave and tidal breakdown, *J. Geophys. Res.*, *86*, 9707-9714, 1981.
- Lipson, J.B., M.J. Elrod, T.W. Beiderhase, L.T. Molina, and M.J. Molina, Temperature dependence of the rate constant and branching ratio for the OH + ClO reaction, *J. Chem. Soc. Faraday Trans.*, *93*, 2665-2673, 1997.

LOWER STRATOSPHERIC PROCESSES

- London, J., The observed distribution of atmospheric ozone and its variations, in *Ozone in the Free Atmosphere*, edited by R.C. Whitten and S.S. Prasad, pp. 11-80, Van Nostrand-Reinhold, Princeton, N. J., 1985.
- Longfellow, C.A., T. Imamura, A.R. Ravishankara, and D.R. Hanson, HONO solubility and heterogeneous reactivity on sulfuric acid surfaces, *J. Phys. Chem. A.*, *102*, 3323-3332, 1998.
- Lovejoy, E.R., and D.R. Hanson, Measurement of the kinetics of reactive uptake by submicron sulfuric acid particles, *J. Phys. Chem.*, *99*, 2080-2087, 1995.
- Mackenzie, I.A., R.S. Harwood, L. Froidevaux, W.G. Read, and J.W. Waters, Chemical loss of polar vortex ozone inferred from UARS MLS measurements of ClO during the Arctic late winters of 1993, *J. Geophys. Res.*, *101*, 14505-14518, 1996.
- Mahlman, J.D., H. Levy II, and W.J. Moxim, Three-dimensional simulations of stratospheric N₂O predictions for other trace constituents, *J. Geophys. Res.*, *91*, 2687-2707, 1986.
- Manney, G.L., L. Froidevaux, J.W. Waters, and R.W. Zurek, Evolution of Microwave Limb Sounder ozone and the polar vortex during winter, *J. Geophys. Res.*, *100*, 2953-2972, 1995a.
- Manney, G.L., R.W. Zurek, L. Froidevaux, J.W. Waters, A. O'Neill, and R. Swinbank, Lagrangian transport calculations using UARS data: Part II, Ozone, *J. Atmos. Sci.*, *52*, 3069-3081, 1995b.
- Manney, G.L., R. Swinbank, S.T. Massie, M.E. Gelman, A.J. Miller, R. Nagatani, A. O'Neill, and R.W. Zurek, Comparison of UK Meteorological Office and US National Meteorological Center stratospheric analyses during northern and southern winter, *J. Geophys. Res.*, *101*, 10311-10334, 1996.
- Manney, G.L., L. Froidevaux, M.L. Santee, R.W. Zurek, and J.W. Waters, MLS observations of Arctic ozone loss in 1996-97, *Geophys. Res. Lett.*, *24*, 2697-2700, 1997.
- Manzini, E., and L. Bengtsson, Stratospheric climate and variability from a general circulation model and observations, *Climate Dyn.*, *12*, 615-639, 1996.
- Martin, S.C., D. Salcedo, L.T. Molina, and M.J. Molina, Deliquescence of sulfuric acid tetrahydrate following volcanic eruption or denitrification, *Geophys. Res. Lett.*, *25*, 31-34, 1998.
- McIntyre, M.E., Middle atmosphere dynamics and transport: Some current challenges to our understanding, in *Dynamics, Transport and Photochemistry in the Middle Atmosphere of the Southern Hemisphere*, NATO Advanced Research Workshop, edited by A. O'Neill, pp. 1-18, Kluwer, Dordrecht, Holland, 1990.
- McIntyre, M.E., The stratospheric polar vortex and subvortex: Fluid dynamics and midlatitude ozone loss, *Proc. R. Soc. London*, *A352*, 227-240, 1995.
- McIntyre, M.E., and T.N. Palmer, Breaking planetary waves in the stratosphere, *Nature*, *305*, 593-600, 1983.
- McKinney, K.A., J.M. Pierson, and D.W. Toohey, A wintertime in situ profile of BrO between 17 and 27 km in the Arctic vortex, *Geophys. Res. Lett.*, *24*, 853-856, 1997.
- Medvedev, A.S., and G.P. Klaassen, Vertical evolution of gravity wave spectra and the parameterization of associated wave drag, *J. Geophys. Res.*, *100*, 25841-25853, 1995.
- Meilinger, S.K., T. Koop, B.P. Luo, T. Huthwelker, K.S. Carslaw, P.J. Crutzen, and T. Peter, Size-dependent stratospheric droplet composition in lee wave temperature fluctuations and their potential role in PSC freezing, *Geophys. Res. Lett.*, *22*, 3031-3034, 1995.
- Michelsen, H.A., R.J. Salawitch, M.R. Gunson, C. Aellig, N. Kampfer, M.M. Abbas, M.C. Abrams, T.L. Brown, A.Y. Chang, A. Goldman, F.W. Irion, M.J. Newchurch, C.P. Rinsland, G.P. Stiller, and R. Zander, Stratospheric chlorine partitioning: Constraints from shuttle-borne measurements of [HCl], [ClNO₂], and [ClO], *Geophys. Res. Lett.*, *23*, 2361-2364, 1996.
- Mickley, L.J., J.P.D. Abbatt, J.E. Frederick, and J.M. Russell III, Response of summertime odd nitrogen and ozone at 17 mb to Mount Pinatubo aerosol over the southern mid-latitudes: Observations from HALOE, *J. Geophys. Res.*, *102*, 23573-23582, 1998.
- Minschwaner, K., A.E. Dessler, J.W. Elkins, C.M. Volk, D.W. Fahey, M. Loewenstein, J.R. Podolske, A.E. Roche, and K.R. Chan, The bulk properties of isentropic mixing into the tropics in the lower stratosphere, *J. Geophys. Res.*, *101*, 9433-9439, 1996.

- Moore, T.A., M. Okumura, M. Tagawa, and T.K. Minton, Dissociation dynamics of ClONO₂ and relative Cl and ClO product yields following photoexcitation at 308 nm, *Faraday Discuss. Chem. Soc.*, *100*, 295-307, 1995.
- Morris, G.A., D.B. Considine, A.E. Dessler, S.R. Kawa, J. Kumer, J. Mergenthaler, A. Roche, and J.M. Russell III, Nitrogen partitioning in the middle stratosphere as observed by the Upper Atmosphere Research Satellite, *J. Geophys. Res.*, *102*, 8955-8965, 1997.
- Mote, P.W., K.H. Rosenlof, M.E. McIntyre, E.S. Carr, J.C. Gille, J.R. Holton, J.S. Kinnnersley, H.C. Pumphrey, J.M. Russell III, and J.W. Waters, An atmospheric tape recorder: The imprint of tropical tropopause temperatures on stratospheric water vapor, *J. Geophys. Res.*, *101*, 3989-4006, 1996.
- Mote, P.W., T.J. Dunkerton, M.E. McIntyre, E.A. Ray, P.H. Haynes, and J.M. Russell III, Vertical velocity, vertical diffusion, and dilution by midlatitude air in the tropical lower stratosphere, *J. Geophys. Res.*, *103*, 8651-8666, 1998.
- Müller, R., and T. Peter, The numerical modelling of the sedimentation of polar stratospheric cloud particles, *Ber. Bunsenges. Phys. Chem.*, *96*, 353-361, 1992.
- Müller, R., P.J. Crutzen, J.-U. Grooß, C. Brühl, J.M. Russell, and A.F. Tuck, Chlorine activation and ozone depletion in the Arctic vortex: Observations by the Halogen Occultation Experiment on the Upper Atmosphere Research Satellite, *J. Geophys. Res.*, *101*, 12531-12554, 1996.
- Müller, R., P.J. Crutzen, J.-U. Grooß, C. Brühl, J.M. Russell, H. Gernandt, D.S. McKenna, and A.F. Tuck, Severe chemical ozone loss in the Arctic during the winter 1995-96, *Nature*, *389*, 709-712, 1997.
- Murphy, D.M., and D.W. Fahey, An estimate of the flux of stratospheric reactive nitrogen and ozone into the troposphere, *J. Geophys. Res.*, *99*, 5325-5332, 1994.
- Murphy, D.M., and B.L. Gary, Mesoscale temperature fluctuations and polar stratospheric clouds, *J. Atmos. Sci.*, *52*, 1753-1760, 1995.
- Murphy, D.M., and A.R. Ravishankara, Temperature averages and rates of stratospheric reactions, *Geophys. Res. Lett.*, *21*, 2471-2474, 1994.
- Murphy, D.M., A.F. Tuck, K.K. Kelly, K.R. Chan, M. Loewenstein, J.R. Podolske, M.H. Proffitt, and S.E. Strahan, Indicators of transport and vertical motion from correlations between in-situ measurement in the airborne Antarctic ozone experiment, *J. Geophys. Res.*, *94*, 11669-11685, 1989.
- Murphy, D.M., D.W. Fahey, M.H. Proffitt, S.C. Liu, K.R. Chan, C.S. Eubank, S.R. Kawa, and K.K. Kelly, Reactive nitrogen and its correlation with ozone in the lower stratosphere and upper troposphere, *J. Geophys. Res.*, *98*, 8751-8773, 1993.
- Nevison, C.D., S. Solomon, R.R. Garcia, D.W. Fahey, E.R. Keim, M. Loewenstein, J.R. Podolske, R.S. Gao, R.C. Wamsley, S.G. Donnelly, and L.A. Del Negro, Influence of Antarctic denitrification on two-dimensional model NO_y/N₂O correlations in the lower stratosphere, *J. Geophys. Res.*, *102*, 13183-13192, 1997.
- Newchurch, M.J., M. Allen, M.R. Gunson, R.J. Salawitch, G.B. Collins, K.H. Huston, M.M. Abbas, M.C. Abrams, A.Y. Chang, D.W. Fahey, R.S. Gao, F.W. Irion, M. Loewenstein, G. Manney, H.A. Michelsen, J.R. Podolske, C.P. Rinsland, and R. Zander, Stratospheric NO and NO₂ abundances from ATMOS solar-occultation measurements, *Geophys. Res. Lett.*, *23*, 2373-2376, 1996.
- Newell, R.E., and S. Gould-Stewart, A stratospheric fountain, *J. Atmos. Sci.*, *38*, 2789-2796, 1981.
- Newman, P.A., L.R. Lait, M.R. Schoeberl, M. Seablom, L. Coy, R. Rood, R. Swinbank, M. Proffitt, M. Loewenstein, J.R. Podolske, J.W. Elkins, C.R. Webster, R.D. May, D.W. Fahey, G.S. Dutton, and K.R. Chan, Measurements of polar vortex air in the midlatitudes, *J. Geophys. Res.*, *101*, 12879-12891, 1996.
- Newman, P.A., J.F. Gleason, R.D. McPeters, and R.S. Stolarski, Anomalous low ozone over the Arctic, *Geophys. Res. Lett.*, *24*, 2689-2692, 1997.
- Ngan, K., and T.G. Shepherd, Comments on some recent measurements of anomalously steep N₂O and O₃ tracer spectra in the stratospheric surf zone, *J. Geophys. Res.*, *102*, 24001-24004, 1997.
- Nicolaisen, S.L., R.R. Friedl, and S.P. Sander, Kinetics and mechanism of the ClO + ClO reaction: Pressure and temperature dependences of the bimolecular and termolecular channels and thermal decomposition of chlorine peroxide, *J. Phys. Chem.*, *98*, 155-169, 1994.

LOWER STRATOSPHERIC PROCESSES

- Nickolaisen, S.L., S.P. Sander, and R.R. Friedl, Pressure-dependent yields and product branching ratios in the broadband photolysis of chlorine nitrate, *J. Phys. Chem.*, *100*, 10165-10178, 1996.
- Nolt, I.G., P.A.R. Ade, F. Alboni, B. Carli, M. Carlotti, U. Cortesi, M. Epifani, M.J. Griffin, P.A. Hamilton, C. Lee, G. Lepri, F. Mencaraglia, A.G. Murray, J.H. Park, K. Park, P. Raspollini, M. Ridolfi, and M.D. Vanek, Stratospheric HBr concentration profile obtained from far-infrared emission spectroscopy, *Geophys. Res. Lett.*, *24*, 281-284, 1997.
- Norton, W.A., Breaking Rossby waves in a model stratosphere diagnosed by a vortex-following coordinate system and a contour advection technique, *J. Atmos. Sci.*, *51*, 654-673, 1994.
- Norton, W.A., and M. Chipperfield, Quantification of the transport of chemically activated air from the Northern Hemisphere polar vortex, *J. Geophys. Res.*, *100*, 25817-25850, 1995.
- O'Sullivan, D., Cross-equatorially radiating stratospheric Rossby waves, *Geophys. Res. Lett.*, *24*, 1483-1486, 1997.
- O'Sullivan, D., and P. Chen, Modeling the quasi-biennial oscillation's influence on tracer transport in the tropics, *J. Geophys. Res.*, *101*, 6811-6822, 1996.
- Oelhaf, H., T.V. Clarmann, H. Fischer, F. Friedl-Vallon, C. Fritzsche, A. Linden, C. Piesch, M. Seefeldner, and W. Volker, Stratospheric ClONO₂ and HNO₃ profiles inside the Arctic vortex from MIPAS-B limb emission spectra obtained during EASOE, *Geophys. Res. Lett.*, *21*, 1263-1266, 1994.
- Oltmans, S.J., and D.J. Hofmann, Increase in lower stratosphere water vapour at a mid-latitude Northern Hemisphere site from 1981 to 1994, *Nature*, *374*, 146-149, 1995.
- Oppliger, R., A. Allanic, and M.J. Rossi, Real-time kinetics of the uptake of ClONO₂ on ice and in the presence of HCl in the temperature range 160 to 200 K, *J. Phys. Chem. A.*, *101*, 1903-1911, 1997.
- Orsolini, Y.J., G. Hansen, U.P. Hoppe, G.L. Manney, and K.H. Fricke, Dynamical modelling of wintertime lidar observations in the Arctic: Ozone laminae and ozone depletion, *Quart. J. Roy. Meteorol. Soc.*, *123*, 785-800, 1997.
- Ortland, D., Rossby wave propagation into the tropical stratosphere observed by the high resolution Doppler imager, *Geophys. Res. Lett.*, 1999-2002, 1997.
- Osterman, G.B., R.J. Salawitch, B. Sen, G.C. Toon, R.A. Stachnik, H.M. Pickett, J.J. Margitan, J.F. Blavier, and D.B. Peterson, Balloon-borne measurements of stratospheric radicals and their precursors: Implications for the production and loss of ozone, *Geophys. Res. Lett.*, *24*, 1107-1110, 1997.
- Pan, L., S. Solomon, W. Randel, J.F. Lamarque, P. Hess, J. Gille, E.W. Chiou, and M.P. McCormick, Hemispheric asymmetries and seasonal variations of the lowermost stratospheric water vapor and ozone derived from SAGE II data, *J. Geophys. Res.*, *102*, 28177-28184, 1997.
- Peter, T., Microphysics and chemistry of polar stratospheric cloud particles, *Ann. Rev. Phys. Chem.*, *48*, 785-822, 1997.
- Peter, T., R. Müller, P.J. Crutzen, and T. Deshler, The lifetime of leewave-induced ice particles in the Arctic stratosphere: II, Stabilization due to NAT-coating, *Geophys. Res. Lett.*, *21*, 1331-1334, 1994.
- Peters, D., and D.W. Waugh, Influence of barotropic shear on the poleward advection of upper tropospheric air, *J. Atmos. Sci.*, *53*, 3013-3031, 1996.
- Pierrehumbert, R.T., Large-scale horizontal mixing in planetary atmospheres, *Phys. Fluids*, *A3*, 1250-1260, 1991.
- Plumb, R.A., A "tropical pipe" model of stratospheric transport, *J. Geophys. Res.*, *101*, 3957-3972, 1996.
- Plumb, R.A., and J. Eluszkiewicz, The Brewer-Dobson circulation: Dynamics of the tropical upwelling, *J. Atmos. Sci.*, in press, 1998.
- Plumb, R.A., and M.K.W. Ko, Interrelationships between mixing ratios of long-lived stratospheric constituents, *J. Geophys. Res.*, *97*, 10145-10156, 1992.
- Plumb, R.A., D.W. Waugh, R.J. Atkinson, P.A. Newman, L.R. Lait, M.R. Schoeberl, E.V. Browell, A.J. Simmons, and M. Loewenstein, Intrusions into the lower stratospheric Arctic vortex during the winter of 1991-1992, *J. Geophys. Res.*, *99*, 1089-1105, 1994.
- Pollock, W.A., L.E. Heidt, R.A. Lueb, J.F. Vedder, M.J. Mills, and S. Solomon, On the age of stratospheric air and ozone depletion potentials in the polar regions, *J. Geophys. Res.*, *97*, 12993-12999, 1992.
- Polvani, L.M., D.W. Waugh, and R.A. Plumb, On the subtropical edge of the stratospheric surf zone, *J. Atmos. Sci.*, *52*, 1288-1309, 1995.
- Poole, L.R., and M.P. McCormick, Polar stratospheric clouds and the Antarctic ozone hole, *J. Geophys. Res.*, *93*, 8423-8430, 1988.

- Portmann, R.W., S. Solomon, R. Garcia, L.W. Thomason, L.R. Poole, and M.P. McCormick, Role of aerosol variations in anthropogenic ozone depletion in the polar regions, *J. Geophys. Res.*, *101*, 22991-23006, 1996.
- Potter, B.E., and J.R. Holton, The role of monsoon convection in the dehydration of the lower tropical stratosphere, *J. Atmos. Sci.*, *52*, 1034-1050, 1995.
- Prabhakara, C., D.P. Kratz, J.M. Yoo, G. Dalu, and A. Vernekar, Optically thin cirrus clouds: Radiative impact on the warm pool, *J. Quant. Spectrosc. Radiat. Transfer*, *49*, 467-483, 1993.
- Prather, M., and A.H. Jaffe, Global impact of the Antarctic ozone hole: Chemical propagation, *J. Geophys. Res.*, *95*, 3473-3492, 1990.
- Pullen, S., and R.L. Jones, Accuracy of temperatures from UKMO analyses of 1994/95 in the Arctic winter stratosphere, *Geophys. Res. Lett.*, 845-848, 1997.
- Pundt, I., J.P. Pommereau, and F. Lefèvre, Investigation of stratospheric bromine and iodine oxides using the SAOZ balloon sonde, in *Atmospheric Ozone: Proceedings of the XVIII Quadrennial Ozone Symposium*, edited by R.D. Bojkov and G. Visconti, pp. 575-578, Parco Scientifico e Tecnologico D'Abruzzo, L'Aquila, Italy, 1998.
- Pyle, J.A., and A.M. Zavody, The modelling problems associated with spatial averaging, *Quart. J. Roy. Meteorol. Soc.*, *116*, 753-766, 1990.
- Pyle, J.A., M.P. Chipperfield, I. Kilbane-Dawe, A.M. Lee, R.M. Stimpfle, D. Kohn, W. Renger, and J.W. Waters, Early modeling results from the SESAME and ASHOE campaigns, *Faraday Discuss. Chem. Soc.*, *100*, 371-387, 1995.
- Randel, W.J., and J.B. Cobb, Coherent variations of monthly mean total ozone and lower stratospheric temperature, *J. Geophys. Res.*, *99*, 5433-5447, 1994.
- Randel, W.J., and F. Wu, Isolation of the ozone QBO in SAGE II data by singular value decomposition, *J. Atmos. Sci.*, *53*, 2546-2559, 1996.
- Randel, W.J., and F. Wu, Cooling of the Arctic and Antarctic polar stratosphere due to ozone depletion, *J. Climate*, in press, 1998.
- Randel, W.J., J.C. Gille, A.E. Roche, J.B. Kumer, J.L. Mergenthaler, J.W. Waters, E.F. Fishbein, and W.A. Lahoz, Planetary wave mixing in the subtropical stratosphere observed in UARS constituent data, *Nature*, *365*, 533-535, 1993.
- Randel, W.J., F. Wu, J.M. Russell III, J.W. Waters, and L. Froidevaux, Ozone and temperature changes in the stratosphere following the eruption of Mount Pinatubo, *J. Geophys. Res.*, *100*, 16753-16764, 1995.
- Randel, W.J., F. Wu, J.M. Russell III, A. Roche, and J.W. Waters, Seasonal cycles and QBO variations in stratospheric CH₄ and H₂O observed in UARS HALOE data, *J. Atmos. Sci.*, *55*, 163-185, 1998.
- Rasch, P.J., B.A. Boville, and G.P. Brasseur, A 3-dimensional general circulation model with coupled chemistry for the middle atmosphere, *J. Geophys. Res.*, *100*, 9041-9071, 1995.
- Ravishankara, A.R., Heterogeneous and multiphase chemistry in the troposphere, *Science*, *276*, 1058-1065, 1997.
- Ravishankara, A.R., and D.R. Hanson, Differences in the reactivity of type-I polar stratospheric clouds depending on their phase, *J. Geophys. Res.*, *101*, 3885-3890, 1996.
- Reichardt, J., A. Ansmann, M. Serwazi, C. Weitkamp, and W. Michaelis, Unexpected low ozone concentration in mid-latitude tropospheric ice clouds: A case study, *Geophys. Res. Lett.*, *23*, 1929-1932, 1996.
- Reid, S.J., and G. Vaughan, Lamination in ozone profiles in the lower stratosphere, *Quart. J. Roy. Meteorol. Soc.*, *117*, 825-844, 1991.
- Reid, S.J., G. Vaughan, and E. Kyrö, Occurrence of ozone laminae near the boundary of the stratospheric polar vortex, *J. Geophys. Res.*, *98*, 8883-8890, 1993.
- Renard, J.-B., M. Pirre, C. Robert, and D. Huguenin, OBrO est-il present dans la stratosphere? Is OBrO present in the stratosphere? *C. R. Acad. Sci. Paris, Sciences de la terre et des planetes*, *325*, 921-924, 1997.
- Rex, M., P. von der Gathen, G.O. Braathen, N.R.P. Harris, E. Reimer, A. Beck, R. Alfier, R. Krüger-Carstensen, M. Chipperfield, H. De Backer, D. Balis, F. O'Connor, H. Dier, V. Dorokhov, H. Fast, A. Gamma, M. Gil, E. Kyrö, Z. Litynska, I.S. Mikkelsen, M. Molyneux, G. Murphy, S.J. Reid, M. Rummukainen, and C. Zerefos, Chemical ozone loss in the Arctic winter 1994/95 as determined by the Match technique, *J. Atmos. Chem.*, in press, 1998.
- Richter, A., M. Eisenger, A. Ladstatter-Weissenmayer, and J.P. Burrows, DOAS zenith sky observations: 2, Seasonal variation of BrO over Bremen (53N) 1994-1995, *J. Atmos. Chem.*, in press, 1998.

LOWER STRATOSPHERIC PROCESSES

- Rinsland, C.P., M.R. Gunson, R.J. Salawitch, H.A. Michelsen, R. Zander, M.J. Newchurch, M.M. Abbas, M.C. Abrams, G.L. Manney, A.Y. Chang, F.W. Irion, A. Goldman, and E. Mahieu, ATMOS/ATLAS 3 measurements of stratospheric chlorine and reactive nitrogen partitioning inside and outside the November 1994 Antarctic vortex, *Geophys. Res. Lett.*, *23*, 2365-2368, 1996a.
- Rinsland, C.P., M.R. Gunson, R.J. Salawitch, M.J. Newchurch, R. Zander, M.M. Abbas, M.C. Abrams, G.L. Manney, H.A. Michelsen, A.Y. Chang, and A. Goldman, ATMOS measurements of $\text{H}_2\text{O} + 2\text{CH}_4$ and total reactive nitrogen in the November 1994 Antarctic stratosphere: Dehydration and denitrification in the vortex, *Geophys. Res. Lett.*, *23*, 2397-2400, 1996b.
- Robinson, G.D., The transport of minor atmospheric constituents between troposphere and stratosphere, *Quart. J. Roy. Meteorol. Soc.*, *106*, 227-254, 1980.
- Robinson, G.N., D.R. Worsnop, J.T. Jayne, and C.E. Kolb, Heterogeneous uptake of ClONO_2 and N_2O_5 by sulfuric acid solutions, *J. Geophys. Res.*, *102*, 3583-3601, 1997.
- Roche, A.E., J.B. Kumer, J.L. Mergenthaler, R.W. Nightingale, W.G. Uplinger, G.A. Ely, J.F. Potter, D.J. Wuebbles, P.S. Connell, and D.E. Kinnison, Observations of lower-stratospheric ClONO_2 , HNO_3 , and aerosol by the UARS CLAES experiment between January 1992 and April 1993, *J. Atmos. Sci.*, *51*, 2877-2902, 1994.
- Rogaski, C.A., D.M. Golden, and L.R. Williams, Reactive uptake and hydration experiments on amorphous carbon treated with NO_2 , SO_2 , O_3 , HNO_3 , and H_2SO_4 , *Geophys. Res. Lett.*, *24*, 381-384, 1997.
- Rood, R.B., A.R. Douglass, J.A. Kaye, M.A. Geller, Y. Chi, D.J. Allen, E.M. Larson, E.R. Nash, and J.E. Nielsen, Three-dimensional simulations of winter-time ozone variability in the lower stratosphere, *J. Geophys. Res.*, *96*, 5055-5071, 1991.
- Rosenfield, J.E., D.B. Considine, P.E. Meade, J.T. Bacmeister, C.H. Jackman, and M.R. Schoeberl, Stratospheric effects of Mount Pinatubo aerosol studied with a coupled two-dimensional model, *J. Geophys. Res.*, *102*, 3649-3670, 1997.
- Rosenlof, K.H., Seasonal cycle of the residual mean meridional circulation in the stratosphere, *J. Geophys. Res.*, *100*, 5173-5191, 1995.
- Rosenlof, K.H., A.F. Tuck, K.K. Kelly, J.M. Russell III, and M.P. McCormick, Hemispheric asymmetries in water vapor and inferences about transport in the lower stratosphere, *J. Geophys. Res.*, *102*, 13213-13234, 1997.
- Rowley, D.M., M.H. Harwood, R.A. Freshwater, and R.L. Jones, A novel flash photolysis/UV absorption system employing charge-coupled device (CCD) detection: A study of the $\text{BrO} + \text{BrO}$ reaction at 298 K, *J. Phys. Chem.*, *100*, 3020-3029, 1996.
- Russell, J.M. III, C.B. Farmer, C.P. Rinsland, R. Zander, L. Froidevaux, G.C. Toon, B. Gao, J. Shaw, and M. Gunson, Measurements of odd nitrogen compounds in the stratosphere by the ATMOS experiment on Spacelab 3, *J. Geophys. Res.*, *93*, 1718-1736, 1988.
- Russell, J.M. III, M. Luo, R.J. Cicerone, and L.E. Deaver, Satellite confirmation of the dominance of chlorofluorocarbons in the global stratospheric chlorine budget, *Nature*, *379*, 526-529, 1996.
- Salawitch, R.J., S.C. Wofsy, E.W. Gottlieb, L.R. Lait, P.A. Newman, M.R. Schoeberl, M. Loewenstein, J.R. Podolske, S.E. Strahan, M.H. Proffitt, C.R. Webster, R.D. May, D.W. Fahey, D. Baumgardner, J.E. Dye, J.C. Wilson, K.K. Kelly, J.W. Elkins, and J.G. Anderson, Chemical loss of ozone in the Arctic polar vortex in the winter of 1991-1992, *Science*, *261*, 1146-1149, 1993.
- Salawitch, R.J., S.C. Wofsy, P.O. Wennberg, R.C. Cohen, J.G. Anderson, D.W. Fahey, R.S. Gao, E.R. Keim, E.L. Woodbridge, R.M. Stimpfle, J.P. Koplrow, D.W. Kohn, C.R. Webster, R.D. May, L. Pfister, E.W. Gottlieb, H.A. Michelsen, G.K. Yue, M.J. Prather, J.C. Wilson, C.A. Brock, H.H. Jonsson, J.E. Dye, D. Baumgardner, M.H. Proffitt, M. Loewenstein, J.R. Podolske, J.W. Elkins, G.S. Dutton, E.J. Hints, A.E. Dessler, E.M. Weinstock, K.K. Kelly, K.A. Boering, B.C. Daube, K.R. Chan, and S.W. Bowen, The diurnal variation of hydrogen, nitrogen, and chlorine radicals: Implications for the heterogeneous production of HNO_2 , *Geophys. Res. Lett.*, *21*, 2551-2554, 1994.
- Sander, S.P., R.P. Friedl, and Y.L. Yung, Rate of formation of the ClO dimer in the polar stratosphere: Implications for ozone loss, *Science*, *245*, 1095-1098, 1989.

- Santee, M.L., W.G. Read, J.W. Waters, L. Froidevaux, G.L. Manney, D.A. Flower, R.A. Jarnot, R.S. Harwood, and G.E. Peckham, Interhemispheric differences in polar stratospheric HNO₃, ClO, and O₃, *Science*, *267*, 849-852, 1995.
- Schauffler, S.M., L.E. Heidt, W.H. Pollock, T.M. Gilpin, J.F. Vedder, S. Solomon, R.A. Lueb, and E.L. Atlas, Measurements of halogenated organic compounds near the tropical tropopause, *Geophys. Res. Lett.*, *20*, 2567-2570, 1993.
- Schmidt, U., and A. Khedim, In situ measurements of carbon dioxide in the winter arctic vortex and at mid-latitudes: An indicator of the age of stratospheric air, *Geophys. Res. Lett.*, *18*, 763-766, 1991.
- Schneider, H.R., M.K.W. Ko, and C.A. Peterson, Interannual variations of ozone: Interpretation of 4 years of satellite observations of total ozone, *J. Geophys. Res.*, *96*, 2889-2896, 1991.
- Schoeberl, M.R., L.R. Lait, P.A. Newman, and J.E. Rosenfield, The structure of the polar vortex, *J. Geophys. Res.*, *97*, 7859-7882, 1992.
- Schoeberl, M.R., A.E. Roche, J.M. Russell III, D. Ortland, P.B. Hays, and J.W. Waters, An estimation of the dynamical isolation of the tropical lower stratosphere using UARS wind and trace gas observations of the quasi-biennial oscillation, *Geophys. Res. Lett.*, *24*, 53-56, 1997.
- Schoeberl, M.R., C.H. Jackman, and J.E. Rosenfield, A Lagrangian estimate of aircraft effluent lifetime, *J. Geophys. Res.*, *103*, 10817-10825, 1998.
- Searle, K., M.P. Chipperfield, S. Bekki, and J.A. Pyle, The impact of spatial averaging on calculated polar ozone loss: 1. Model experiments, *J. Geophys. Res.*, *103*, 25397-25408, 1998a.
- Searle, K., M.P. Chipperfield, S. Bekki, and J.A. Pyle, The impact of spatial averaging on calculated polar ozone loss: 2. Theoretical analysis, *J. Geophys. Res.*, *103*, 25409-25416, 1998b.
- Seisel, S., and M.J. Rossi, The heterogeneous reaction of HONO and HBr on ice and on sulfuric acid, *Ber. Bunsenges. Phys. Chem.*, *101*, 943-955, 1997.
- Selkirk, H.B., The tropopause cold trap in the Australian Monsoon during STEP/AMEX, *J. Geophys. Res.*, *98*, 8591-8610, 1993.
- Sen, B., G.C. Toon, G.B. Osterman, J.F. Blavier, J.J. Margitan, R.J. Salawitch, and G.K. Yue, Measurements of reactive nitrogen in the stratosphere, *J. Geophys. Res.*, *103*, 3571-3585, 1998.
- Shepherd, T.G., K. Semeniuk, and J.N. Koshyk, Sponge layer feedbacks in middle atmosphere models, *J. Geophys. Res.*, *101*, 23447-23464, 1996.
- Shindell, D.T., D. Rind, and P. Lonergan, Climate change and the middle atmosphere: Part IV, Ozone photochemical response to doubled CO₂, *J. Climate*, *11*, 895-918, 1998a.
- Shindell, D.T., D. Rind, and P. Lonergan, Increased polar stratospheric ozone losses and delayed eventual recovery owing to increasing greenhouse-gas concentrations, *Nature*, *392*, 589-592, 1998b.
- Silvente, E., R.C. Richter, M. Zheng, and A.J. Hynes, Relative quantum yields for O(¹D) production in the photolysis of ozone between 301 and 336 nm: Evidence for the participation of a spin-forbidden channel, *Chem. Phys. Lett.*, *264*, 309-315, 1997.
- Slusser, J.R., D.J. Fish, E.K. Strong, R.L. Jones, H.K. Roscoe, and A. Sarkissian, Five years of NO₂ vertical column measurements at Faraday (65°S): Evidence for the hydrolysis of BrONO₂ on Pinatubo aerosols, *J. Geophys. Res.*, *102*, 12987-12993, 1997.
- Sobel, A., R.A. Plumb, and D.W. Waugh, On methods of calculating transport across the polar vortex edge, *J. Atmos. Sci.*, *25*, 2241-2260, 1997.
- Solomon, S., R.R. Garcia, and A.R. Ravishankara, On the role of iodine in ozone depletion, *J. Geophys. Res.*, *99*, 20491-20499, 1994.
- Solomon, S., R.W. Portmann, R.R. Garcia, L.W. Thomason, L.R. Poole, and M.P. McCormick, The role of aerosol trends and variability in anthropogenic ozone depletion at northern midlatitudes, *J. Geophys. Res.*, *101*, 6713-6727, 1996.
- Solomon, S., S. Borrmann, R.R. Garcia, R. Portmann, L. Thomason, L.R. Poole, D. Winker, and M.P. McCormick, Heterogeneous chlorine chemistry in the tropopause region, *J. Geophys. Res.*, *102*, 21411-21429, 1997.
- Solomon, S., R.W. Portmann, R.R. Garcia, W. Randel, R. Nagatani, J. Gleason, L. Thomason, L.R. Poole, and M.P. McCormick, Ozone depletion at mid-latitudes: Coupling of volcanic aerosols and temperature variability to anthropogenic chlorine, *Geophys. Res. Lett.*, *25*, 1871-1874, 1998.
- Sparling, L.C., J.A. Kettleborough, P.H. Haynes, M.E. McIntyre, J.E. Rosenfield, M.R. Schoeberl, and P.A. Newman, Diabatic cross-isentropic dispersion in the lower stratosphere, *J. Geophys. Res.*, *102*, 25817-25829, 1997.

LOWER STRATOSPHERIC PROCESSES

- Sparling, L.C., A.R. Douglass, and M.R. Schoeberl, An estimate of the effect of unresolved structure on modeled ozone loss from aircraft observations of ClO, *Geophys. Res. Lett.*, *25*, 305-308, 1998.
- Steil, B., M. Dameris, C. Brühl, P.J. Crutzen, V. Grewe, M. Ponater, and R. Sausen, Development of a chemistry module for GCMs: First results of a multiannual integration, *Ann. Geophys.*, *16*, 205-228, 1998.
- Stimpfle, R.M., J.P. Koplrow, R.C. Cohen, D.W. Kohn, P.O. Wennberg, D.M. Judah, D.W. Toohey, L.M. Avallone, J.G. Anderson, R.J. Salawitch, E.L. Woodbridge, C.R. Webster, R.D. May, M.H. Proffitt, K. Aiken, J.J. Margitan, M. Loewenstein, J.R. Podolske, L. Pfister, and K.R. Chan, The response of ClO radical concentrations to variations in NO₂ radical concentrations in the lower stratosphere, *Geophys. Res. Lett.*, *21*, 2543-2546, 1994.
- Strahan, S.E., and J.D. Mahlman, Evaluation of the SKYHI general circulation model using aircraft N₂O measurements: 2, Tracer variability and diabatic meridional circulation, *J. Geophys. Res.*, *99*, 10319-10332, 1994.
- Swinbank, R., and A. O'Neill, A stratosphere-troposphere data assimilation system, *Mon. Weather Rev.*, *122*, 686-702, 1994.
- Tabazadeh, A., and O.B. Toon, The presence of metastable HNO₃/H₂O solid phases in the stratosphere inferred from ER-2 data, *J. Geophys. Res.*, *101*, 9071-9078, 1996.
- Tabazadeh, A., R.P. Turco, K. Drdla, M.Z. Jacobson, and O.B. Toon, A study of type I polar stratospheric cloud formation, *Geophys. Res. Lett.*, *21*, 1619-1622, 1994.
- Tabazadeh, A., O.B. Toon, and P. Hamill, Freezing behavior of stratospheric sulfate aerosols inferred from trajectory studies, *Geophys. Res. Lett.*, *22*, 1725-1728, 1995.
- Takahashi, K., M. Kishigami, Y. Matsumi, M. Kawasaki, and A.J. Orr-Ewing, Observation of the spin-forbidden O(¹D) + O₂(X³Σ_g⁻) channel in the 317-327 nm photolysis of ozone, *J. Chem. Phys.*, *105*, 5290-5293, 1996.
- Takahashi, M., Simulation of the stratospheric quasi-biennial oscillation using a general circulation model, *Geophys. Res. Lett.*, *23*, 661-664, 1996.
- Talukdar, R.K., C.A. Longfellow, M.K. Gilles, and A.R. Ravishankara, Quantum yield of O(¹D) in the photolysis of ozone between 289 and 329 nm as a function of temperature, *Geophys. Res. Lett.*, *25*, 143-146, 1998.
- Tan, D.G.H., P.H. Haynes, A.R. MacKenzie, and J.A. Pyle, The effects of fluid-dynamical stirring and mixing on the deactivation of stratospheric chlorine, *J. Geophys. Res.*, *103*, 1585-1605, 1998.
- Teitelbaum, H., J. Moustououi, J. Ovarlez, and H. Kelder, The role of atmospheric waves in the laminated structure of ozone profiles at high latitude, *Tellus*, *48A*, 442-455, 1996.
- Thompson, D.W.J., and J.M. Wallace, Observed linkages between Eurasian surface air temperature, the North Atlantic Oscillation, Arctic sea level pressure, and the stratospheric polar vortex, *Geophys. Res. Lett.*, *25*, 1297-1300, 1998.
- Thuburn, J., and D.G.H. Tan, A parameterization of mixdown time for atmospheric chemicals, *J. Geophys. Res.*, *102*, 13037-13049, 1997.
- Tie, X.X., and G. Brasseur, The response of stratospheric ozone to volcanic eruptions: Sensitivity to atmospheric chlorine loading, *Geophys. Res. Lett.*, *22*, 3035-3038, 1995.
- Tie, X., G.P. Brasseur, B. Briegleb, and C. Granier, Two-dimensional simulation of Pinatubo aerosol and its effect on stratospheric ozone, *J. Geophys. Res.*, *99*, 20545-20562, 1994.
- Tie, X., C. Granier, W. Randel, and G.P. Brasseur, Effects of interannual variation of temperature on heterogeneous reactions and stratospheric ozone, *J. Geophys. Res.*, *102*, 23519-23527, 1997.
- Toon, G.C., C.B. Farmer, L.L. Lowes, P.W. Schaper, J.F. Blavier, and R.H. Norton, Infrared aircraft measurements of stratospheric composition over Antarctica during September 1987, *J. Geophys. Res.*, *94*, 16571-16596, 1989a.
- Toon, O.B., R.P. Turco, J. Jordan, J. Goodman, and G. Ferry, Physical processes in polar stratospheric ice clouds, *J. Geophys. Res.*, *94*, 11359-11380, 1989b.
- Toon, O.B., E.V. Browell, S. Kinne, and J. Jordan, An analysis of Lidar observations of polar stratospheric clouds, *Geophys. Res. Lett.*, *17*, 393-396, 1990.
- Tsias, A., A.J. Prenni, K.S. Carslaw, T.P. Onasch, B.P. Luo, A.A. Tolbert, and T. Peter, Freezing of polar stratospheric clouds in orographically induced strong warming events, *Geophys. Res. Lett.*, *24*, 2303-2306, 1997.

- Tsuda, T., Y. Murayama, H. Wiryosumarto, S.W.B. Harijono, and S. Kato, Radiosonde observations of equatorial atmospheric dynamics over Indonesia: 1, Equatorial waves and diurnal tides, *J. Geophys. Res.*, *99*, 10491-10506, 1994.
- Tuck, A.F., A comparison of one-, two-, and three-dimensional model representations of stratospheric gases, *Phil. Trans. R. Soc. London A*, *2909*, 477-494, 1979.
- Tuck, A.F., Synoptic and chemical evolution of the Antarctic vortex in late winter and early spring, *J. Geophys. Res.*, *94*, 11687-11737, 1989.
- Tuck, A.F., T. Davies, S.J. Hovde, M. Noguera-Alba, D.W. Fahey, S.R. Kawa, K.K. Kelly, D.M. Murphy, M.R. Proffitt, J.J. Margitan, M. Loewenstein, J.R. Podolske, S.E. Strahan, and K.R. Chan, Polar stratospheric cloud processed air and potential vorticity in the Northern Hemisphere lower stratosphere at mid-latitudes during winter, *J. Geophys. Res.*, *97*, 7883-7904, 1992.
- Tuck, A.F., D. Baumgardner, K.R. Chan, J.E. Dye, J.W. Elkins, S.J. Hovde, K.K. Kelly, M. Loewenstein, J.J. Margitan, R.D. May, J.R. Podolske, M.H. Proffitt, K.H. Rosenlof, W.L. Smith, C.R. Webster, and J.C. Wilson, The Brewer-Dobson circulation in light of high altitude in situ aircraft observations, *Quart. J. Roy. Meteorol. Soc.*, *123*, 1-71, 1997.
- Tung, K.K., and H. Yang, Global QBO in circulation and ozone: Part I, Reexamination of observational evidence, *J. Atmos. Sci.*, *51*, 2699-2707, 1994.
- Turnipseed, A.A., M.K. Gilles, J.B. Burkholder, and A.R. Ravishankara, Kinetics of the IO radical: 1, Reaction of IO with ClO, *J. Phys. Chem. A*, *101*, 5517-5525, 1997.
- Tyndall, G.S., C.S. Kegley-Owen, J.J. Orlando, and J.G. Calvert, Quantum yield for Cl(²P), ClO, and O(³P) in the photolysis of chlorine nitrate at 308 nm, *Faraday Trans. Chem. Soc.*, *93*, 2675-2682, 1997.
- Vaughan, G., and C. Timmis, Transport of tropospheric air into the lower midlatitude stratosphere, *Quart. J. Roy. Meteorol. Soc.*, *124*, 1559-1578, 1998.
- Vohralik, P.F., L.K. Randeniya, I.C. Plumb, and K.R. Ryan, Use of correlations between long-lived atmospheric species in assessment studies, *J. Geophys. Res.*, *103*, 3611-3627, 1998.
- Volk, C.M., J.W. Elkins, D.W. Fahey, R.J. Salawitch, G.S. Dutton, J.M. Gilligan, M.H. Proffitt, M. Loewenstein, J.R. Podolske, K. Minschwaner, J.J. Margitan, and K.R. Chan, Quantifying transport between the tropical and mid-latitude lower stratosphere, *Science*, *272*, 1763-1768, 1996.
- Volk, C.M., J.W. Elkins, D.W. Fahey, G.S. Dutton, J.M. Gilligan, M. Loewenstein, J.R. Podolske, and K.R. Chan, On the evaluation of source gas lifetimes from stratospheric observations, *J. Geophys. Res.*, *102*, 25543-25564, 1997.
- von Clarmann, T., G. Wetzel, H. Oelhaf, F. Friedl-Vallon, A. Linden, G. Maucher, M. Seefeldner, O. Trieschmann, and F. Lefèvre, ClONO₂ vertical profile and estimated mixing ratios of ClO and HOCl in winter Arctic stratosphere from Michelson interferometer for passive atmospheric sounding limb emission spectra, *J. Geophys. Res.*, *102*, 16157-16168, 1997.
- von der Gathen, P., M. Rex, N.R.P. Harris, D. Lucic, B.M. Knudsen, G.O. Braathen, H. DeBacker, R. Fabian, H. Fast, M. Gil, E. Kyrö, R.M. Mikkelsen, J. Stahelin, and C. Varotsos, Observational evidence for chemical ozone depletion over the Arctic in winter 1991-92, *Nature*, *375*, 131-134, 1995.
- Wamsley, P.R., J.W. Elkins, D.W. Fahey, and G.S. Dutton, Distribution of halon-1211 in the upper troposphere and lower stratosphere and the 1994 total bromine budget, *J. Geophys. Res.*, *103*, 1513-1526, 1998.
- Wang, P.H., M.P. McCormick, L.R. Poole, W.P. Chu, G.K. Yue, G.S. Kent, and K.M. Skeens, Tropical high cloud characteristics derived from SAGE II extinction measurements, *Atmos. Res.*, *34*, 53-83, 1994.
- Waters, J.W., G.L. Manney, W.G. Read, L. Froidevaux, D.A. Flower, and R.F. Jarnot, UARS MLS observations of lower stratospheric ClO in the 1992-93 and 1993-94 winter vortices, *Geophys. Res. Lett.*, *22*, 823-826, 1995.
- Wauben, W.M.F., R. Bintanja, P.F.J. van Velthoven, and H. Kelder, On the magnitude of transport out of the Antarctic polar vortex, *J. Geophys. Res.*, *102*, 1229-1238, 1997.
- Waugh, D.W., Seasonal variation of isentropic transport out of the tropical stratosphere, *J. Geophys. Res.*, *101*, 4007-4023, 1996.

LOWER STRATOSPHERIC PROCESSES

- Waugh, D.W., R.A. Plumb, R.J. Atkinson, M.R. Schoeberl, L.R. Lait, P.A. Newman, M. Loewenstein, D.W. Toohey, L.M. Avallone, C.R. Webster, and R.D. May, Transport of material out of the stratospheric Arctic vortex by Rossby wave breaking, *J. Geophys. Res.*, *99*, 1071-1078, 1994.
- Waugh, D.W., R.A. Plumb, D.W. Fahey, K.A. Boering, G.S. Dutton, E. Keim, R.S. Gao, B.C. Daube, S.C. Wofsy, M. Loewenstein, J.R. Podolske, K.R. Chan, M.H. Proffitt, K.K. Kelly, P.A. Newman, and L.R. Lait, Mixing of polar air into middle latitudes as revealed by tracer-tracer scatter plots, *J. Geophys. Res.*, *102*, 13119-13134, 1997a.
- Waugh, D.W., T.M. Hall, W.J. Randel, K.A. Boering, S.C. Wofsy, B.C. Daube, J.W. Elkins, D.W. Fahey, G.S. Dutton, C.M. Volk, and P. Vohralik, Three-dimensional simulations of long-lived tracers using winds from MACCM2, *J. Geophys. Res.*, *102*, 21493-21513, 1997b.
- Weaver, C.J., A.R. Douglass, and R.B. Rood, Thermodynamic balance of three-dimensional stratospheric winds derived from a data assimilation procedure, *J. Atmos. Sci.*, *50*, 2987-2993, 1993.
- Weaver, C.J., A.R. Douglass, and D.B. Considine, A 5 year simulation of supersonic aircraft emission transport using a three-dimensional model, *J. Geophys. Res.*, *101*, 20975-20984, 1996.
- Webster, C.R., R.D. May, L. Jaeglé, H. Hu, S.P. Sander, M.R. Gunson, G.C. Toon, J.M. Russell III, R.M. Stimpfle, J.P. Koplów, R.J. Salawitch, and H.A. Michelsen, Hydrochloric acid and the chlorine budget of the lower stratosphere, *Geophys. Res. Lett.*, *21*, 2575-2578, 1994.
- Weinstock, E.M., E.J. Hintsa, A.E. Dessler, and J.G. Anderson, Measurements of water vapor in the tropical lower stratosphere during the CEPEX campaign: Results and interpretation, *Geophys. Res. Lett.*, *22*, 3231-3234, 1995.
- Wennberg, P.O., R.C. Cohen, R.M. Stimpfle, J.P. Koplów, J.G. Anderson, R.J. Salawitch, D.W. Fahey, E.L. Woodbridge, E.R. Keim, R.S. Gao, C.R. Webster, R.D. May, D.W. Toohey, L.M. Avallone, M.H. Proffitt, M. Loewenstein, J.R. Podolske, K.R. Chan, and S.C. Wofsy, Removal of stratospheric O₃ by radicals: In situ measurements of OH, HO₂, NO, NO₂, ClO, and BrO, *Science*, *266*, 398-404, 1994.
- Wennberg, P.O., T.F. Hanisco, R.C. Cohen, R.M. Stimpfle, L.B. Lapsón, and J.G. Anderson, In situ measurements of OH and HO₂ in the upper troposphere and stratosphere, *J. Atmos. Sci.*, *52*, 3413-3420, 1995.
- Wennberg, P.O., J.W. Brault, T.F. Hanisco, R.J. Salawitch, and G.H. Mount, Atmospheric column abundance of IO: Implications for stratospheric ozone, *J. Geophys. Res.*, *102*, 8887-8898, 1997.
- Williams, L.R., and F.S. Long, Viscosity of supercooled sulfuric acid solutions, *J. Phys. Chem.*, *99*, 3748-3751, 1995.
- WMO (World Meteorological Organization), *Scientific Assessment of Ozone Depletion: 1994*, Global Ozone Research and Monitoring Project—Report No. 37, Geneva, 1995.
- Wofsy, S.C., R.J. Salawitch, J.H. Yatteau, M.B. McElroy, B.W. Gandrud, J.E. Dye, and D. Baumgardner, Condensation of HNO₃ on falling ice particles: Mechanism for denitrification of the polar stratosphere, *Geophys. Res. Lett.*, *17*, 449-452, 1990.
- Woodman, R.F., and P.K. Rastogi, Evaluation of effective eddy diffusive coefficients using radar observations of turbulence in the stratosphere, *Geophys. Res. Lett.*, *11*, 243-246, 1984.
- Wyslouzil, B.E., K.L. Carleton, D.M. Sonnenfroh, W.T. Rawlins, and S. Arnold, Observation of hydration of single, modified carbon aerosols, *Geophys. Res. Lett.*, *21*, 2107-2110, 1994.
- Yokelson, R.J., J.B. Burkholder, and A.R. Ravishankara, Photodissociation of ClONO₂: 2, Time-resolved absorption studies of product quantum yields, *J. Phys. Chem. A.*, *101*, 6667-6678, 1997.
- Yulaeva, E., J.R. Holton, and J.M. Wallace, On the cause of the annual cycle in tropical lower stratospheric temperatures, *J. Atmos. Sci.*, *51*, 169-174, 1994.
- Zhang, R., M.T. Leu, and L.F. Keyser, Hydrolysis of N₂O₅ and ClONO₂ on the H₂SO₄/HNO₃/H₂O ternary solutions under stratospheric conditions, *Geophys. Res. Lett.*, *22*, 1493-1496, 1995.
- Zhang, R., M.T. Leu, and M.J. Molina, Formation of polar stratospheric clouds on preactivated background aerosols, *Geophys. Res. Lett.*, *23*, 1669-1672, 1996.
- Zhang, R., M.T. Leu, and L.F. Keyser, Heterogeneous chemistry of HO₂NO₂ in liquid sulfuric acid, *J. Phys. Chem. A.*, *101*, 3324-3330, 1997.
- Zondlo, M.A., S.B. Barone, and M.A. Tolbert, Uptake of HNO₃ on ice under upper tropospheric conditions, *Geophys. Res. Lett.*, *24*, 1391-1394, 1997.